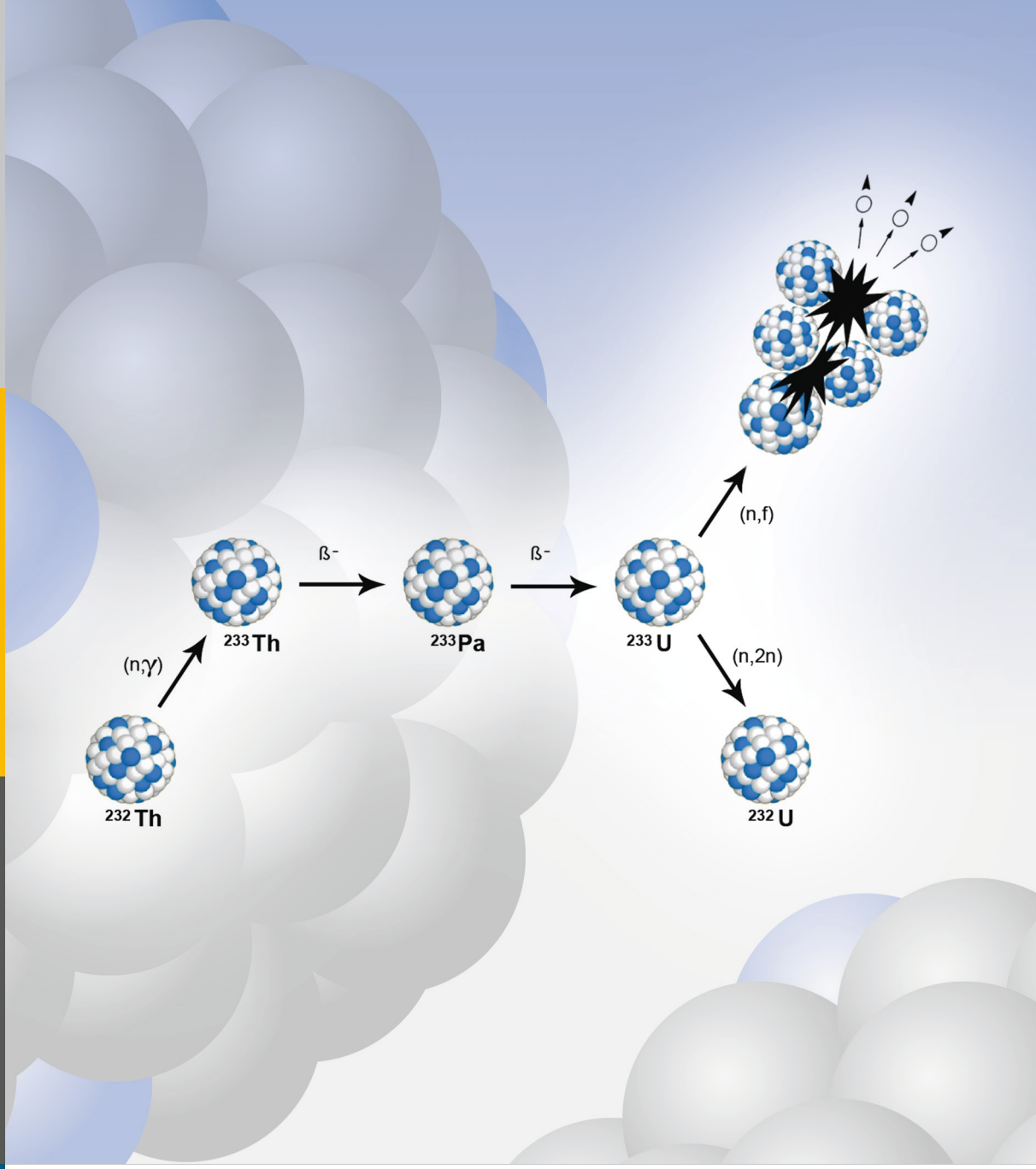

High-Quality Thorium TRISO Fuel Performance in HTGRs

Karl Verfondern, Heinz Nabielek, Michael J. Kania, Hans-Josef Allelein

Member of the Helmholtz Association

JÜLICH
FORSCHUNGSZENTRUM

Schriften des Forschungszentrums Jülich
Reihe Energie & Umwelt / Energy & Environment Band / Volume 174

Forschungszentrum Jülich GmbH
Institut für Energie- und Klimaforschung (IEK)
Nukleare Entsorgung und Reaktorsicherheit (IEK-6)

High-Quality Thorium TRISO Fuel Performance in HTGRs

Karl Verfondern[1], Heinz Nabielek[2], Michael J. Kania[3], Hans-Josef Allelein[1,4]

[1] Research Center Jülich, 52425 Jülich, Germany
[2] Monschauerstr. 61, 52355 Düren, Germany
[3] 20 Beach Road on Burden Lake, Averill Park, NY 12018-3701, USA
[4] RWTH Aachen, 52072 Aachen, Germany

Schriften des Forschungszentrums Jülich
Reihe Energie & Umwelt / Energy & Environment Band / Volume 174

ISSN 1866-1793 ISBN 978-3-89336-873-0

Bibliographic information published by the Deutsche Nationalbibliothek.
The Deutsche Nationalbibliothek lists this publication in the Deutsche Nationalbibliografie; detailed bibliographic data are available in the Internet at http://dnb.d-nb.de.

Publisher and Distributor: Forschungszentrum Jülich GmbH
Zentralbibliothek
52425 Jülich
Tel: +49 2461 61-5368
Fax: +49 2461 61-6103
Email: zb-publikation@fz-juelich.de
www.fz-juelich.de/zb

Cover Design: Grafische Medien, Forschungszentrum Jülich GmbH

Printer: Grafische Medien, Forschungszentrum Jülich GmbH

Schriften des Forschungszentrums Jülich
Reihe Energie & Umwelt / Energy & Environment, Band / Volume 174

ISSN 1866-1793
ISBN 978-3-89336-873-0

The complete volume is freely available on the Internet on the Jülicher Open Access Server (JUWEL) at www.fz-juelich.de/zb/juwel

High-Quality Thorium TRISO Fuel Performance in HTGRs

Karl Verfondern[1], Heinz Nabielek[2], Michael J. Kania[3], Hans-Josef Allelein[1,4]

1 Research Center Jülich, 52425 Jülich, Germany

2 Monschauerstr. 61, 52355 Düren, Germany

3 20 Beach Road on Burden Lake, Averill Park, NY 12018-3701, USA

4 RWTH Aachen, 52072 Aachen, Germany

ABSTRACT

Thorium as a nuclear fuel has received renewed interest, because of its widespread availability and the good irradiation performance of Th and mixed (Th,U) oxide compounds as fuels in nuclear power systems. Early HTGR development employed thorium together with high-enriched uranium (HEU). After 1980, HTGR fuel systems switched to low-enriched uranium (LEU). After completing fuel development for the AVR and the THTR with BISO coated particles, the German program expanded its efforts utilizing thorium and HEU TRISO coated particles in advanced HTGR concepts for process heat applications (PNP) and direct-cycle electricity production (HHT). The combination of a low-temperature isotropic (LTI) inner and outer pyrocarbon layers surrounding a strong, stable SiC layer greatly improved manufacturing conditions and the subsequent contamination and defective particle fractions in production fuel elements. In addition, this combination provided improved mechanical strength and a higher degree of solid fission product retention, not known previously with high-temperature isotropic (HTI) BISO coatings. The improved performance of the HEU $(Th,U)O_2$ TRISO fuel system was successfully demonstrated in three primary areas of development: manufacturing, irradiation testing under normal operating conditions, and accident simulation testing. In terms of demonstrating performance for advanced HTGR applications, the experimental failure statistic from manufacture and irradiation testing are significantly below the coated particle requirements specified for PNP and HHT designs at the time. Covering a range to 1300°C in normal operations and 1600°C in accidents, with burnups to 13% FIMA and fast fluences to 8×10^{25} n/m^2 (E>16 fJ), the performance results exceed the design limits on manufacturing and operational requirements for the German HTR-Modul concept, which are 6.5×10^{-5} for manufacturing, 2×10^{-4} for normal operating conditions, and 5×10^{-4} for accident conditions. These performance statistics for the HEU $(Th,U)O_2$ TRISO fuel system are in good agreement with similar results for the LEU UO_2 TRISO fuel system.

KURZFASSUNG

Dem Thorium als Kernbrennstoff gilt erneut verstärktes Interesse wegen der weiten Verfügbarkeit des Rohstoffs und dem guten Verhalten von Thorium- und (Th,U) Misch-Oxiden bei Bestrahlung in nuklearen Anlagen. Frühe Hochtemperaturreaktoren (HTR) verwendeten Thorium zusammen mit hochangereichertem Uran (HEU), aber HTR Projekte nach 1980 wurden auf niedrig-angereichertes Uran (LEU) umgestellt.

In Deutschland wurde nach der HTR-Brennelemententwicklung für AVR und THTR mit zweifach beschichteten BISO-Partikeln das Programm erweitert auf 3-fach beschichtete TRISO-Partikel für fortgeschrittene Systeme mit Gasturbine im Primärkreislauf (HHT) bzw. Hochtemperatur-Prozeßwärmeanlagen (PNP). Hier hat die Kombination von einer hochdichten, hochfesten Siliziumkarbidschicht, eingebettet in eine innere und äußere LTI-Pyrokohlenstoffschicht (LTI = low-temperature isotropic), zu einem Partikel geführt, das sowohl bei der Herstellung als auch bei Bestrahlung dem alten BISO-Partikel mit HTI-Pyrokohlenstoffschicht (HTI = high temperature isotropic) massiv überlegen war: zum einen bei der Herstellung wegen der sehr viel geringeren Schwermetallkontamination und dem geringerem Anteil von Defektpartikeln und zum anderen im Leistungsbetrieb wegen der höheren Festigkeit und sehr viel besseren Spaltproduktrückhaltung.

Die deutlich verbesserte Qualität von HEU $(Th,U)O_2$ TRISO Brennstoffen wurde auf allen Ebenen erfolgreich demonstriert: bei der Herstellung, unter Normalbetriebsbedingungen und in Störfallsimulationstests. Für die Anwendungen in fortgeschrittenen HHT und PNP-Systemen wurden Ergebnisse erzielt mit Werten deutlich unterhalb der Zielsetzung für den Partikelbruchanteil, und dies in Temperaturbereichen bis 1300°C im Normalbetrieb und in Störfällen bis maximal 1600°C, schnellen Dosiswerten bis zu 8×10^{25} n/m^2 (E>16 fJ) und Abbränden bis zu 13% FIMA. Die erreichten Werte liegen qualitätsmäßig gleich gut wie das später umfangreich demonstrierte LEU UO_2 TRISO-Partikelsystem, ebenfalls unter den Zielwerten für den Partikelbruchanteil, die für das deutsche HTR-Referenzkonzept des HTR-Modul festgelegt worden sind zu: herstellungsbedingt $< 6.5\times10^{-5}$, betriebsbedingt $< 2\times10^{-4}$ und störfallbedingt $< 5\times10^{-4}$.

TABLE OF CONTENTS

EXECUTIVE SUMMARY

Thorium as a nuclear fuel has received renewed interest, because of its widespread availability and the good irradiation performance of Th and mixed (Th,U) oxide and carbide compounds as fuels in nuclear power systems. Early development of large high temperature gas-cooled reactors (HTGR) employed thorium together with high-enriched uranium (HEU) as their reference fuel cycle. After 1980, all HTGR fuel systems switched to the low-enriched uranium (LEU) to avoid proliferation risks with HEU. After completing fuel development for the AVR and the THTR with BISO (bi-isotropic) coated particles, the German program expanded its efforts utilizing HEU $(Th,U)O_2$ TRISO (tri-isotropic) coated particles for advanced HTGR concepts directed to process heat application (PNP) and to direct-cycle electricity production (HHT).

The combination of a low-temperature-isotropic (LTI) inner and outer pyrolytic carbon (PyC) layers surrounding a strong, stable silicon carbide layer greatly improved manufacturing conditions and the subsequent contamination and defective particle fractions in production fuel elements. In addition, this combination provided improved mechanical strength and a higher degree of solid fission product retention, not known previously with high-temperature-isotropic (HTI) BISO coatings.

The improved performance of the HEU $(Th,U)O_2$ TRISO fuel system was successfully demonstrated in three primary areas of development: manufacturing, irradiation testing under normal operating conditions, and accident simulation testing. In terms of demonstrating performance for advanced HTGR applications, the experimental failure statistic from manufacture and irradiation testing are significantly below the coated particle requirements specified for the PNP and HHT designs. In the mid-1970s, there were no passive safety requirements specified for PNP/HHT as these were large HTGR plant designs and the unrestrained core heatup event was the dominant accident scenario.

Based on the performance statistics compiled from the German Advanced Fuel Development Program in the period from 1977 through 1990, the following assessment of HEU (~93%) $(Th,U)O_2$ TRISO fuel system can be presented:

- Forty-six (46) reference HTGR fuel elements from manufacturing, containing 487,480 TRISO fuel particles were evaluated using reference quality control methods. The results yielded a 95% on-sided upper confidence level for the combined contamination and defective particle fraction of 2.2×10^{-5}. This value is lower than the PNP/HHT specification value by a factor of about 3 and is below the specification for the German HTR-Modul at $< 6.5\times10^{-5}$.

- In-reactor testing included accelerated MTR irradiation experiments (comprising 126,664 TRISO particles) and nine reference fuel elements (94,320 TRISO particles) in the real-time AVR environment. Extensive testing and in-reactor monitoring under normal operating conditions yielded an in-reactor failure level of 6.5×10^{-5} at the upper 95% confidence level. Considering the experimental results for reference fuel elements only, the in-reactor failure level was 4.4×10^{-5} at the upper 95% confidence level. Both of these levels are below the PNP/HHT specification by a factor > 3 and well below the in-reactor operation design limit for the German HTR-Modul at $< 2\times10^{-4}$.

- Accident testing conducted on five reference fuel elements (61,970 TRISO particles) yielded failure fraction of 4.8×10^{-5} at the upper 95% confidence level. This failure level represents the fraction of failed fuel particles expected at accident temperatures ≤ 1600ºC. This value is lower than the German HTR-Modul specification of $< 5\times10^{-4}$ for temperatures ≤ 1620ºC by an order of magnitude.

Not all the accident testing results described above were carried out in a traditional accident simulation testing program. A major portion of the results were obtained in a high-temperature annealing program designed to evaluate AVR irradiated fuel element performance at temperatures between 1500ºC and 2500ºC. This program did not have access to the sophisticated experimental facilities for accident simulation testing that were developed after 1983. For this reason and because of the limited number of tests completed, additional accident condition testing on HEU $(Th,U)O_2$ TRISO fuels is strongly recommended. Such tests should be conducted under conditions simulating modern HTGR design-basis events and in current accident testing facilities.

The performance statistics for the HEU $(Th,U)O_2$ TRISO fuel system are in good agreement with similar results for the LEU UO_2 TRISO fuel system [Nabielek 2010]. This comparison is based on the experimental results obtained on reference 60 mm diameter fuel elements for both the $(Th,U)O_2$ and the UO_2 TRISO fuel systems. The results for each fuel designs exceed the design limits on manufacturing and operational requirements for the German HTR-Modul concept, which were:

- $< 6.5\times10^{-5}$ for manufacturing;
- $< 2\times10^{-4}$ for normal operating conditions; and
- $< 5\times10^{-4}$ for accident conditions.

Based on the review of historical experimental data, the performance of HEU thorium based fuels exceeds the performance of similar uranium based fuels for high temperature reactors and could be considered for future high temperature reactor applications.

In the 1980s, international nuclear non-proliferation policies resulted in a change from HEU to LEU fissile fuel materials. As a result of this political decision, the development efforts for the thorium and HEU fuel systems were stopped. This included all fabrication, irradiation, accident condition testing and reprocessing efforts.

- In 1981 in the USA, the reference HTGR concept remained based on a two-particle system, but with a 350 µm diameter fissile UCO fuel kernel with 19.9 wt% ^{235}U, and a 500 µm diameter fertile UCO fuel kernel containing natural uranium. Both the reference HTGR fissile and fertile particles employ TRISO coatings [Stansfield 1991, IAEA 1997].

- In Germany, development of the HEU/Th fuel cycle was terminated in 1980, with a switch to a LEU cycle, with a 500 um diameter pure UO_2 fuel kernel. In an intermediate phase, some experimental effort was undertaken with a medium-enriched uranium (MEU)/Th fuel cycle as an alternative and back-up solution to HEU. The MEU fuel cycle is advantageous with regard to non-proliferation and the design selected was a ~20 wt% ^{235}U and a heavy metal loading of 8 g per spherical element.

1. THORIUM FUEL

The production and use of nuclear fuels was initially based on the U/Pu fuel cycle, since ^{235}U is the only naturally occurring material that will fission with thermal neutrons. But soon afterwards, when projecting a rapid growth of nuclear power and an anticipated shortage in uranium supply, the Th/U cycle was also considered driven by its advantages of:

- expanding the nuclear fuel base by converting the fertile ^{232}Th to fissile ^{233}U; and
- improved uranium utilization in thermal reactors due to the superior physical and nuclear properties of the thorium fuel cycle over the uranium fuel cycle.

In the 1980s, the interest in further developing the alternative thorium fuel cycle decreased due to the availability of low-price uranium, the absence of commercial reprocessing capabilities, and nuclear proliferation concerns. This decrease in interest was also fostered by the severe nuclear accidents at Three Mile Island and Chernobyl.

Thorium as a nuclear fuel has received renewed interest with regard to future (fourth generation) nuclear reactor concepts and, in particular, the Gen-IV requirements for safety, sustainability, proliferation resistance, and economy. Here, the important aspect of reduced plutonium and minor actinide production, which minimizes radioactive waste and improves proliferation resistance, and the expected lower fuel cycle costs in the long term come into play. A Th/Pu cycle is even capable of burning plutonium through fission in a thermal reactor. The favorable neutronics properties of thorium also lead to more efficient utilization of low-cost uranium reserves which can delay the exhaustion of low-cost ore. The thorium's greater abundance makes it attractive to countries to enlarge their degree of energy independence.

1.1. Properties of Thorium-Based Fuels

The naturally abundant form of thorium as mined is practically a single isotope, ^{232}Th, and therefore can be used in thermal reactors with no need for isotope separation. Traces of other thorium isotopes can be found as the result of decay of naturally occurring uranium (Figure 1).

Due to the absence of fissile thorium isotopes, some driver fissile material or another neutron source is necessary to initiate the fuel cycle and achieve criticality. The driver fuel could be either enriched uranium as the optimal choice, but also plutonium if the aim is Pu burning. The thermal absorption cross section of ^{232}Th, is nearly three times that of the fertile ^{238}U in uranium which would indicate enhanced conversion in a thermal reactor. The fission cross-section of ^{238}U in the fast spectrum is three to five times that of ^{232}Th. In a conventional PWR, ^{232}Th fission represents only ~2% of the total energy generated, whereas ^{238}U fission accounts for 7 to 8%.

In thorium fuel, ^{233}U is produced in-reactor through neutron capture in ^{232}Th, followed by two subsequent beta decays of ^{233}Th and ^{233}Pa, respectively, as is shown in Figure 1. The generated ^{233}U can either be used *in-situ* or reprocessed, i.e., chemically separated from the thorium and recycled into new fuel. This thermal breeding of fissile material is unique to thorium-based fuels and cannot be done with uranium fuels. Thermal breeding is favored by a

heterogeneous fuel arrangement where fissile and fertile materials are physically separated, because it allows the better supply with surplus neutrons [WNA 2011].

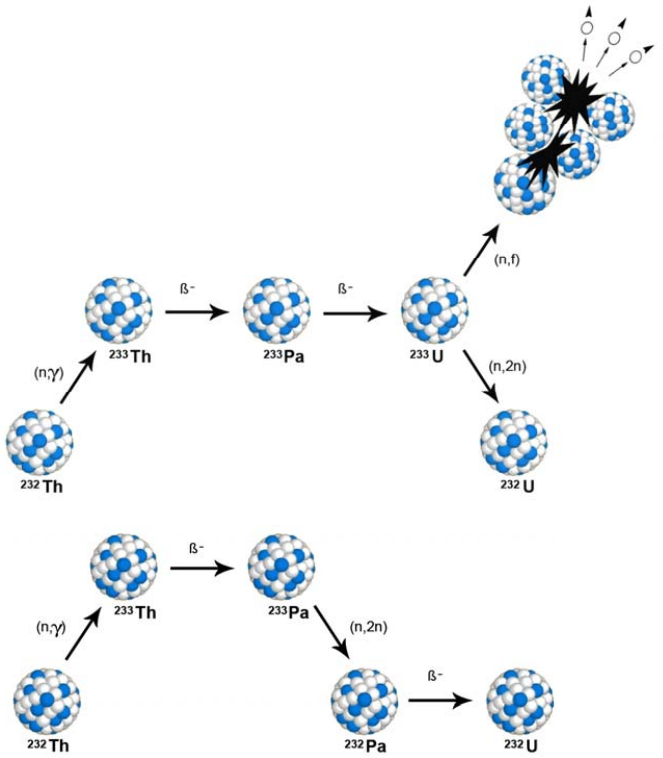

Figure 1. Buildup of fissile U-233 and of U-232 from thorium.

A major challenge is the comparatively long interval, over which ^{232}Th breeds to ^{233}U. The half-life of ^{233}Pa is rather high at ~27 days which is ten times longer than the half-life of ^{239}Np (2.3 d), the respective interim product in the plutonium breeding process. As a result, substantial amounts of ^{233}Pa accumulate in thorium-based fuels representing a significant neutron absorber, which may lead to shutdown control problems. Although it will eventually breed into fissile ^{235}U (requiring two additional neutron absorptions), this process degrades neutron economy and increase the likelihood of transuranic elements production.

Thorium-based fuels display a number of favorable physical and chemical properties which improve reactor and repository performance. The fissile ^{233}U isotope is a very valuable material because of the high number of neutrons produced per neutron absorbed in the thermal neutron spectrum. The fission cross-section of ^{233}U is high with the ratio of production/absorption by fission being 2.29 over a wide range of energies. On the other hand, the capture cross-section is low, which restricts transmutation and improves neutron economy.

These properties can be the basis for a thermal breeder reactor. Theoretical studies to evaluate different thorium breeder systems indicate that gas-cooled high temperature reactors, heavy-water-moderated reactors and molten-salt reactors are particularly promising. In advanced

thorium converters, it may be even possible to breed ^{233}U sufficiently to achieve a self-sustaining recycle system without the need for supplementary driver fuel input. The ultimate uranium conservation is given in a fuel cycle where no driver material would be required and in which, in equilibrium, no natural uranium would be necessary.

In a thermal reactor neutron spectrum, the asymptotic stable concentration of ^{233}U in thorium is about 1.5%. In contrast, the higher thermal capture cross-section of ^{232}Th in combination with the thermal absorption cross-section of Pu isotopes, which is more than twice that of ^{233}U, enhances the Pu consumption rate and limits the Pu content in uranium rods to ~1%, even after a long residence time at high neutron flux.

Fissile ^{233}U produced in thorium fuels is inevitably connected with the in-pile formation of ^{232}U (see Figure 1) which has two significant high-energy gamma emitting decay products, thallium-208 (^{208}Th) with its 2.6 MeV gamma and bismuth-212 (^{212}Bi) with its 1.8 MeV gamma as can be seen from the decay chain in Figure 2. Since ^{232}U can not be chemically separated from ^{233}U, this path represents a radiological hazard that necessitates strong shielding and remote handling for all operations of recycling, manufacture, transport, or disposal.

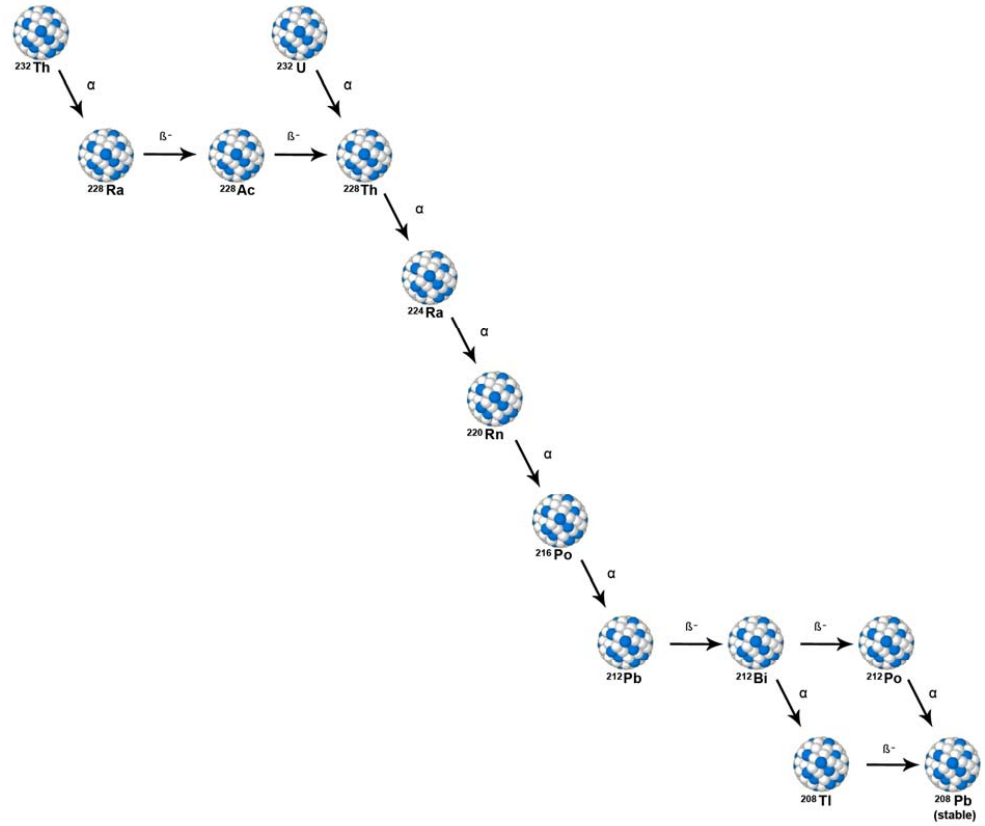

Figure 2. Natural decay chain in the thorium fuel cycle.

On the other hand, the strong gamma radiation of the irradiated fuel provides inherent proliferation resistance and aids in the passive detection of such materials. This holds also for recycled thorium because of the presence of ^{228}Th, which is part of the ^{232}U decay sequence. This is different from Pu fuel that can easily be handled in a glove box.

Compared to the largely employed UO_2, thorium dioxide (ThO_2) has one of the highest melting points of all oxides, 3300°C, compared to 2700°C for UO_2. This applies also to their metallic forms (1750°C vs. 1130°C). Above ~500°C, thorium is significantly stronger than uranium. Furthermore, ThO_2 has a higher thermal conductivity, and a lower coefficient of thermal expansion. It exhibits greater chemical stability and, different from UO_2, does not further oxidize. The characteristic properties for ThO_2 are its stability, refractiveness and radiation resistance which provides more operational freedom. Also, the irradiation behavior of thorium fuels is superior to UO_2 fuel allowing higher burnups to be achieved.

There are two classes of thorium fuel cycle options: (i) the closed cycle where the ^{233}U is recycled into fresh fuel, and (ii) the open or once-through cycle which aims at high burnups before the spent fuel is ready for directly disposal (or interim storage for potential recycling at a later stage). The former has the primary advantage of a reduced natural uranium consumption, while the latter option favors thorium fuels with a low Pu generation rate. If nuclear waste (americium and curium) were added to the Th/U fuel, this fuel system could even be used to incinerate long-lived radiotoxic isotopes.

The Th/Pu cycle could be of interest in a transition period to the full use of a thorium fuel cycle. Plutonium from available stockpiles or from reprocessing LWR fuels (or from both sources) could serve as a feed fissile material to initiate a closed thorium cycle considered as a possible long-term option.

The potential radiotoxicity of the long-lived isotopes in irradiated fuel is lower in thorium fuel. Being a lighter element than the uranium and plutonium isotopes, ^{232}Th produces fewer minor actinides (americium and curium) than ^{238}U does. This fact appears beneficial in waste management. Still, some long-lived actinide products constitute a long-term radiological impact, especially ^{231}Pa.

Due to the high achievable burnups, the question is whether or not reprocessing is necessary and reasonable. Nevertheless, a reprocessing technology has been developed. From the technical point of view, the treatment of thorium fuels at the back-end has become feasible using the so-called THOREX process. It was tested on laboratory and pilot scale in the USA, Germany, and recently in India. However, because of insufficient experience, particularly for high-burnup fuels, this process has never proceeded to industrial application up to now and requires further development work. [Greneche 2007]

Reprocessing is delicate since the accumulated ^{233}Pa demands long cooling times (positive aspect though with regard to non-proliferation). Also, ThO_2 is insoluble in nitric acid and the THOREX process uses highly corrosive agents. Up to now, the interest has mainly focused on partitioning of the Th/U, while the TRU separation was neglected. Therefore, no complex flowsheets are available for the joint partitioning of U, Th, Pu, Np and the Am and Cm actinides from spent fuel. Based solely on laboratory experiments, the losses expected for the THOREX process are similar to those in the PUREX process of the U/Pu fuel cycle which are an estimated 0.1% for U and Th, and 1-2% for Pa. [Gruppelaar 2000]

1.2. Thorium Fuels in High Temperature Reactors

Because of the unique arrangement of coated particle fuel embedded in a graphite matrix serving as moderator, the HTGR has an inherent flexibility to accommodate many types of fuel cycles. A variety of mixtures of fissile and fertile materials can be employed without significant modification to the fuel element geometry or core design. The feasible fuel cycles for HTGRs can be grouped into four categories: (i) low-enriched uranium (LEU); (ii) mixed oxide (MOX); (iii) plutonium only; and (iv) thorium-based fuel [IAEA 2010].

With regard to once-through cycles (with the *in-situ* consumption of the ^{233}U) in an HTGR, the HEU U/Th cycle is, from the economic point of view, similar to the LEU UO_2 cycle. For closed cycles, however, the U/Th cycle is by far superior promising a reduction in the annual uranium demand by at least 60%. Today, nearly all current commercial projects are based on the LEU UO_2 fuel cycle, since it appears the most appropriate one for near-term commercial HTGR deployment.

But a look back into the past reveals that the nuclear HTGR programs in Germany and the U.S. have shown from the beginning a substantial interest in the utilization of thorium in power reactors. The HEU/Thorium cycle became the reference HTGR fuel cycle in both countries. Requirements to the coated fuel particle design were principally defined through the selected fuel cycle, the chemical behavior of the fuel kernel during irradiation, and through the overall irradiation performance. The heavy metal loading considered favorable in the HEU fuel cycle was 11 g/sphere. For the closed thorium cycle, 16 g/sphere were considered appropriate to achieve a high conversion rate. The breakeven breeding ratio to reach a breed rate of 1.0 is 32 g/sphere. For practical reasons, however, the limit is 20 g for cold pressing, and 30-40 g, respectively, for warm pressing of the spheres.

Since the early 1960s, the development of HTGR fuel in Germany was based on thorium fuel cycles with HEU. Utilizing the experience from the OECD project Dragon reactor where various types of coated particle fuels were inserted, among them three variants for a Th/U fuel cycle, work on spherical fuel elements was dedicated to development of a gas-cooled pebble-bed converter reactor concept using thorium as fertile material. The production process in Germany for spherical fuel elements containing particle kernels with a 10:1 ratio of Th to ^{235}U as fuel for AVR and THTR-300 was fully established and licensed in the 1970s [IAEA 1997]. Three HEU fuel reference concepts were selected for advanced HTGR concepts directed to process heat applications (PNP) and direct-cycle electricity production (HHT) as will be explained in more detail in Chapter 2. In support of the process heat and direct cycle HTGR concept development, a significant number of irradiation tests were executed with the HEU $(Th,U)O_2$ TRISO fuel system in the period 1977 to 1981.

Coated fuel particle development in the USA during the 1970s and early 1980s concentrated on a two-particle concept with a 200 µm UC_2 or UCO fuel kernel with a TRISO coating as the fissile particle, plus a 500 µm ThO_2 fuel kernel with an LTI-BISO coating. The two-particle concept in the closed U/Th cycle facilitates fuel reprocessing, but also calls for two different fabrication processes. The SiC layer was employed here in particular as a means to allow separation of the bred fissile ^{233}U from make-up ^{235}U and its activation product ^{236}U. The US fuel fabrication became much advanced with good experience.

Besides the Dragon test reactor, four more HTGR test and prototype power reactors were designed, constructed and operated in the 1960s and 1970s with this type of fuel cycle. The

first thorium-utilizing reactor concept taken up actively was the AVR pebble-bed reactor aimed at the demonstration of high conversion rates and high burnup values. More than 80% of all the fuel elements inserted into the AVR contained thorium fuel and achieved maximum burnups of up to ~150 GWd/t_{HM}. The AVR also provided important experience with different fuel concepts, such as the one-particle and two-particle concepts, that were evaluated for the follow-on project – the prototype Thorium High Temperature Reactor (THTR-300). The THTR-300 was designed for the HEU U/Th fuel cycle only, with ~620,000 fuel spheres used in reactor operation and also achieved maximum burnups of ~150 GWd/t_{HM}.

A decisive step in the German HTGR fuel design was the move from BISO to TRISO coatings. The combination of an LTI inner and outer PyC layers surrounding a strong and stable SiC layer greatly improved manufacturing conditions and the subsequent contamination and defective particle fractions in production fuel elements. In addition, this combination provided improved mechanical strength and a higher degree of solid fission product retention, not previously known with HTI-BISO coatings. Irradiation stability and good irradiation performance of the mixed oxide (ThO_2+UO_2) fuel system was demonstrated.

In the USA, manufacture of the fuel for cores 1 and 2 of Peach Bottom Unit 1 was based on the HEU/Th fuel cycle comprising about 3500 kg of BISO coated, HEU (Th,U)C_2 particles assembled into more than 48,000 annular fuel compacts in cylindrical fuel elements. With regard to fuel fabrication for the Fort St. Vrain reactor, the six segments of the initial core consumed more than 800 kg of high-enriched ^{235}U and 15,000 kg of Th in 1482 fuel elements. Together with four reload fuel segments, a total of ~25,000 kg of thorium was processed for the production of 7.1 million fuel compacts with the fissile HEU (Th,U)C_2 kernels in a ratio of 1 to 3.6, and the fertile ThC_2 kernels. Both the fissile and fertile Particles employed LTI-TRISO coatings.

In the 1980s, the international nuclear non-proliferation policies eventually resulted in a change from HEU to LEU fissile fuel. As a result of this political decision, the development of thorium fuel fabrication and reprocessing efforts was stopped. The new focus of research activities was on questions of reactor safety and on waste treatment. In the USA, the new reference HTGR concept selected in 1981 remained based on the two-particle system, but now with a 350 µm diameter fissile UCO fuel kernel containing 19.9 wt% enriched uranium and a 500 µm diameter fertile UCO fuel kernel containing natural uranium. Furthermore, it was recommended that the reference HTGR fertile particles also employ a TRISO coating [Stansfield 1991, IAEA 1997].

In Germany, the development of HTGR fuel cycles with HEU/Th was terminated in 1980, after having decided to switch all HTGR fuel cycle efforts from HEU to a LEU cycle, with a pure oxide fuel. In an intermediate phase, work was done on a MEU/Th cycle as an alternative and back-up solution to HEU. Medium-enriched uranium is advantageous with regard to non-proliferation. Its design was selected with a ~20 wt% ^{235}U and with a heavy metal loading of 8 g per fuel sphere.

Within the German HTGR fuel program, the fabrication of HEU/Th fuel has been developed to a fully qualified process on an industrial scale. Of the seven experimental and prototype HTGR reactors that were or still are in operation, five gained valuable experience with thorium fuels. Estimated quantities of thorium that were employed in the manufacture of HTGR fuel are listed in Table 1.

Table 1. Thorium fuel used in high temperature reactors.

HTGR	**Thorium [kg]**
Dragon, OECD	~100
AVR, Germany	~1360
Peach Bottom, USA	~3500
THTR-300, Germany	~6400
Fort St. Vrain, USA	~26,500*

* The prismatic design of Fort St. Vrain requires much higher initial heavy metal loading than the pebble-bed design of THTR that has no burnable poisons and where the fissile loading is only gradually increased.

Renewed interest in thorium fuel for future reactors in Europe re-materialized in the PUMA Project of the EU 6th Framework Programme which investigated the use of thorium in a VHTR with particular emphasis on the Th/Pu cycle [Kuijper 2010]. Further studies employing the Th/Pu cycle have shown that a reduction in the ever increasing Pu reserves without producing significant new amounts of Pu.

But there are also some other nuclear reactor concepts which are well suited for being charged with thorium fuels. Heavy water cooled reactors, especially the advanced CANDU reactors exhibit an excellent neutron economy. The fissile driver fuel could be plutonium or even low-enriched uranium. Another concept appropriate for thorium fuel is the molten salt reactor which contains the fuel in form of fluorides as part of a salt mixture serving both as coolant and fuel carrier. In a chemical processing unit which is part of the primary circuit, fission products can be separated as well as the generated ^{233}U [IAEA 2012b].

2. $(TH,U)O_2$ TRISO COATED PARTICLE FUEL DESIGN

The High Temperature Gas-Cooled Reactor (HTGR) is characterized by an all-ceramic core structure with nuclear grade graphite being used for moderator, reflector, core support and primary fuel element material. The basic fuel is also a ceramic with a sequence of high-temperature ceramic-coatings surrounding a uranium oxide, carbide or mixed compound. The use of these refractory core materials combined with a single phase inert helium coolant permit high outlet coolant temperatures up to 950°C along with a high thermal efficiency. The selection of these materials provide several inherent safety advantages, including a low-power density reactor core with a large heat capacity and an inert coolant, not subject to phase changes, that can mitigate severe fuel consequences during loss-of-coolant accident scenarios.

Two concepts of the HTGR have been developed since the mid-1950s: (i) the pebble-bed concept; and (ii) the prismatic core concept. Both HTGR core concepts employ an all ceramic core, ceramic fuel and use helium as coolant, but differ substantially in the type of fuel elements employed by each.

- The pebble-bed HTGR [Schulten 1959, Schulten 1978] employs a spherical fuel element, 60-mm diameter, manufactured by a cold-isostatic molding process (Figure 3). This element is a two-part design with an inner 50 mm-diameter fuel zone surrounded by a 5 mm-thick fuel-free shell of graphitized fuel matrix material. The fuel zone contains the coated particles, overcoated with matrix material and then homogenously dispersed within the graphitized matrix. The pebble bed concept was initially pursued in Germany, Russia and later South Africa, and today China is where the pebble-bed HTGR is being developed.

- The prismatic-core HTGR [Fortescue 1965, Dahlberg 1969] employs fuel elements fabricated from nuclear-grade graphite machined into a hexagonal shape, ~800 mm-high by ~360 mm across-the-flats (Figure 3). Separate fuel and coolant holes are drilled into the graphite block with six fuel holes surrounding each coolant hole in a hexagonal pattern. Pre-fabricated fuel compacts, ~12.5 mm-diameter by ~50 mm long contain the over-coated fuel particle in a close-packed array, dispersed within a carbonaceous matrix. The fuel compacts are then stacked in the fuel holes. The prismatic core concept was initially pursued in the United States of America (USA), United Kingdom (UK) and Japan. Today, the traditional prismatic-core HTGR continues development in the USA and Russia, while in Japan, the prismatic concept takes the form of a Pin-in-Block design with a different fuel configuration and coolant path.

Although the fuel elements of the two HTGR core concepts differ substantially as shown in Figure 4, their basic fuel-containing unit - the coated particle - is essentially the same. Coated fuel particle development has been underway since the mid-1960s. Originally the coatings on particle fuel were designed to provide oxidation resistance for carbide fuel kernels in air. Since that time, the coated particle has developed into a sophisticated fission-product containment system that can operate at the relatively high temperature, high burnup environment of an HTGR. Each coated particle is a miniature fuel element with a ceramic kernel that contains fissile or fertile fuel material protected by a sequence of ceramic coating layers that perform specific design functions as will be explained below [IAEA 2010].

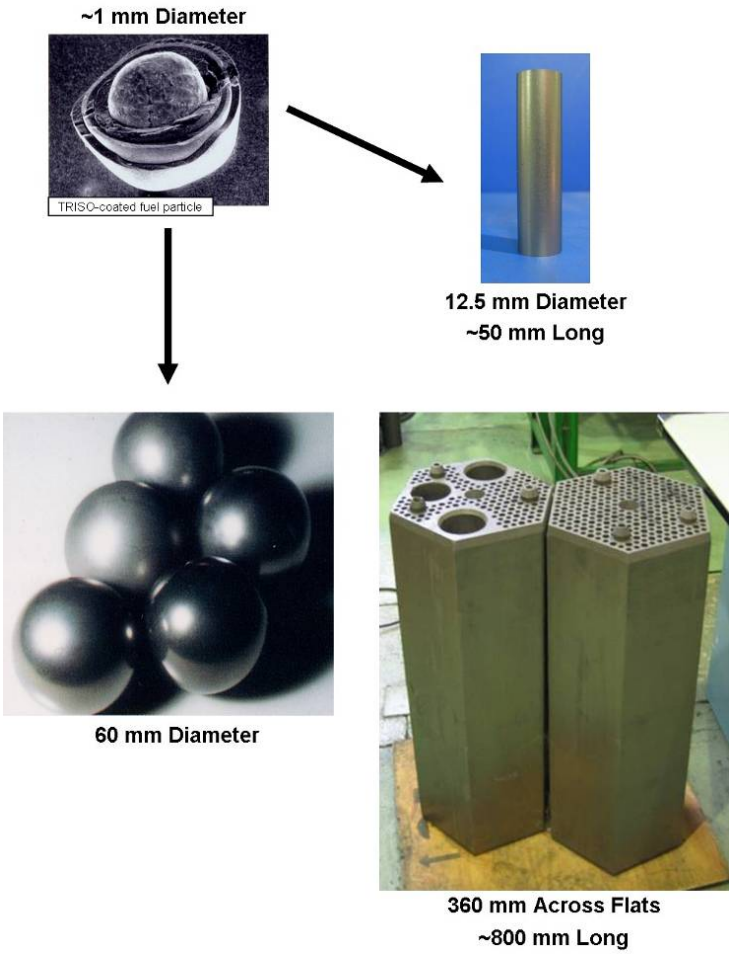

Figure 3. Fuel element designs for the pebble-bed core concept and the prismatic core concept.

The TRISO coated fuel particle, with a SiC layer sandwiched between two dense pyrocarbon (PyC) layers is generally accepted worldwide as the reference particle concept for today's HTGRs. The TRISO particle consists of a dense heavy metal spherical kernel of oxide, carbide or a mixture (oxy-carbide) enclosed within four successive ceramic coatings, as shown in Figure 4.

Research and development continues today on an international effort to further improve and extend the TRISO particle fuel performance envelope independent of differences in HTGR designs. To date, these R&D efforts have achieved various levels of success worldwide; however, one program - the HTGR Fuel Development Program undertaken in Germany, for nearly three decades until its termination in the mid-1990s, can be characterized as the most successful.

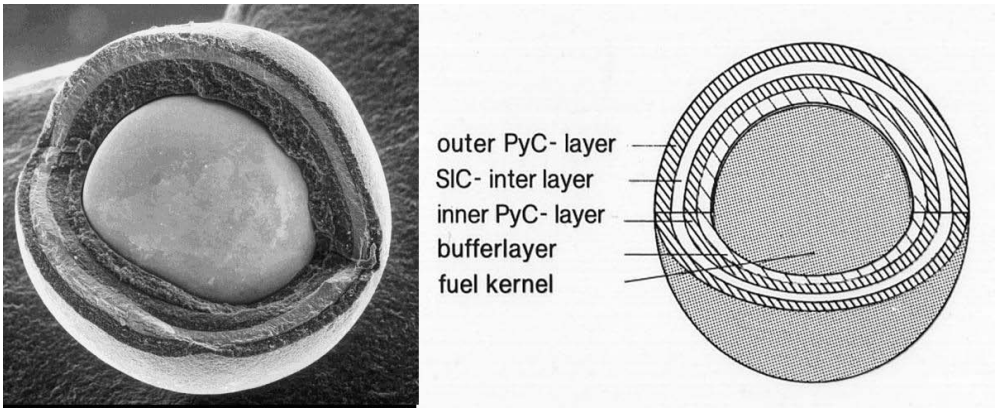

Figure 4. Scanning Electron Microscope image (left) and schematic (right) of a TRISO coated particle with an oxide kernel showing the pyrocarbon layers and the load bearing SiC fission product barrier.

The German HTGR Fuel Development Program, outlined in Table 2, successfully developed, licensed and manufactured many thousands of spherical fuel elements with high-enriched Uranium (HEU)-Thorium oxide (HEU $(Th,U)O_2$), HTI-BISO-coated fuel particles. This fuel type was used to power the experimental Arbeitsgemeinschaft Versuchsreaktor (AVR, 1967-1988) [Ivens 1990] and successfully licensed for the HTGR prototype Thorium-Hochtemperaturreaktor (THTR-300, 1986-1989) [Bäumer 1990]. By the mid-1970s, three fuel particle types were under development for the high-enriched uranium-thorium fuel cycle:

(i) high-enriched uranium (HEU) and thorium mixed oxide particle, $(Th,U)O_2$, with a 400 μm diameter fuel kernel surrounded by an HTI-BISO coating;

(ii) low-enriched uranium (LEU) oxide particle, UO_2, with a 500 μm diameter fuel kernel surrounded by an LTI-TRISO coating; and

(iii) two-particle (heterogeneous) system consisting of a HEU or LEU particle, UC_2 (UCO), in a 200 μm (300 μm) diameter fissile kernel, and a thorium containing particle, ThO_2, with a 500 μm diameter fertile kernel, both kernel types were surrounded by an LTI-TRISO coating.

The dense HEU $(Th,U)O_2$ fuel kernel was successfully used in the AVR and the THTR. Coupling this kernel material with an LTI-TRISO coating was eventually qualified for the PNP (Prototype Nuclear Process Heat) [Kugeler 1975] and the HHT (HTGR with Helium Turbine) [HHT 1977] HTGR concepts in Germany. Irradiation testing of the HEU $(Th,U)O_2$ TRISO particle system in real-time AVR tests and accelerated European Material Test Reactor (MTR) tests demonstrated the superior manufacturing process for this fuel and its excellent irradiation performance.

Table 2. Historical overview of irradiation tests conducted within the German Fuel Development Program.

R&D program	**Old LEU**	**HEU Program for process heat and gas turbine applications**			**LEU program**
	1972-76	**1977-1981**			**1982-2010**
Coated particle	UO_2 TRISO UO_2 BISO	**Variant 1** $(Th,U)O_2$ BISO	**Variant 2** $(Th,U)O_2$ TRISO	**Variant 3** UC_2 (UCO) TRISO + ThO_2 TRISO	UO_2 TRISO
Test goal					
Particle performance	HFR-M5 DR-S6	BR2-P24	BR2-P25	BR2-P23	HFR-P4 SL-P1
Fission product transport in intact particles	DR-S4	FRJ2-P22	FRJ2-P23	FRJ2-P24	FRJ2-P27
Release from kernel	–	FRJ2-P25	FRJ2-P25	FRJ2-P25	FRJ2-P28
Chemical effects	FRJ2-P16	–	–	HFR-P3	HFR-P5
Fuel element tests					
Fuel element performance	DR-K5	HFR-K1	R2-K12 R2-K13	R2-K12	HFR-K3
FE fission product transport	–	–	FRJ2-K11	FRJ2-K10	FRJ2-K13 FRJ2-K15
Large-scale demonstration	AVR 6	AVR 14 AVR 18	AVR 15 AVR 20	AVR 13	AVR 19 AVR 21
Proof test	–	–	–	–	HFR-K5 HFR-K6
High-burnup test	–	–	–	–	FRJ2-K15 HFR-EU1
High-temperature test	–	–	–	–	HFR-EU1bis

In the early 1980s another program direction change was made in Germany to a LEU UO_2 TRISO-coated particle system coupled with high-quality manufacturing specifications designed to meet new HTGR plant design needs. These needs included inherent safety under normal operation and all design-basis accident conditions. Once again, the German fuel development program met and exceeded these challenges by manufacturing, qualifying and licensing the LEU UO_2 TRISO-fuel system for the HTR-Modul design. The LEU UO_2 TRISO fuel design produced in this program is often referred to as 'modern HTGR fuel'. These fuel elements contain near defect free UO_2 TRISO coated particles, homogeneously distributed within a graphite matrix with very low levels of uranium contamination ($\sim 6\times10^{-5}$). The processes used to manufacture the LEU UO_2 TRISO fuel are being used worldwide (China, France, Korea, Japan, USA) to reproduce the German high-quality fuel of the 1980s.

The purpose of this document is to provide a reliable performance assessment for the HEU $(Th,U)O_2$ TRISO fuel system based upon the data generated in the German Fuel Development Program in the period 1977 to 1990. Data from the German program will be assessed in three primary areas: (1) fuel manufacture and quality control; (2) irradiation testing under normal operating conditions and post-irradiation examinations/analysis; and (3) accident condition testing on irradiated fuels.

The HEU-thorium fuel cycle was studied extensively in early HTGR development and considered the reference cycle from the beginning of HTGR development until the late 1970s. The primary advantage of this fuel cycle is the significant reduced consumption of natural uranium when operated in a closed cycle. The HEU-thorium cycle can potentially reach very high conversion factors and with ^{233}U recycling, significantly reduce natural uranium requirements. The competitiveness of the HEU-thorium fuel cycle today is questionable in several aspects: one in regard to the cost of thorium as the market for this material is nearly non-existent; second, the technical requirements for ^{233}U recycle in which fuel fabrication most likely would have to take place in remote, shielded hot cells; and finally, but most significantly, the use of HEU and ^{233}U and their associated problem of proliferation.

The HEU $(Th,U)O_2$ TRISO coated particle design was originally envisioned for advanced applications to nuclear process heat and direct-cycle electricity producing HTGR concepts – the so-called PNP (Prototype Nuclear Process Heat) and HHT (HTGR with Helium Turbine), Variant 2 in Table 2. From 1975 to 1980, this was the German reference coated particle fuel design. The LTI-TRISO coating provided a greater resistance to fast neutron damage than the previous HTI-BISO PyC coating design, and a significantly better fission product retention capability under the anticipated operating conditions of higher temperature, burnup and fast neutron fluence in the PNP and HHT concepts.

The $(Th,U)O_2$ TRISO-coated fuel particle consists of a dense HEU thorium oxide fuel kernel, with a Th:U mole ratio of 5:1 or 10:1 depending on the HTGR concept application, enclosed within four successive ceramic coatings of the TRISO coating. Each of these coatings have one or more design functions as outlined in the Table 3.

Table 3. Design functions of the ceramic coating layers of the TRISO coated fuel particle.

TRISO particle coating layer	**Design function**
Buffer (50% dense PyC)	Provides void volume for gaseous fission products and carbon-oxygen reaction products (CO, CO_2) released from fuel kernel Accommodates fuel kernel swelling Protects PyC and SiC layers from fission product recoil
Inner PyC (density ≥1.85 Mg/m^3)	Diffusion barrier to fission products, retain gaseous fission products Impermeable layer prevents Cl_2 from reaching kernel during SiC deposition, and prevents CO from interacting with SiC during irradiation Provides mechanical substrate for deposition of SiC layer Induces compressive stresses in SiC due to irradiation induced shrinkage
SiC (near theoretical density of 3.21 Mg/m^3)	Primary barrier to fission products, retains all gaseous and solid fission products at normal operating temperatures (< 1250°C) and in accidents up to 1600°C Load-bearing layer for particle
Outer PyC (density ≥ 1.85 Mg/m^3)	Creates compressive stress on SiC due to irradiation induced shrinkage Retains gaseous fission products Provides bonding layer with carbonaceous fuel element matrix

The first coating is a low-density, porous PyC layer, called the buffer, which provides void volume for the accumulation of gaseous fission products released from the fuel kernel, accommodates fuel kernel swelling, and serves as a sacrificial layer to attenuate fission fragments. The second coating is a high-density, isotropic PyC layer, called the inner PyC (IPyC). The IPyC is a gas-tight coating that protects the kernel from hot gaseous chlorine compounds during SiC deposition and provides a smooth substrate for SiC deposition. The IPyC also serves as a diffusion barrier to gaseous and metallic fission products, and during irradiation it shrinks and this contraction helps to reduce tensile stresses on the SiC. The third coating is a near theoretical density, isotropic SiC layer which serves as the pressure bearing component of the particle and the primary metallic fission product diffusion barrier. The fourth coating is another high-density, isotropic PyC layer, called the outer PyC (OPyC). This layer serves as a further diffusion barrier for gaseous and metallic fission products, and like the IPyC layer, it too contracts during irradiation helping to reduce tensile stress on the SiC. The OPyC also protects the SiC during particle handling and sphere/compact formation, and provides a bonding surface for the overcoating process.

The HEU (Th,U)O_2 TRISO coated particle batches of particular interest to this assessment are identified in Table 4. They were selected from the German database and have the highest degree of commonality with today's modern HTGR fuel processing capabilities. That means fuel types that employed fuel kernel aqueous, wet chemistry manufacturing processes and chemical vapor deposition (CVD) processes to produce the all ceramic TRISO coatings. Figure 5 shows a simulation of the significant variation in the packing fraction (number of particles per sphere) in the R2-K13 test elements with 20,050 particles, compared to the other fuel elements listed in Table 4 that contain either 10,480 or 10,660 particles. Despite the different appearance, no negative influence of particle density has been observed in the irradiation performance, presented in the analysis of MTR irradiations in Chapter 4.2.

Table 4. Four (Th,U)O_2 LTI-TRISO coated fuel particle batches of interest to this fuel performance assessment.

Particle batch	**(Th,U)O_2 kernel composition N=Th/^{235}U**	**Enrichment [^{235}U wt%]**	**Fuel kernel diameter [µm]**	**Irradiation tests**	**No. particles per fuel sphere**
EO 1607	5.01	89.57	494	BR2-P25* R2-K12 FRJ2-P23* FRJ2-K11 FRJ2-P25*	10,830
AVR XV BP-S1 (HT 150-160, 162-167)	5.00	92.46	500	AVR XV	10,480
EO 1674	10.02	89.01	496	R2-K13	20,050
AVR XX BP-S1 AVR XX BP-S2	4.97	92.39	495	AVR XX	10,660

* These irradiation tests contained non-reference fuel elements consisting of either coupons, cylindrical compacts, or cylinders extruded from a 20 mm-diameter fuel zone sphere.

The four specific (Th,U)O_2 LTI-TRISO particle batches all have similar characteristics such as fuel kernel diameter, enrichment, composition, and a TRISO coating design shown in Table 5. This particle is different from the earlier (Th,U)O_2 HTI-BISO particle design manufactured in large numbers for AVR and THTR and the UO_2 HTI-TRISO in Dragon and the UK, but is based on these prior experiences.

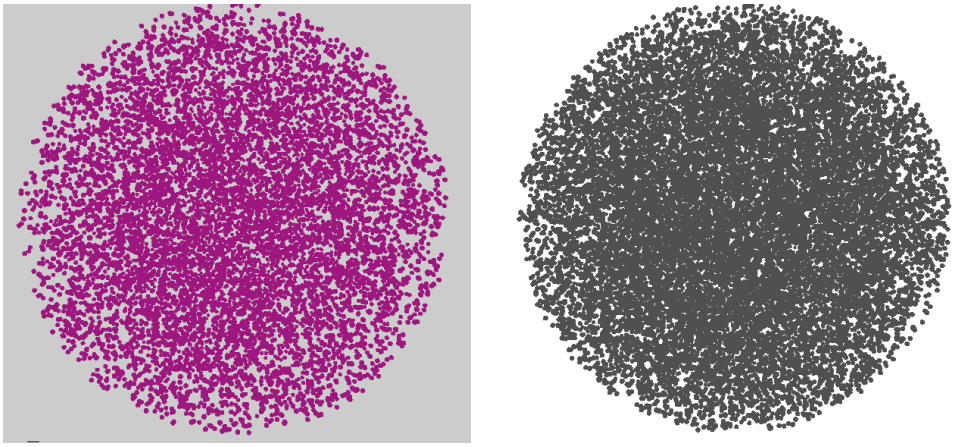

Simulation of 10,000 fuel kernels in a spherical fuel element as in R2-K12 and GO_2 balls

Simulation of 20,000 fuel kernels in a spherical fuel element as in the R2-K13 test elements

Figure 5. Spherical fuel elements with (Th,U)O_2 TRISO particles tested with two different packing fractions.

Table 5. Nominal dimensions of the (Th,U)O_2 LTI-TRISO particle design.

TRISO Particle Component	**Dimensions [µm]**
(Th,U)O_2 kernel diameter	500
Buffer layer thickness	90
IPyC layer thickness	40
SiC layer thickness	35
OPyC layer thickness	40

Collectively, these four batches of, high quality HEU (Th,U)O_2 TRISO coated particles were produced in full-size production facilities by the company NUKEM, GmbH., Germany. The particles were then fabricated into either: special irradiation test specimens and subsequently tested in six accelerated irradiation MTR tests (1978 through 1982); or 60 mm diameter reference spherical elements as part of two large AVR fuel element reload campaigns where ~20,900 elements were irradiation tested under a real-time HTGR environment in the AVR (1981 & 1985). A timeline for the in-reactor irradiation tests is shown in Figure 6.

Following irradiation, fuel specimens were carefully selected for destructive and non-destructive post-irradiation examinations and design basis accident simulation testing. Details of the (Th,U)O_2 TRISO fuel performance under irradiation and post-irradiation evaluations are provided in Chapter 4 of this document. Details of the design basis accident simulation tests and the (Th,U)O_2 TRISO fuel performance under these conditions are provided in Chapter 5 of this document.

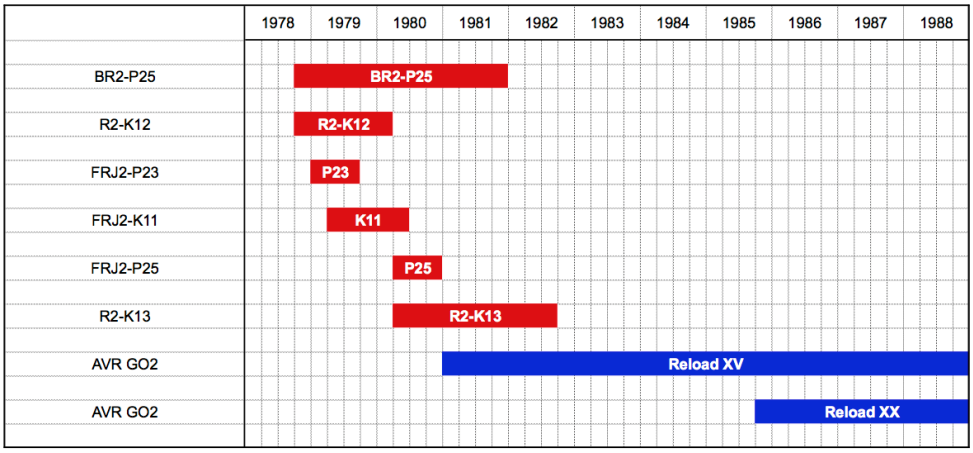

Figure 6. Timeline of irradiation tests in the period 1978-1988 containing HEU (Th,U)O_2 LTI-TRISO fuels in MTRs (red) and AVR (blue).

3. HTGR FUEL MANUFACTURE

3.1. Kernel Manufacture

Increasing quality and performance requirements favor wet chemical processes over dry agglomeration processes employed in the 1960s and early 1970s, and were used to produce fissile, fertile, and mixed oxide fuel kernels. The flow sheet described in Figure 7 represents the process used to produce the 500 µm-diameter HEU $(Th,U)O_2$ fuel kernels in the TRISO coating batches described in Table 4. Aqueous solutions containing uranium and/or thorium nitrate with additives are transformed into droplets by vibrating nozzles. In the kernel forming process shown in Figure 8, droplets pre-consolidate while falling through gaseous ammonia into an aqueous solution of ammonia.

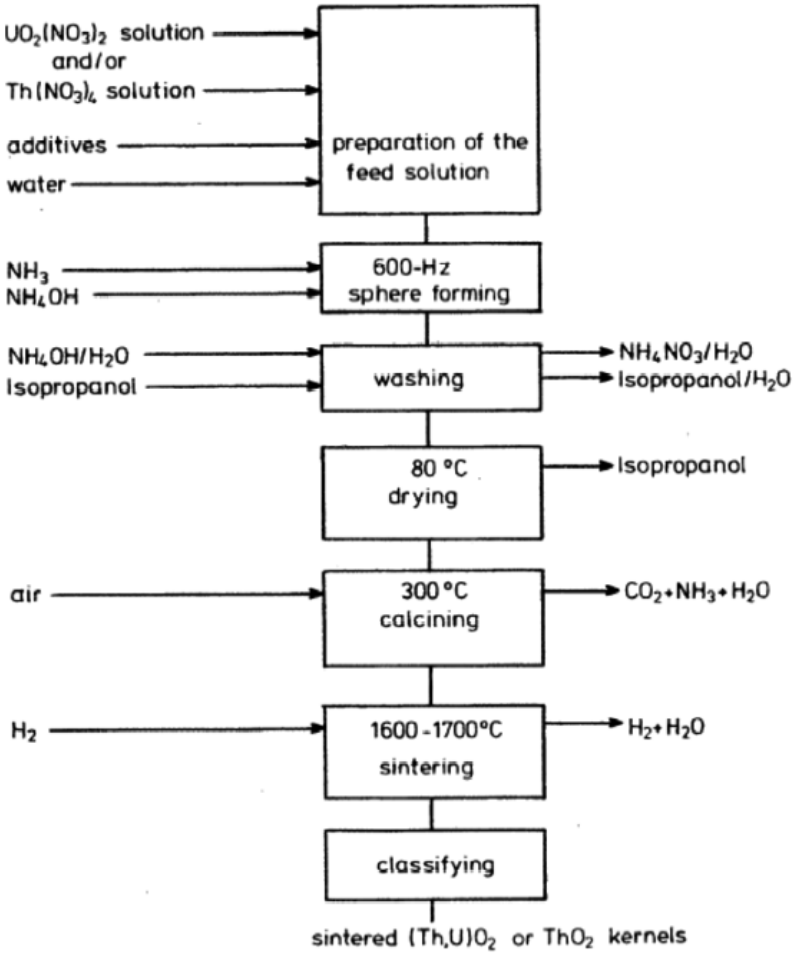

Figure 7. Flow sheet for sintered ThO_2 or $(Th,U)O_2$ fuel kernel manufacture.

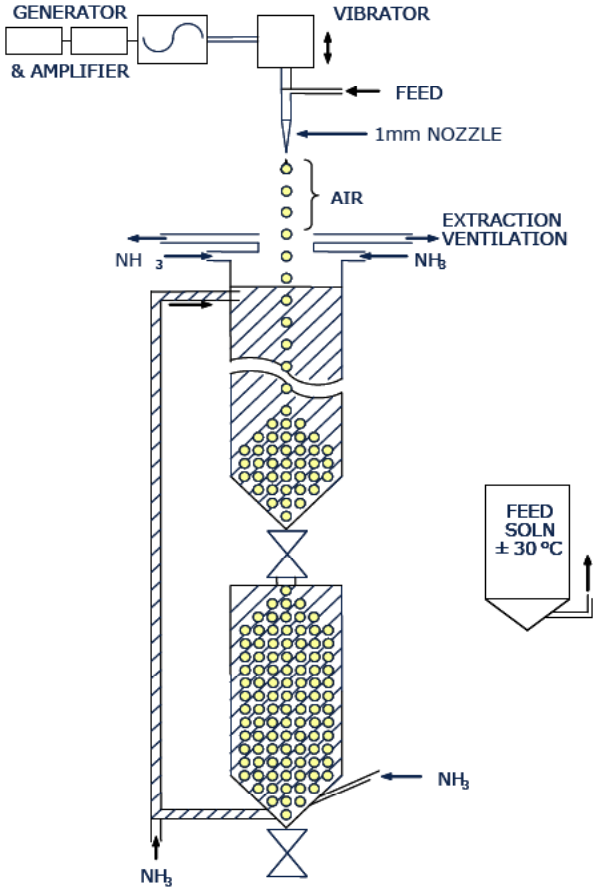

Figure 8. Schematic diagram of the German kernel casting process.

The reaction with ammonia produces thorium hydroxide and ammonium nitrate that is removed from the kernel in a subsequent washing step. The kernels are then dried, calcined and sintered to produce a dioxide kernel (or, reaction sintered to produce carbide kernels). Characteristics of the HEU $(Th,U)O_2$ fuel kernels produced with the process outlined in Figure 7 and used in the particle batches EO 1607, AVR XV BP-S1 (HT 150-160, 162-167), EO 1674 and AVR XX BP-S1 & BP-S2 are listed in Table 6. With the exception of the N-value (Th to ^{235}U ratio) of particle batch EO 1674, all of the kernel characteristics listed the four particle batches of interest are quite similar indicating a fabrication process that is stable and reproducible from kernel batch to kernel batch.

Table 6. Measured parameters for the HEU (Th,U)O_2 fuel kernels and their LTI-TRISO coatings of the four particle batches that are part of this fuel performance assessment.

	HEU (Th,U)O_2 LTI-TRISO particle batch characteristics			
	EO 1607	**AVR XV BP-S1 (HT 150-160, 162-167)**	**EO 1674**	**AVR XX BP-S1 / AVR XX BP-S2**
HEU (Th,U)O_2 kernel characteristics				
Kernel diameter				
mean [$\bar{x}$, µm]	494	500	495	495
standard deviation [$s_{\bar{x}}$, µm]	13.8	9.9	14.0	2 *
Enrichment [^{235}U wt%]	89.57	92.48	89.01	92.39 / 92.47
Density [Mg/m^3]	10.12	10.08	10.10	10.18
U content [%]	16.20	15.77	8.96	7.95 / 8.08
N-value (Th/^{235}U)	5.01	5.00	10.02	4.91 / 4.91
LTI-TRISO coating characteristics				
Buffer layer				
mean thickness [$\bar{x}$, µm]	85	91	89	94 / 100.2
standard deviation [$s_{\bar{x}}$, µm]	10.2	8.8	11.5	13.0 / 12.7
density [Mg/m^3]	1.09	n.m.	1.06	n.m.
IPyC layer				
mean thickness [$\bar{x}$, µm]	39	45	37	40 / 41
standard deviation [$s_{\bar{x}}$, µm]	3.5	4.6	3.0	4.5 / 3.0
density [Mg/m^3]	1.93	1.90	1.90	1.90 / 1.91
anisotropy (BAF_o)	1.030	1.018	1.029	1.04 / 1.03
SiC layer				
mean thickness [$\bar{x}$, µm]	37	33	33	35 / 35
standard deviation [$s_{\bar{x}}$, µm]	2.0	2.1	1.7	3.0 / 3.4
density [Mg/m^3]	3.20	3.20	3.19	3.20 / 3.20
defect fraction (burn-leach)	$< 0.4\times10^{-6}$	$< 2\times10^{-6}$	$< 2\times10^{-6}$	$< 2\times10^{-6}$
OPyC layer				
mean thickness [$\bar{x}$, µm]	39	39	39	39 / 39
standard deviation [$s_{\bar{x}}$, µm]	2.8	4.6	3.2	3.0 / 2.9
density [Mg/m^3]	1.93	1.91	1.90	1.91 / 1.91
anisotropy (BAF_o)	1.017	1.018	1.013	1.03 / 1.02

n.m. = not measured

* 2 µm is the value of the original Quality Control/Quality Assurance (QC/QA) document and has been confirmed by the acceptance inspection. However, the number appears unusually small.

3.2. TRISO Coating Technology

The process schematic [Huschka 1977] for the uninterrupted TRISO coating deposition is given in Figure 9. The four coating layers are deposited on kernels in a fluidized-bed coating furnace [Kadner 1977], Figure 10, in a process called chemical vapor deposition (CVD). Flowing gases forced into the furnace suspend the kernels so that they form a fluidized-bed. Coating gases were selected which decompose and deposit, at temperatures up to 1600°C, certain of their constituents onto the surfaces of the fuel kernels. The materials of the layers formed by this process are described as pyrolytic, because they are formed by pyrolysis (thermochemical decomposition) of an organic material, brought about by heat.

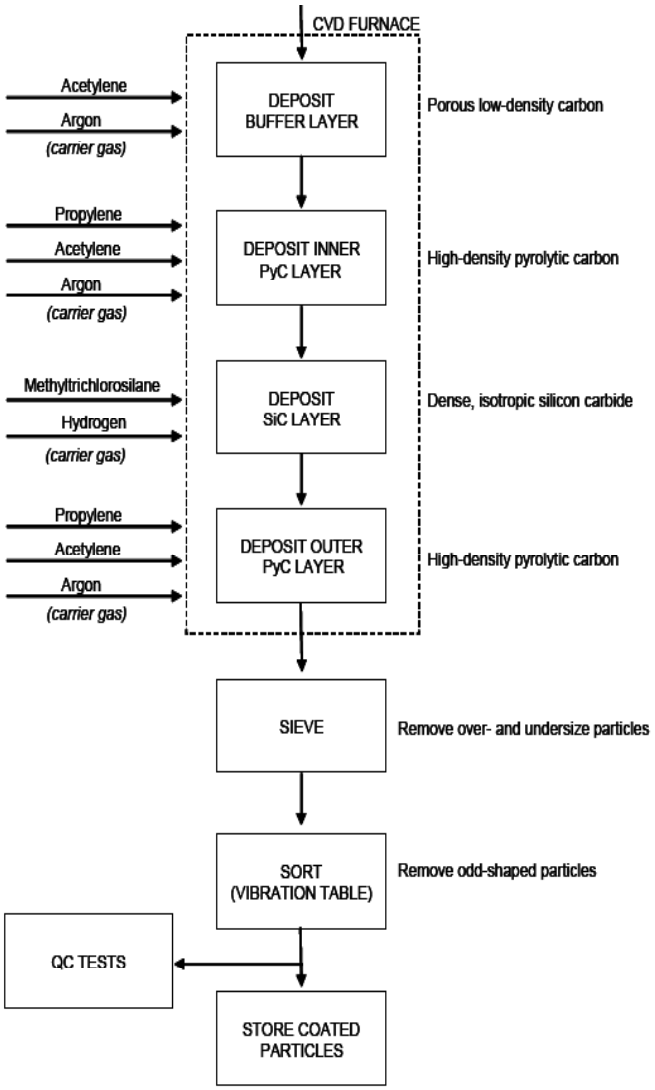

Figure 9. Flowsheet for the LTI-TRISO coating deposition process [IAEA 2012].

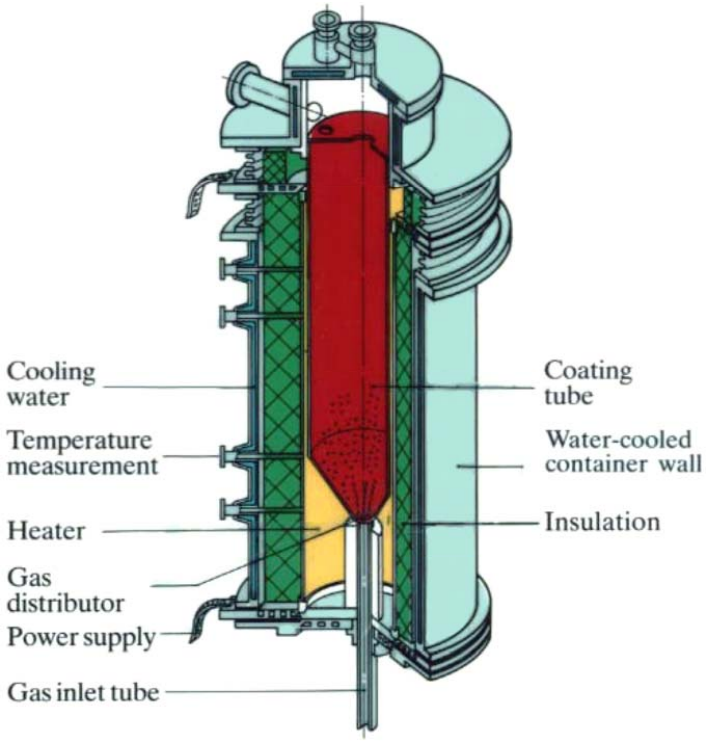

Figure 10. Schematic diagram of a high temperature fluidized-bed coating furnace used in HTGR fuel fabrication [IAEA 2012].

The process for depositing the four LTI-TRISO coating layers is as follows:

- Deposit a low-density, porous pyrocarbon (PyC) layer (the "buffer" layer) onto the fuel kernels by the decomposition of ethyne, C_2H_2, according to the reaction:

$$C_2H_2(g) \rightarrow 2\ C(s) + H_2(g)$$

- Deposit an inner, dense layer of isotropic pyrocarbon (IPyC) onto the porous PyC buffer layer by the decomposition of a mixture of propene, C_3H_6, and ethyne:

$$C_2H_2(g) \rightarrow 2\ C(s) + H_2(g)$$

$$C_3H_6(g) \rightarrow 3\ C(s) + 3\ H_2(g)$$

- Deposit a dense, isotropic layer of SiC onto the IPyC layer by the decomposition of methyltrichlorosilane, CH_3SiCl_3, according to the reaction:

$$CH_3SiCl_3\ (g) \rightarrow SiC(s) + 3\ HCl\ (g)$$

- Deposit an outer, dense layer of isotropic pyrocarbon (OPyC) on the SiC layer by the decomposition of propene and ethyne (similar to the inner dense layer).

Waste handling of the contaminated reaction product HCl during SiC deposition requires scrubbers and large filters be connected to the fluidized-bed furnace and represents a significant operational hazard. The addition of ethyne to the propene coating gas was to improve the heat balance during the deposition of PyC onto the surfaces of the spherical particles within the CVD fluidized-bed coating furnace. Nominal values of the key process parameters used to deposit the four layers that make up a LTI-TRISO coating are provided in Table 7.

Table 7. Typical processing parameters for the deposition of an LTI-TRISO coating onto a HEU (Th,U)O_2 fuel kernel.

Coating layer	**Decomposition gas**	**Carrier gas**	**Deposition temperature [°C]**	**Deposition rate [µm/min]**
Low density carbon	C_2H_2	Argon	1250	10
Inner dense isotropic PyC	Mixture of C_2H_2 and C_3H_6	Argon	1300	5
Isotropic SiC	CH_3SiCl_3	Hydrogen	1500	0.2
Outer dense isotropic PyC	Mixture of C_2H_2 and C_3H_6	Argon	1300	5

All four layers of the LTI-TRISO coating are deposited in an uninterrupted sequential process in the same fluidized-bed coating furnace. The conditions under which layer deposition takes place are very important as they determine the material properties of the coated particles formed. Parameters such as time, temperature, pressure, gas composition and gas ratios all play an important role in fixing the coated particle properties. The nominal layer thicknesses that were applied in the reference German HTGR HEU (Th,U)O_2 LTI-TRISO coated fuel particle design were listed previously.

Key material property requirements for good irradiation performance are for dense isotropic PyC layers:

- impermeable,
- isotropic texture, and
- deposited at low enough temperature to avoid heavy metal contamination;

and a good SiC layer:

- beta-SiC with a cubic structure of type 3C,
- density > 3.19 Mg/m^3,
- equi-axed microstructure with fine grains and few flaws,
- sufficient strength of PyC-SiC interfaces.

The characteristics of the TRISO coatings applied to the four HEU $(Th,U)O_2$ particle batches were listed in Table 6 along with the key $(Th,U)O_2$ kernel characteristics. All of the coating batches exhibit PyC coatings with typically high densities (close to the PyC theoretical density of 2.0 Mg/m^3), low anisotropy (illustrated by BAF_o values close to 1.000) and thicknesses close to the nominal values listed in Table 5. Similarly, the SiC layers in each of the batches have thicknesses close to the nominal value of 35 μm, densities ≥ 3.19 Mg/m^3, and SiC defect fractions, as measured by the burn-leach procedure, typically in the low 10^{-6} range. The similarity from coating batch to coating batch are indications that the deposition process, outlined in Figure 9, together with adherence to strict process control of the conditions listed in Table 7 results in a consistent, reproducible TRISO coating from coating batch to coating batch.

Ceramographic sections [Gontard 1981] of one particle from coating batch EO 1607 in one of the R2-K12 fuel elements are shown in Figure 11. These ceramographic sections are typical for the HEU $(Th,U)O_2$ LTI-TRISO fuel particle design of this performance assessment.

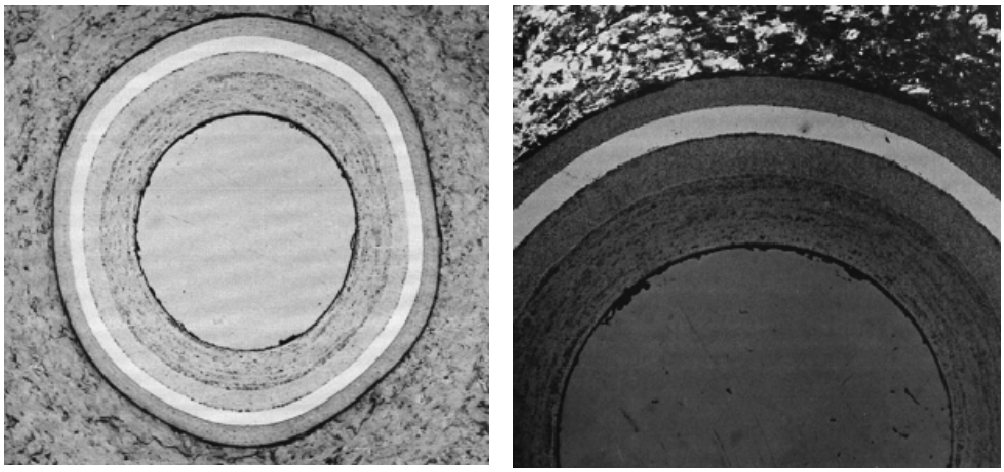

x100, normal light x200, polarized light

Figure 11. Single particle from coating batch EO 1607 photographed in bright (left) and polarized (right) light. Photographs taken from ceramographic section of companion spherical fuel element manufactured for irradiation test R2-K12 [Gontard 1981].

The final production steps are sieving to remove any under- and over-sized particles, followed by sorting to remove any odd-shaped particles. Sorting is performed on a vibrating table that is slightly inclined to allow spherical particles to roll down-hill following a parabola while odd-shaped particles are vibration transported along a perpendicular direction and collected for recycling.

3.3. Fabrication of Spherical Fuel Elements for Pebble-Bed HTGRs

The fabrication process for HTGR spherical fuel elements, described in the flowchart of the individual fabrication steps in Figure 12 was developed and improved by the NUKEM company. A pictorial display of the same process is provided in Figure 13. The primary steps in spherical fuel element processing are:

- resinated graphitic matrix powder preparation;
- overcoating of particles;
- pre-molding of fuel zone;
- high-pressure isostatic pressing of the complete fuel element;
- machining;
- carbonization at 800°C; and
- final heat treatment at 1900-1950°C.

This same or nearly similar spherical fuel element fabrication process has been used in the past in Russia and South Africa, and is currently being employed in China for fabrication of reference 60 mm diameter fuel elements for the HTR-PM concept.

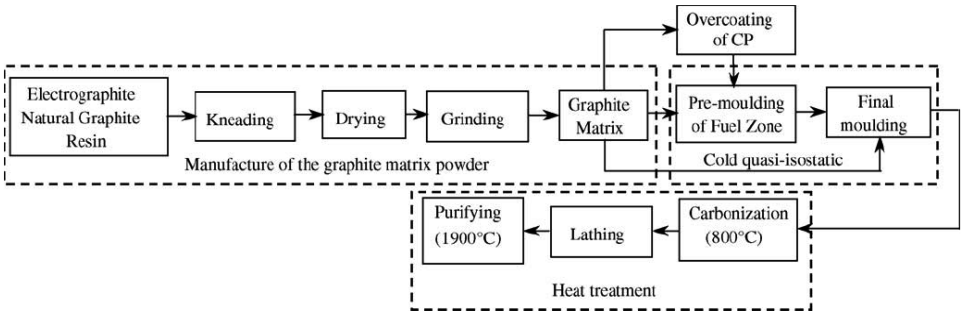

Figure 12. Flow chart of individual processes involved in spherical fuel element fabrication [Zhao 2006].

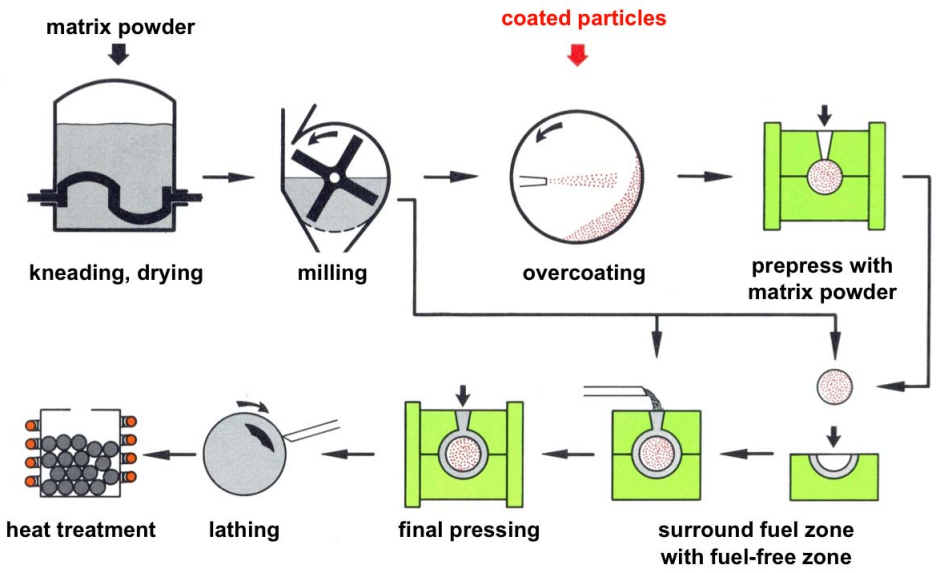

Figure 13. Pictorial flowchart of the German fabrication method for spherical fuel elements [Hrovat 1973, Hrovat 1988].

3.3.1. Preparation of Resinated Graphitic Matrix Powder

Two types of matrix graphite [Schulze 1982] designated A3-3 and A3-27 were developed by the NUKEM company for spherical fuel element production in Germany. The composition and fabrication differences between the two matrix types are illustrated in Table 8. Both matrix types are based on the same filler components – natural graphite and artificial electro-graphite. The primary difference is in the type of binder employed and how it is processed or synthesized. In general, the matrix graphite for spherical fuel elements consists of ~64% natural graphite, ~16% electro-graphite powders, and ~20% phenol resin binder.

The manufacturing process for the graphitic matrix powder is the following seven step process:

1. Natural graphite and electro-graphite powders are mixed in a four-to-one ratio in a conical mixer.

2. Depending on the type of matrix required, either A3-3 or A3-27, the binder materials are added in different manner and the binder is synthesized differently:

    a. standard A3-3 matrix, a phenolic resin is dissolved in alcohol (Methanol) to form the binder in a separate process step, added to the natural- and electro-graphite powders and then the mixture homogenized. This mixture is then fed into a kneading machine.

b. A3-27 matrix, all of the raw materials – the natural and electro-graphite powders, are warm-mixed together with the binder components – phenol and hexamethylenetetramine at a temperature of ~130ºC and where the binder synthesized. This process eliminates the need for kneading and steps 3 and 4 below.

3. The paste-like mixture is extruded through a punched screen creating strings that are cut into small pieces.

4. These small pieces are placed in drying trays which are heated to approximately 100°C.

5. The graphitic mass is then transferred into a hopper that feeds a hammer mill used to grind the material into powder of the desired grain size.

6. The dried graphitic mass is transferred into a hopper that feeds a hammer mill used to grind the material into powder of the desired grain size.

7. The milled powder is homogenized and ready for pressing.

Table 8. Composition and fabrication parameters for the two types of graphite matrix materials used in spherical fuel element fabrication.

Material and fabrication	**Standard matrix A3-3**	**Matrix with synthesized resin A3-27**
Composition of raw materials [wt%]:		
natural graphite	64	62.4
petroleum coke graphite	16	15.6
resin binder	22	22.0
Binder	Phenolic resin pre-fabricated from phenol and formaldehyde	Resin synthesized from phenol and hexamethylenetetramine during matrix formation
Moulding method	Quasi-isostatic cold moulding	
High-temperature treatment [°C]		
fuel elements	1800 or 1950	1950
fuel-free matrix spheres	1800	1950

* for AVR fuel elements: A3-3 and A3-27, for THTR fuel elements: A3-3.

The two resin binders exhibit differences in regard to the binder type and cross-linking. The phenolic resin binder used for the standard A3-3 matrix graphite is thermoplastic and the polymers are cross-linked primarily two dimensionally. In the A3-27 matrix material, the binder synthesized from phenol and hexamethylenetetramine is duroplastic and the polymers are cross-linked primarily three-dimensionally. Thus, the binder cokes formed from the resin binders during the carbonization and heat treatment processes are of different structure.

The material properties of the two fuel matrix types are provided in Table 9. A comparison of the data on the standard A3-3 matrix shows an improvement in the corrosion rate with the higher 1950ºC heat-treatment compared to the lower 1800ºC heat-treatment data. The falling strength and corrosion rate data for the A3-27 matrix material are significantly higher than those of the standard A3-3 at the higher heat-treatment temperature of 1950ºC.

3.3.2. Overcoating the TRISO particles

Overcoating of the TRISO particles takes place in a rotating drum as shown in Figure 14. The photograph on the left is the old manual overcoating drum that was used at the NUKEM company in the production of the HEU (Th,U)O_2 TRISO coated particles that are the subject of this performance assessment. The photograph on the right is a relatively new, automated overcoating facility located at the Institute of New and Nuclear Energy Technology (INET), Tsinghua University, China [Liang 2010].

Figure 14. Old manual overcoating drum that was used by NUKEM in the production of the HEU (Th,U)O_2 TRISO coated particles (left); new automated overcoating facility used at present by INET in the production of LEU UO_2 TRISO particles (right).

The purpose of the overcoating is to prevent direct particle-to-particle contact which may induce cracking of the particle coating layers during sphere formation. The overcoating is ~200 µm thick on the rigid TRISO coated particles and of the same composition as the fuel element graphite matrix. The dry resinated graphitic matrix material and a solvent are added simultaneously into the rotating drum in order to maximize adherence and obtain a uniform thickness. The moist overcoated particles are then dried at ~80°C to remove any of the remaining solvent. The dried overcoated particles are sieved to select the proper sized particles within the range of 1.1 mm and 1.5 mm and are once again sorted on an inclined vibrating table to remove oddly shaped, twin, or non-spherical overcoated particles.

Table 9. Material properties for the two types of graphite matrix used in the fabrication of spherical fuel elements [Hrovat 1973, Schulze 1982, IAEA 2012].

Property		**A3-3**		**A3-27**	**Generic specification**
heat-treated @		1800°C	1950°C	1950°C	
Carbon mass [g]		n.a.	n.a.	n.a.	≥ 190
Geometrical density [kg/m^3]		1700	1730	1740	≥ 1700
Young's modulus [10^4 kN/m^2]	∥	1020	1000	1070	n.s.
	⊥	991	970	1020	
Thermal expansion coefficient 20–500°C [10^{-6}/K]	∥	2.80	2.89	2.43	≤ 5
	⊥	2.92	3.45	2.69	
Thermal conductivity [W/(m·K)]					
@ room temperature:	∥	59	70	69	n.s.
	⊥	63	63	64	n.s.
@ 1000°C:	∥	38	41	44	≥ 30
	⊥	38	37	39	≥ 30
Specific electrical resistance [10^{-3} Ω cm]	∥	1.56	1.46	1.43	n.s.
	⊥	1.60	1.48	1.48	n.s.
Falling strength (# falls from height of 4 m onto A3-3 spheres until fracture)		521	437	652	≥ 50
Corrosion rate (@ 1000°C, 0.1 MPa in helium with 1 vol.% H_2O over 10 h [mg/(cm^2·h)])		1.19	0.97	0.73	≤ 1.5
Abrasion [mg/h per sphere]		1.81		2.89	≤ 6
Anisotropy factor		1.19			≤ 1.3
Crushing strength [kN]	∥	24.9		23.7	≥ 18
	⊥	23.1		26.3	
Impurities [µg/g]		60 (S:36; Si:6)		32 (Cl:16; Ca:7)	
Ash		50		30	≤ 300
B equivalent		–		–	≤ 1.3
Li		–		–	≤ 0.05

∥ = parallel, ⊥ = perpendicular to equatorial plane of matrix sphere; n.a. = not applicable; n.s. = not specified

3.3.3. Molding and Pressing of Fuel Spheres

The fuel spheres are manufactured by quasi-isostatic pressing at room temperature using silicon rubber molds. The pressing operation consists of taking overcoated TRISO particles together with graphite matrix powder and molding them in a pre-pressing operation to form the internal fueled spherical zone, ~50 mm diameter. Then additional matrix material is added to form the fuel-free shell, ~5 mm thick, around the fueled core using a final high pressure molding process.

Figure 15 is a photograph of the sphere pressing line, based on the NUKEM process that is currently in place at the INET at Tsinghua University in China. Figure 16 presents a photograph of silicon rubber molds for fuel spheres.

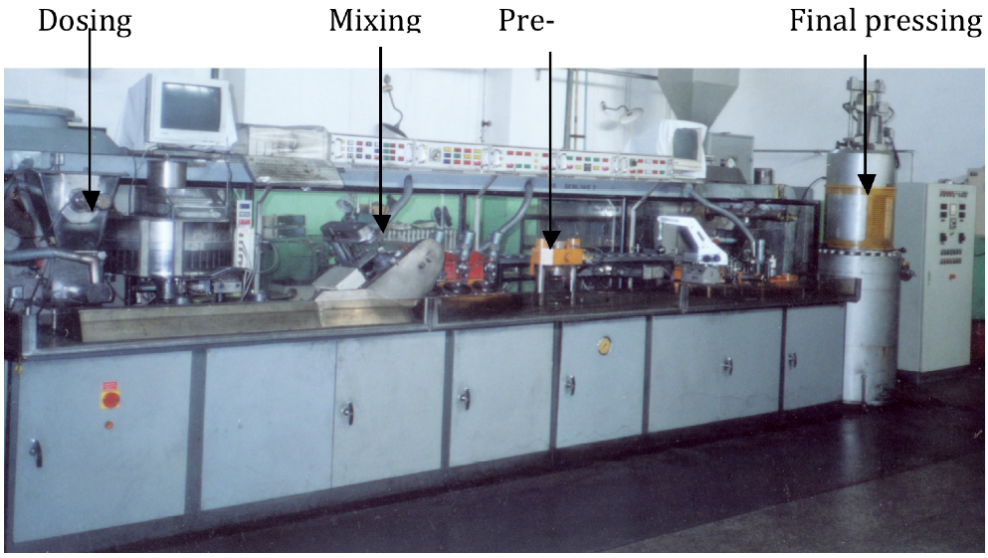

Figure 15. Molding and pressing line for green fuel spheres at the INET in China [Liang 2010].

The sphere molding and pressing process consists of the following steps:

- Combine overcoated particles with matrix graphite powder to form the fuel zone. The matrix graphite powder volume is carefully controlled along with the overcoated particle volume and the mixture is homogenized.
- The homogenized mixture is injected into the pre-pressing mold and pressed at ~5 MPa pressure.
- The pressed fuel zone spheres are then transferred into the final mold. The lower half of the final mold contains matrix graphite powder. The fuel zone sphere is placed into the center of the bottom mold and the second half of the mold is placed on top. More matrix material is added through a feeder tube to completely fill the internal annulus between fuel zone sphere and top final mold. Final pressing process is performed at ~300 MPa pressure.

Figure 16. Silicon rubber dies for fuel spheres [Heit 2001].

3.3.4. Lathing the Elements

After pressing, the green fuel spheres are transported to the lathing equipment where they are machined in a two-step process to obtain uniform spheres with specified dimensions.

3.3.5. Carbonization and Removal of Impurities

After machining, the spheres are heat-treated in two distinct processes; carbonization and annealing. In the carbonizing process, the green fuel spheres are heated to 800°C in an inert argon atmosphere furnace to carbonize the phenolic resin binder to provide strength. The annealing process is carried out under vacuum at a temperature range between 1800-1950°C for one hour to eliminate residual impurities in the matrix graphite. The upper 1950ºC final heat treatment temperature was used for all of the 60 mm diameter spherical elements that contain the HEU (Th,U)O_2 TRISO fuels that are part of this performance assessment. The switch to the higher 1950ºC temperature was made in the mid-1980s and remains the reference final heat treatment temperature today. Following a cool-down phase, the spherical elements are removed for inspection. This final heat treatment step is also important for the coated particle, and the strength and corrosion resistance of the sphere.

Photographs of X-ray images taken at different orientations illustrate the final pre-irradiation appearance and internal particle distribution within the fuel zone of the 60 mm diameter elements in experiment R2-K12, shown in Figure 17 for the example of the spherical fuel element in capsule 2. The element is sitting within a steel ring for the three images. Note that there are no coated particles located in the ~5 mm thick fuel-free zones that surrounds the ~50 mm diameter fuel zones.

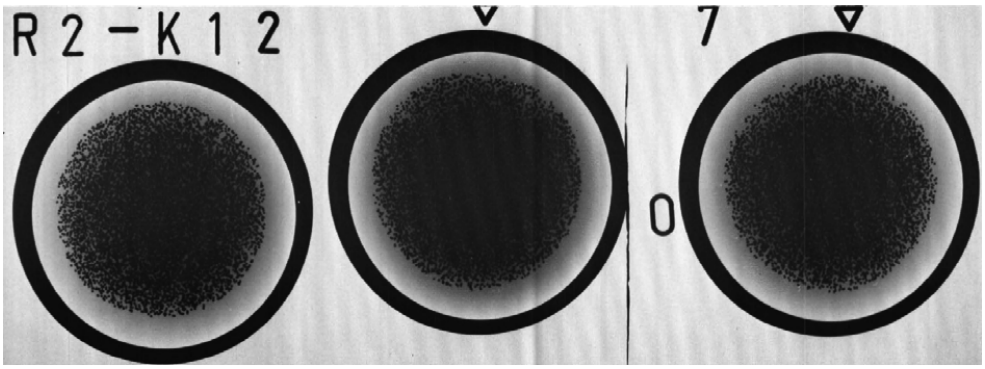

Figure 17. Photograph of the X-ray images taken at different orientations prior to irradiation of the spherical fuel element R2-K12/2 [Gontard 1981].

3.4 Quality Control and Characterization Data for Thorium Fuels

The German fuel qualification program fuel quality characteristics were specified in-detail and then proven by destructive and non-destructive examinations carried out under a statistically based Quality Assurance Program. This applied to all the raw materials, both the fuel kernels and the TRISO coated particles, and to the spherical fuel elements. Initial QC/QA procedures and techniques were developed for the HEU (Th,U)O_2 HTI-BISO fuel fabricated for the AVR and THTR where nearly 10^6 spherical fuel elements were manufactured and qualified. With improvements in the fuel development program and the subsequent quality level of advanced HTGR TRISO fuels, the QC/QA procedures were improved and updated to accommodate characterization and qualification of HEU (Th,U)O_2 LTI-TRISO and LEU UO_2 LTI-TRISO fuels. In their final manifestation as currently in-use today in China, the quality control procedures are outlined in Figure 18.

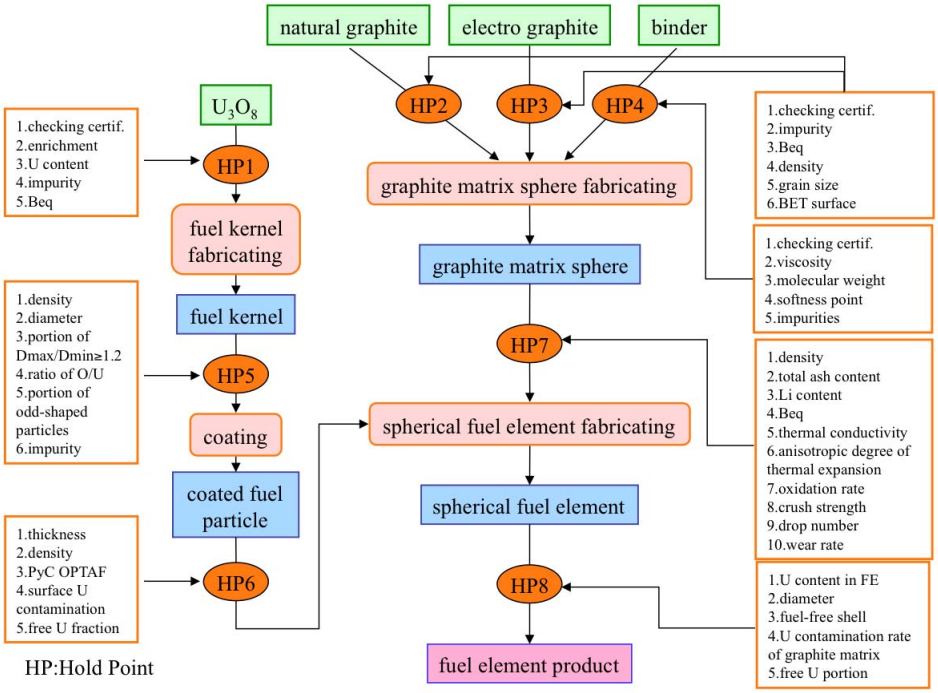

Beq= Boron Equivalent

Figure 18. Fabrication process and quality control diagram for modern TRISO fuel [Zhao 2006, Liu 2011].

The major characteristics examined and the standard testing methods which were established and used in Germany are presented in detail in [Delle 1976] and [Hantke 1992]. For reference 60 mm diameter spherical elements irradiated in three MTR experiments – R2-K12, R2-K13, and FRJ2-K11, and the ~17,940 elements irradiated in the AVR from two reloads – AVR XV and AVR XX, Table 10 contains the fuel particle and fuel element characterization data related to their manufacture. A full set of fuel element quality control data obtained on a statistically significant population of as-fabricated type GO2 elements containing HEU $(Th,U)O_2$ LTI-TRISO fuels for AVR Reloads XV and XX are given in Table 11.

Table 10. Fuel particle and fuel element characterization data related to the manufacture of reference 60 mm diameter spherical elements irradiated in MTR experiments and in the AVR from two reloads – AVR XV and AVR XX.

	R2-K12	**R2-K13**	**AVR XV & FRJ2-K11**	**AVR XX**
TRISO coating batch	EO 1607	EO 1674	AVR XV BP-S1 (HT 150-167)	AVR XX BP-S1 AVR XX BP-S2
$(Th,U)O_2$ kernel				
Diameter [µm]	494	495	500	495
N=Th/^{235}U	5.01	10.02	5.00	4.97 / 4.97
Enrichment [wt% ^{235}U]	89.57	89.01	92.48	92.39 / 92.47
Density [M/m^3]	10.12	10.10	10.08	10.18
Weight [µg]	639	645	660	646
Spherical Fuel Element				
Fuel matrix type	A3-27	A3-27	A3-27	A3-27
Final heat treatment temperature [°C]	1950	1950	1950	1950
Weight [g]				
^{235}U	1.002	1.020	1.000	1.000
U_{tot}	1.119	1.146	1.081	1.081
Th	5.021	10.221	5.000	4.97
$(Th,U)O_2$	6.983	12.931	6.918	6.885
Total element	203.2	207.9	200.4 – 201.0	201.7 – 203.6
Particles/FE (calc.)	~10,830	~20,050	~10,480	~10,660
SiC defect fraction*	$< 0.4\times10^{-6}$	$< 2\times10^{-6}$	$< 6.3\times10^{-5}$	$< 9.5\times10^{-6}$
Particle volume loading in fuel zone [vol%]	7.8	14.4	7.5	7.6

* R2-K12, R2-K13 SiC defect fraction from burn-leach on TRISO fuel particle batches;
AVR XV, AVR XX SiC defect fraction data from burn-leach on as-fabricated spherical elements.

Table 11. Fuel element quality control data for GO2 Spheres with HEU (Th,U)O_2 LTI-TRISO particles in AVR Reloads XV and XX.

				AVR XV				AVR XX					
				Lot#1	**Lot#2**	**Lot#3**	**Lot#4**	**Lot#1**	**Lot#2**	**Lot#3**	**Lot#4**	**Lot#5**	**Lot#6**
Number of spheres				1600	1600	1600	1450	2000	2000	2000	2000	2000	2000
Property	**Test frequency**	**Specif ication**											
Density [Mg/m^3]	5 per lot	–	mean*	1.75	1.75	1.75	1.74	1.74	1.74	1.74	1.74	1.75	1.75
			σ	0.005	0.005	0.005	0.005	0.005	0.004	0.004	0.005	0.005	0.005
Thermal conductivity [W/(m·K)] @ 20°C	3 each per lot	to be recorded	x_{smin}	73	68	73	71	76	70	76	73	75	73
			x_{pmean}	75	70	76	78	79	75	81	77	78	76
Thermal conductivity [W/(m·K)] @ 1000°C		≥ 25	x_{smin}	33	36	37	43	33	32	34	35	35	34
			x_{smean}	35	37	37	44	34	36	36	35	36	36
			x_{pmin}	35	37	38	44	39	39	36	36	39	37
			x_{pmean}	36	38	38	45	40	44	41	37	42	42
CTE [µm/(m·K)] (0-500°C)	3 each per lot	to be recor ded	x_{smean}	2.60	2.56	2.42	2.45	2.58	2.49	3.15	2.77	2.85	2.67
			x_{pmean}	2.27	2.14	2.17	2.22	2.27	2.36	2.74	2.49	2.54	2.38
Anisotropy factor		≤ 1.3		1.15	1.19	1.12	1.10	1.14	1.06	1.15	1.11	1.12	1.12
Bending strength [MPa]	3 each per lot	to be recor ded	x_{smean}	25.0	24.7	24.4	24.7	26.0	26.8	27.3	26.6	26.7	27.5
			x_{pmean}	26.0	24.5	25.4	25.0	28.3	26.6	28.2	26.3	26.9	28.5

Dynamic E-modulus [GPa]	3 each per lot	to be recor ded	x_{smean}	10.1	10.2	10.2	10.2	10.6	10.7	10.5	10.5	10.5	10.7
			x_{pmean}	10.6	10.8	11.0	10.7	11.1	11.1	11.2	10.7	10.7	11.2
Specific electrical resistance [μΩ·m]	3 each per lot	to be recor ded	x_{smean}	14.9	15.0	15.0	15.1	14.3	14.3	14.4	14.4	14.3	14.2
			x_{pmean}	14.1	14.2	13.9	14.3	13.8	13.9	13.7	14.2	14.1	13.5
Drop strength (number of drops)	5 per lot	≥ 50	T_U	186	343	166	343	262	511	168	273	419	397
Crushing strength [kN]	5 per lot	≥ 18	T_U	25.92	22.39	18.20	20.63	24.00	21.80	24.20	23.70	25.10	22.30
Corrosion resistance [mg/(cm^2·h)] @ 900°C	3 each per lot	≤ 0.3	x_{mean}	0.07	0.06	0.06	0.06	0.10	0.10	0.09	0.11	0.11	0.10
Corrosion resistance [mg/(cm^2·h)] @ 1000°C		≤ 1.5	x_i	0.59	0.57	0.55	0.58	0.91	0.85	0.88	0.78	0.81	0.83
		≤ 1.0	x_{mean}	0.53	0.51	0.46	0.56	0.69	0.77	0.73	0.77	0.75	0.71
Burn-leach test [wt% of free U]	5-AVR15 or 4-AVR20 per lot	≤ 0.02	x_{mean}	0.002 0.001 0.001 0.001	0.002 0.024 0.001 0.001	0.001 0.015 0.001 0.001	0.002 0.001 0.001 0.001	< 0.001					
Abrasion [mg/h]	20 per delivery	≤ 6	x_{mean}	4.10	3.21	4.70	3.63	3.44					

* x_{smean}, x_{pmean}: "s" stands for "square (⊥)", and "p" stands for "parallel (∥)" to the grain; this is determined by the sphere pressing direction.

3.5. Burn-Leach Testing

One of the essential characterization techniques for quality assurance is the burn-leach testing of HTGR fuel. During a "burn-and-leach" test, the graphite of the sample to be measured (loose coated particles, spherical element, fuel compact or coupon) is burnt away in a combustion chamber at around 800°C in air down to the SiC layer of the coated particles. This process is complete when the sample weight remains constant which is ~90 hours for a spherical fuel element. The residual of ash and particles is treated with a nitric acid solution at 100°C and the amount of dissolved uranium and thorium analyzed. Since the SiC layer is corrosion resistant, the heavy metal found in the solution includes the natural U/Th content of the matrix material and the U/Th content of those particles with a defective SiC layer. Also particles with an incomplete coating will be identified. The test results are presented as the ratio (in percent) of the measured free uranium to the total uranium contained in the spherical element, U_{free}/U_{total}. The detection limit is typically at a level of $1\text{-}3\times10^{-6}$ depending on the U/Th content of the sample. This uncertainty is much lower than the heavy metal content of a single defective coated particle which is on the order of 60 to 104 µg.

Tables 12 and 13 contain the burn-leach results from the AVR type GO2 fuel elements with HEU $(Th,U)O_2$ LTI-TRISO particles from AVR Reload XV manufactured in the year 1978 and AVR Reload XX manufactured in the year 1983. Tables 14 and 15 show defect particle fractions in comparison to later AVR Reloads XIX and XXI, which contained the AVR types GLE3 and GLE4 elements, respectively. The AVR type GLE3 and GLE4 spherical elements were manufactured with LEU UO_2 LTI-TRISO particles in 1981 and 1985, respectively. All of the burn leach results are well suited for a modern, inherently safe, small modular HTGR. However, the extremely low burn-leach levels of AVR XX with the equivalent of zero defects and AVR XXI/2 with a defect fraction $\sim9\times10^{-6}$ are of the highest quality recorded for any HTGR fuel production campaign; unfortunately, the exact reasons why their quality levels are so spectacularly low are not known.

A graphical presentation of the number of defective particles per spherical fuel element as a function of the number of particles per fuel element obtained on statistical significant samples is displayed in Figure 19 for the AVR reload production campaigns evaluated. Based on the data show here, there is evidence of a step-change improvement in the spherical fuel element production with TRISO fuel particles and it occurred in the time period 1983-85, both for HEU $(Th,U)O_2$ and LEU UO_2 fuels.

Table 12. Free uranium fraction and the equivalent number of defective particles from 16 burn-leach tests conducted on as-fabricated fuel spheres from AVR Reload XV [Hauer 1978].

	AVR XV Lot #1	**AVR XV Lot #2**	**AVR XV Lot #3**	**AVR XV Lot #4**
Fraction of U_{free}/U_{total} from burn-leach [%]				
Sphere 1	0.002	0.002	0.001	0.001
Sphere 2	0.001	0.024	0.015	0.001
Sphere 3	0.001	0.001	0.001	0.001
Sphere 4	0.001	0.001	0.001	0.001
Number of defective particles				
Sphere 1	0	0	0	0
Sphere 2	0	3	2	0
Sphere 3	0	0	0	0
Sphere 4	0	0	0	0

Table 13. Free uranium fraction and the equivalent number of defective particles from 30 burn-leach tests conducted on as-fabricated fuel spheres from AVR Reload XX [Hauer 1983].

	AVR XX Lot #1	**AVR XX Lot #2**	**AVR XX Lot #3**	**AVR XX Lot #4**	**AVR XX Lot #5**	**AVR XX Lot #6**
Fraction of U_{free}/U_{total} from burn-leach [%]						
Sphere 1	< 0.001	< 0.001	< 0.001	< 0.001	< 0.001	< 0.001
Sphere 2	< 0.001	< 0.001	< 0.001	< 0.001	< 0.001	< 0.001
Sphere 3	< 0.001	< 0.001	< 0.001	< 0.001	< 0.001	< 0.001
Sphere 4	< 0.001	< 0.001	< 0.001	< 0.001	< 0.001	< 0.001
Sphere 5	< 0.001	< 0.001	< 0.001	< 0.001	< 0.001	< 0.001
Number of defective particles						
Sphere 1	0	0	0	0	0	0
Sphere 2	0	0	0	0	0	0
Sphere 3	0	0	0	0	0	0
Sphere 4	0	0	0	0	0	0
Sphere 5	0	0	0	0	0	0

Table 14. Evaluation of free uranium and defective SiC layers in German HEU (Th,U)O_2 TRISO (Tables 12 and 13) and LEU UO_2 TRISO [Nabielek 1990] fuel elements.

Designation of FE population	**AVR XV HEU**	**AVR XX HEU**	**AVR XIX LEU**	**AVR XXI LEU**	**AVR XXI/2 LEU**
Production year	1978	1983	1981	1983	1985
No. FE lots	4	6	14	11	8
No. FEs produced	6250	12,000	24,600	20,500	14,000
^{235}U enrichment [wt%]	92.5	92.4	9.8	16.7	16.7
N = Th/^{235}U ratio	5.00	4.97	–	–	–
Number of particles/FE	10,480	10,660	16,400	9560	9560
Evaluation of free uranium from burn-leach measurements					
Mean value [ppm]	34	< 10	51	43	8
Number of FEs tested in burn-leach	16	30	70	55	40
No. FEs with 0 part. defects	0	0	31	42	38
No. FEs with 1 part. defects	0	0	26	8	1
No. FEs with 2 part. defects	1	0	9	2	1
No. FEs with 3 part. defects	1	0	4	2	0
No. FEs with 4 part. defects	0	0	0	0	0
No. FEs with 5 part. defects	0	0	0	0	0
No. FEs with 6 part. defects	0	0	0	1	0
No. FEs with ≥7 part. defects	0	0	0	0	0
No. defect particles observed	5	0	56	24	3
Equivalent ppm U_{free} from the number of defects observed	30	0	49	46	8

FE = fuel element

Table 15. Burn-leach manufacturing statistics for all modern oxide TRISO fuels fabricated in AVR reload campaigns over the period 1977-1985.

Type		No. particles tested N	No. defective particles (n)	Expected defect fraction (= n/N)	Upper 95% limit defect fraction
HEU	AVR XV	167,680	5	3.0×10^{-5}	6.3×10^{-5}
	AVR XX	319,800	0	0.	9.4×10^{-6}
LEU	AVR XIX	1,148,000	56	4.9×10^{-5}	6.1×10^{-5}
	AVR XXI	525,800	24	4.6×10^{-5}	6.4×10^{-5}
	AVR XXI/2	382,400	3	7.9×10^{-6}	2.0×10^{-5}

* The upper 95% limit is obtained from the MS Excel function BetaInv(0.95, n+1, N+1-n).

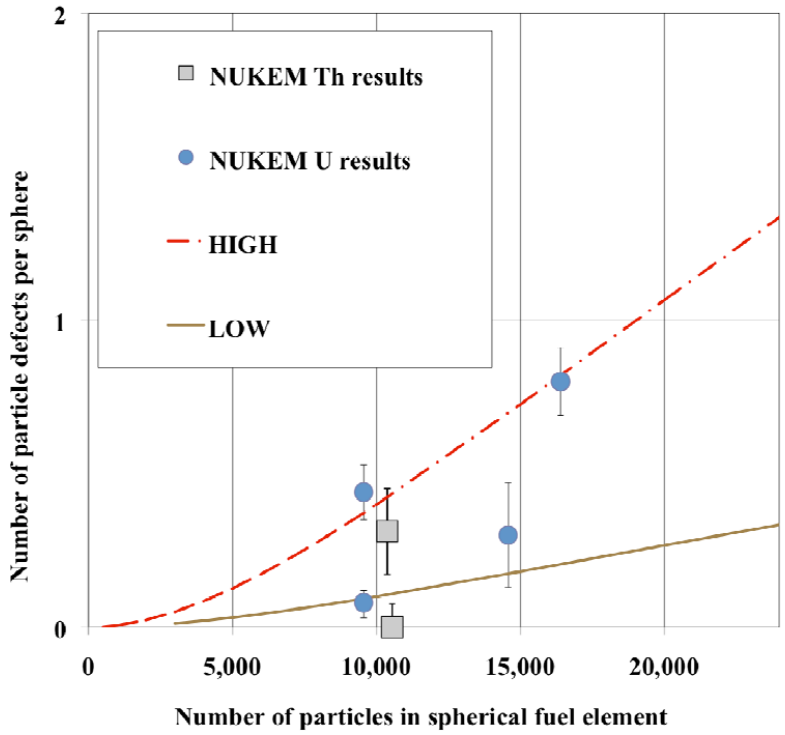

Figure 19. Equivalent TRISO coated particle defects per fuel sphere as a function of particles/element based on burn-leach test results.

4. IRRADIATION BEHAVIOR (NORMAL OPERATING CONDITIONS)

Within a fuel development program, irradiation testing of prototypical fuel specimens under the anticipated operating conditions of design HTGR concepts have been accepted methodology by which fuel performance data on candidate fuel systems have been obtained. This is an expensive, man-power intensive and time-consuming process. It requires extensive in-reactor and out-of-reactor remote test facilities along with a dedicated multi-disciplined team of material science experts. These experts must possess fundamental materials knowledge as well as knowledge of just how radiation affects properties, together with the experimental expertise to design/operate state-of-the instruments necessary to extract fuel performance data. Over a period of nearly four decades, the German program was able to put in place such expertise and successfully apply it to HTGR fuel development.

For the HEU (Th,U)O_2 TRISO fuel system in the period 1976 through 1985, a series of fuel irradiation tests were planned and executed on high quality fuels manufactured to well-defined specifications [Nabielek 1990]. The irradiation testing included accelerated tests in MTRs together with real-time testing in the HTGR environment of the AVR. Six multi-capsule MTR experiments (see Table 2) designated BR2-P25 (BR2 reactor, Belgium), R2-K12 (R2 reactor, Sweden), FRJ2-P23 (FRJ2 reactor, Germany), FRJ2-K11, FRJ2-P25, and R2-K13 were executed and evaluated [Burck 1988, Gontard 1990]. Small fuel lots of a variety of test specimens were fabricated by NUKEM for these MTR irradiation test capsules, including 60 mm diameter reference fuel elements, 20 mm diameter spheres, and cylindrical compacts. The two 60 mm diameter fuel elements FRJ2-K11/3 and /4 contained HEU (Th,U)O_2 TRISO fuel from the AVR XV reload campaign.

Two large-scale AVR fuel element reload campaigns, designated AVR XV and AVR XX, contained HEU (Th,U)O_2 TRISO and were produced in large numbers in production scale facilities by NUKEM. The fuel elements in these reload campaigns were designated as AVR GO2. Reload AVR XV contained 6087 elements and began AVR service in February 1981. Reload AVR XX contained 11,854 elements and began their AVR service in October 1985. Together these two campaigns contributed 17,940 elements. These fuel elements with the HEU (Th,U)O_2 fuels, with the exception of those removed for periodic sampling, remained in the AVR core until its shutdown in 1988.

4.1. Irradiation Envelope

All of the irradiation tests were carried out in the accelerated neutron environments of an MTR as compared to a real-time HTGR neutron environment like the AVR. The European MTRs utilized for the accelerated testing of HEU (Th,U)O_2 TRISO coated particles typically have higher thermal, epithermal and fast neutron fluxes than an actual HTGR. In these environments, fissile fuel burnups and accumulated neutron fluences can be achieved in one to two years, as compared to a typical four year cycle in an HTGR. Thus, the term "accelerated" refers to an irradiation under higher thermal and/or fast neutron flux environments for the purpose of speeding up the normal rate of fuel burnup and fast fluence accumulation. It is, however, important that target values for burnup, temperature and fluence are well covered. Indeed, this has been the case as is shown later in Table 17 and in Figures 21 and 22. The timeline for the German HEU (Th,U)O_2 TRISO coated particle testing program was shown previously in Figure 6.

Irradiation temperatures are typically maintained within the same operating range as expected in an HTGR. This is accomplished by incorporating an active temperature control system into the design of the irradiation tests, and together with stepped gas-gaps and precise tolerances on capsule internal components, it is possible to maintain fuel operating temperatures within the acceptable limits. Each independent capsule is swept with a variable mixture of helium and neon purge gas to compensate for the decrease in fission power throughout irradiation.

The radiograph in Figure 20 shows thermocouple penetrations through the top capsule bulkhead that reach into graphite cups holding the element in place. Each of the four independent capsules contain separate inlet and outlet gas lines that continuously circulates a Ne + He gas mixture to control irradiation temperatures. The gas mixture is different in each capsule depending on the desired temperature. By varying the composition of this gas mixture, the thermal conductivity of the purge gas located in the control gaps can be adjusted to maintain design temperatures. At times when the fission rate is high (high heat production), higher concentrations of helium gas (with a high thermal conductivity) are used. As fuel burnup increases, the fission rate in the fuel decreases and higher concentrations of neon gas (with a low thermal conductivity) are employed. In addition to active temperature control, internal thermocouples make it possible to monitor operating temperatures. Additional instrumentation, both active and passive, is generally included in each irradiation test to provide thermal and fast flux information and accumulated fast and thermal fluences.

The nominal maximum design operating conditions applicable to the process heat and direct cycle gas turbine HTGR concepts are shown in Table 16 [Vorreyer 1978]. The six MTR accelerated irradiation tests were patterned after operating requirements given in Table 17.

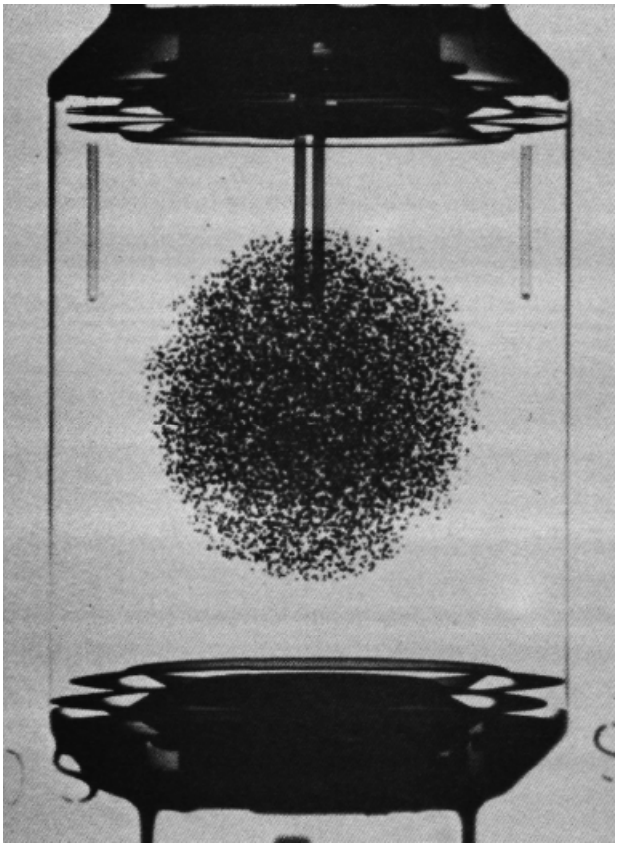

Figure 20. X-Ray image of the heavy metal kernels in a spherical fuel element built into one of the four capsules in the R2-K12 test rig prior to irradiation [Gontard 1981].

Table 16. PNP and HHT reactor operating requirements.

Operating parameter	**Nominal maximum for PNP and HHT**
Fuel element central temperature	1020°C
Fuel burnup	11% FIMA
Accumulated neutron fluence	4.5×10^{25} n/m^2 (E > 16 fJ)

Table 17 lists the corresponding operating temperature ranges, peak burnups and fast fluences for each of the independent test capsules that make up the six MTR irradiation experiments. In Figure 21, the nominal maximum expected PNP/HHT HTGR concepts limit of fast fluence versus temperature is compared with the accumulated fast fluence as a function of irradiation temperature for the six HEU $(Th,U)O_2$ TRISO fueled accelerated MTR tests. These same operational test data are numerically presented in Table 17.

Table 17. Accelerated MTR irradiation tests operating conditions for HEU (Th,U)O_2 TRISO fuel system in the German Fuel Development Program [Burck 1988, Gontard 1990].

Irradiation test/ specimen	Operating temperature range [°C]	Burnup range [% FIMA]	Fluence [10^{25} n/m^2, E > 16fJ]	^{85m}Kr release rate to birth rate Ratio (R/B)*	
				BOL	EOL
BR2-P25/					
1-12	1010 - 1070	13.9 - 15.6	6.2 - 8.1	3×10^{-7} *	1×10^{-6}
R2-K12/					
1	950 - 1100	11.1	5.6	3.9×10^{-9}	3.2×10^{-8}
2	1120 - 1280	12.4	6.9	3.5×10^{-9}	3.4×10^{-8}
FRJ2-P23/					
1	950 - 1200	11.3	1.1	$< 10^{-7}$ *	1.4×10^{-7}
2	1120 - 1200	12.5	1.4	$< 10^{-7}$ *	1.9×10^{-7}
3	1330 - 1600	11.9	1.4	$< 10^{-7}$ *	2.3×10^{-7}
4	1200 - 1400	12.1	1.1	$< 10^{-7}$ *	2.1×10^{-7}
FRJ2-K11/					
3	950 - 1166	9.0	0.062	1.7×10^{-9}	2.7×10^{-7}
4	940 - 1162	8.5	0.051		
FRJ2-P25/**					
2	850 - 1100	10.7	1.4	9.2×10^{-7}	1.5×10^{-5}
R2-K13/					
1	960 - 1170	10.2	8.5	2.2×10^{-9}	2.1×10^{-7}
4	750 - 980	9.8	6.8	1.5×10^{-9}	1.9×10^{-7}

* For this experiment, the short-lived fission gas ^{88}Kr is given.
** Included 1% defective particles

Test specimens irradiated in BR2-P25, R2-K12/1 and 2, and R2-K13/1 and 4 well-exceeded the nominal PNP/HHT maximum fast fluence limit and, with the exception of some specimens in R2-K13/4, these fluences were accumulated at operating temperature higher than the PNP/HHT maximum limit. For those specimens in FRJ2-P25/2 and FRJ2-P23/1, 2, 3, 4 the accumulated fast neutron fluences were in the mid to lower range of the PNP/HHT concept limit. For FRJ2-P25, these fluences were accumulated in the mid to upper range of the PNP/HHT temperature limit, but for FRJ2-P23, all of the capsules' operating temperatures were at or exceeded the PNP/HHT temperature limit, in parts massively so. Also, R2-K12/2 fuel element center temperatures were unusually high, but this did not lead to particle failure even at 12.4% FIMA and a fluence of 6.9×10^{25} n/m^2 (E>16 fJ).

For the spherical fuel elements irradiated in FRJ2-K11/3 and 4, the accumulated fluences were at the lowest range (< 0.1×10^{25}) of the PNP/HHT limits. This is due to the location of the fuel elements outside the core of the DIDO reactor where thermal flux is at a maximum and the fast flux is very low. However, these fluences were accumulated at operating temperatures at the high end or exceeded the PNP/HHT maximum temperature limit.

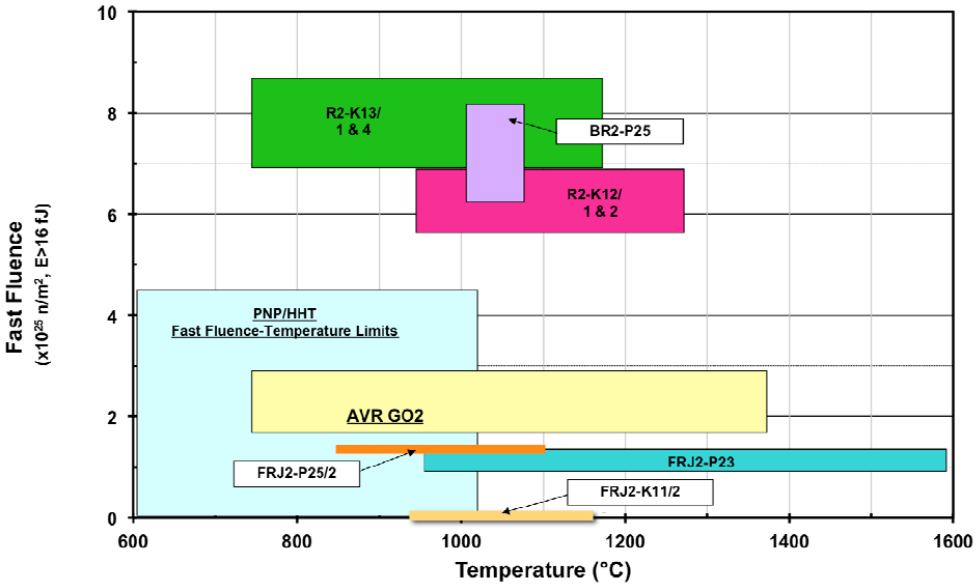

Figure 21. Accumulated fast neutron fluence vs. temperature for HEU (Th,U)O_2 TRISO fueled MTR accelerated irradiation tests compared to the PNP/HHT concept limits.

A comparison of the nominal maximum PNP/HHT HTGR concepts fuel burnup and operating temperature limits with those achieved in the six accelerated HEU (Th,U)O_2 TRISO fuel MTR irradiation tests is shown in Figure 22. Again, these data are numerically presented in Table 17. Test specimens irradiated in BR2-P25, R2-K12/1,2 and FRJ2-P23/1-4 achieved burnups above the nominal PNP/HHT concepts maximum burnup limit at operating temperatures well above the PNP/HHT maximum temperature limit. The specimens irradiated in FRJ2-P25/2 (with 1% defects added) achieved burnup above the nominal PNP/HHT maximum, but the operating temperatures ranged from the mid-range to above the PNP/HHT temperature limit. The fuel specimens in FRJ2-K11/3 and 4, and R2-K13/1 and 4 achieved burnups in the mid to upper range of the PNP/HHT burnup limits with operating temperatures near the upper or well above the PNP/HHT maximum temperature limits. For all of the fuel specimens containing HEU (Th,U)O_2 TRISO fuels, the nominal burnup maximum range achieved at EOL was from ~8.5 to ~15.2% FIMA over an operating temperature range from ~750 to ~1600ºC.

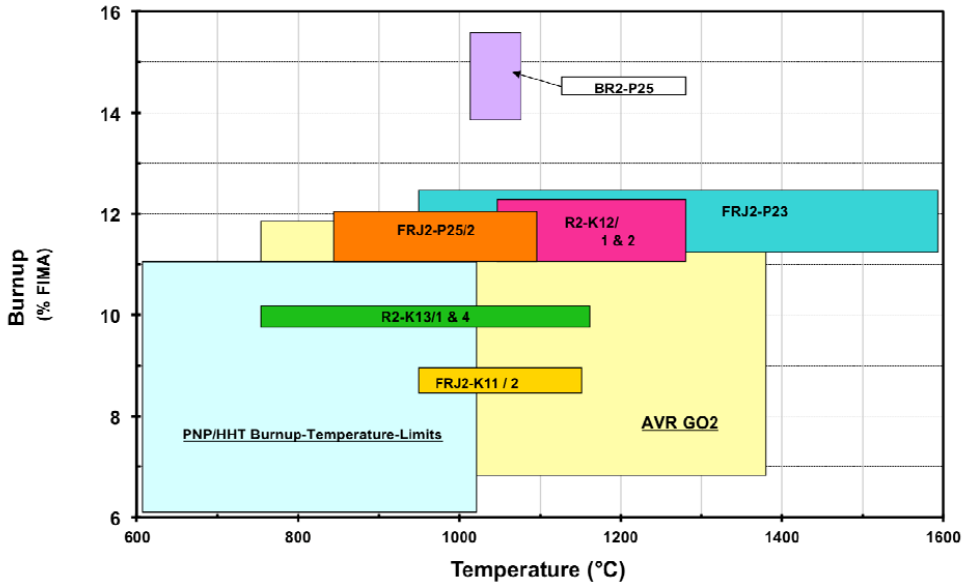

Figure 22. Fuel burnup vs. temperature for HEU (Th,U)O_2 TRISO fueled MTR accelerated irradiation tests compared to the PNP/HHT concept limits.

The presence of an active temperature monitoring system in each of the MTR accelerated tests made it possible to record temperatures and to measure the release rates of gaseous fission products from the fuel under irradiation. As the He + Ne purge gas exits the individual test capsules, a controlled volume sample is taken and gamma counted to quantitatively determine the quantity of short-lived noble gas fission products as a function of irradiation time. Knowing the sample volume, the purge gas flow rate at time of sampling, and the activity released allows a measure of the fission gas release rate (R_i) directly from the fuel particles. Typically the radioactive krypton and xenon isotopes of interest are ^{85m}Kr, ^{87}Kr, ^{88}Kr, ^{89}Kr and ^{133}Xe, ^{135}Xe, ^{137}Xe, and ^{138}Xe. By comparing the measured release-rate of an isotope to the birth-rate (B_i), determined through fuel depletion calculations as a function of time, the ratio $(R/B)_i$ can provide a direct measure of the steady-state release rate behavior of the fuel. This method of monitoring the fission gas release-rate to birth-rate has become the standard technique of assessing in-reactor fuel performance.

Table 17 also lists the beginning-of-life (BOL) and end-of-life (EOL) R/B values for the short lived ^{85m}Kr (4.48 hr) fission gas from experiments R2-K12, FRJ2-K11, FRJ2-P25 and R2-K13. For experiments BR2-P25 and FRJ2-P23, the short-lived ^{88}Kr (2.84 hr) fission gas BOL and EOL measurements are recorded. These measurements will be used later in this section to evaluate the in-reactor performance of the HEU (Th,U)O_2 TRISO particle fuels.

4.2. MTR Irradiation Tests & Analysis

4.2.1. Accelerated Irradiation Tests

The six accelerated irradiation tests designed to qualify the irradiation performance of the HEU (Th,U)O_2 TRISO coated fuel particles under normal operating conditions were carried out over the period from October 1978 to September 1982 [Burck 1988, Gontard 1990]. A description of the test specimens contained within each irradiation test along with the fuel particle population in each irradiation specimen test is presented in Table 18. A population of 131,947 HEU (Th,U)O_2 TRISO fuel particles was irradiated in these six reactor tests.

Table 18. Description of fuel specimens irradiated in MTR irradiation tests for qualification of German HEU (Th,U)O_2 TRISO particles.

Irradiation test (Dates) Duration	**Specimen / Contents**	**(Th,U)O_2 TRISO fuel batch**	**Particles per fuel specimen**	**Total number of particles**
BR2-P25 (10/78-12/81) 350 efpd	1-12/ 20 mm sphere each	EO 1607	1490	17,880
R2-K12 (11/78 – 2/80) 308 efpd	1, 2/ one 60 mm sphere each	EO 1607	10,830	21,660
FRJ2-P23 (1/79 – 9/79) 177 efpd	1-2/ three cylindrical compacts each 3-4/ three cylindrical compacts each	EO 1607 EO 1607	1707 2637	26,064
FRJ2-K11 (4/79 – 6/80) 260 efpd	3, 4/ one 60 mm sphere each	HT 150-160, 162-167	10,480	20,960
FRJ2-P25 (4/80 – 12/80) 187 efpd	2/ three cylindrical compacts with 17 defects per compact	EO 1607	1759	– *
R2-K13 (4/80 - 9/82) 517 efpd	1, 4/ one 60 mm sphere each	EO 1674	20,050	40,100
			MTR tests total	**126,664**

* Experiment FRJ2-P25/Capsule 2 inventory is excluded because it contained 1% intentionally defective fuel.

4.2.1.1. BR2-P25

The BR2-P25 irradiation test [Gontard 1990] was carried out in the BR2-Reactor (HFR) located in Mol, Belgium for 350 effective full power days (efpd) from 31 October 1978 to 10 December 1981. The irradiation of BR2-P25 was interrupted after the initial 40 efpd because of the need to change the beryllium reflector of BR2-reactor. This outage lasted nearly one and a half years and the experiment was re-inserted in mid-1980 and resumed the remainder of its irradiation. The primary objectives of this experiment were to investigate the particle failure mechanisms associated with the HEU (Th,U)O_2 TRISO particle design and to determine its failure rates under PNP/HHT irradiation conditions. Irradiation experiment BR2-P25 contained only one swept-gas capsule with 12 cylindrical fuel specimens stacked on top of each other. The specimens were numbered 1 through 12, beginning at the top. Each of the cylindrical compacts contained one 20-mm diameter fuel sphere at its center. The small spherical fuel specimens were manufactured with the HEU (Th,U)O_2 particle batch EO 1607 and the A3-27 graphite matrix. The irradiation specimens, initially fabricated as 60 mm diameter elements with a 20 mm diameter fuel zone, were machined to their cylindrical shape with the small diameter fuel zone at its center. Configuration data were presented in Table 18; in-reactor irradiation data were provided in Table 17 and are shown in Figure 23.

Extensive post-irradiation examination was carried out on the 12 irradiated fuel specimens from BR2-P25. Specimens #3 and #7 were electrolytically deconsolidated to obtain unbonded irradiated fuel particles. The fission product release fractions were determined on a select number of these particles using quantitative gamma spectrometry and sequentially crushing of the particle coatings down to the fuel kernel. The measured cesium fractional release (based on ^{134}Cs and ^{137}Cs release measurements) from the HEU (Th,U)O_2 was ~45% - 51% for the lower burnup/higher temperature specimen #3, and ~40% - 45% for the higher burnup/lower temperature specimen #7. The cesium release from the coatings was ~0.2% and from the compacts themselves $\leq$ 0.04%. The fractional release data for cesium (^{134}Cs and ^{137}Cs) from the HEU (Th,U)O_2 fuel kernel, TRISO coating and the specimen matrix are presented later in Table 22. The remaining unbonded HEU (Th,U)O_2 TRISO particles from both compacts were analyzed using the Irradiated Microsphere Gamma Analyzer (IMGA) System [Kania 1980] and discussed below.

A total of 1331 and 1291 particles were examined with the IMGA system from the two specimens BR2-P25/#3 and BR2-P25/#7, respectively. Comparisons of the absolute radionuclide activities between the gamma spectrometry measurements (IMGA) and the calculations (provided by FZJ Jülich) agreed to within ±8% for cesium and cerium and to within ±4% for the mean $^{137}Cs/^{144}Ce$ activity ratios. Of the 1331 particles examined from specimen BR2-P25/3, six were identified as failed based on cesium loss ($\leq$ 3 standard deviations of the mean $^{137}Cs/^{144}Ce \equiv$ failed particle). For the specimen BR2-P25/7, eight particles were identified as failed. A detailed examination of the isolated failed particles revealed that at least four had a portion of their TRISO coatings missing, and the remaining nine had no visible damage. This number of failed particles was larger than anticipated based on the EOL ^{85m}Kr R/B data and post-irradiation chlorine-leach measurements. No definitive failure mechanism was identified for the observed particle failures. The IMGA results for the two BR2-P25 particle populations are summarized later in Table 21.

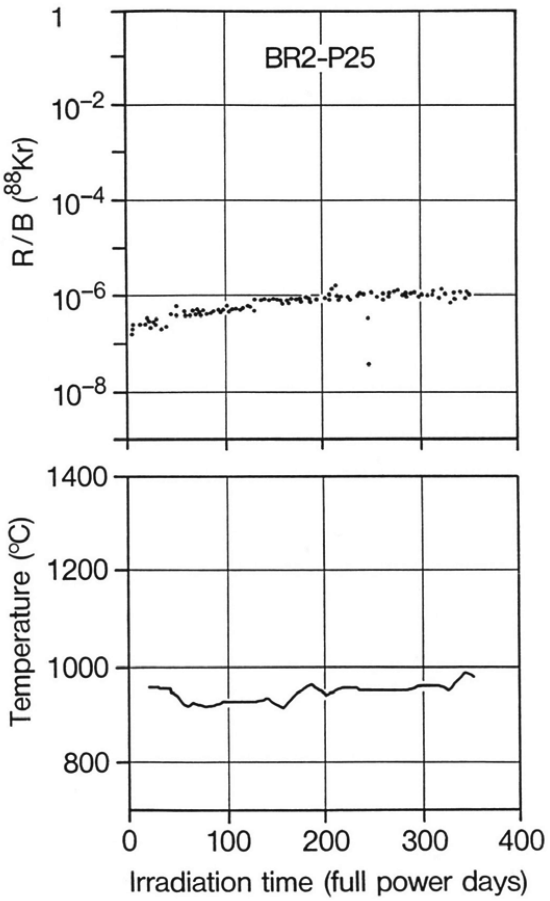

Figure 23. Gas release rates and mini-sphere surface temperatures BR2-P25 [Gontard 1990].

Eight of the 12 compacts in BR2-P25 (#1, #2, #4, #5, #8, #9, #11, and #12) were subjected to a hot chlorination test to measure the free uranium available in the compacts. This technique is useful in detecting failed or defective fuel particles. In compact #1, the ^{137}Cs inventory of one fuel particle was detected. Subsequent uranium isotopic analysis of the leach solution identified the particle as having a HEU $(Th,U)O_2$ fuel kernel of sufficient burnup to match BR2-P25 irradiation conditions. Only one failed particle was detected in the eight compacts examined. Collectively, one failure out of ~11,920 particles examined would yield a failure fraction of 4.0×10^{-4} at the upper 95% confidence limit. The remaining seven compacts contained only uranium contamination which was uncharacteristic for this experiment. This failure fraction measurement is significantly lower than that determined with the IMGA system, described above.

Ceramographic examination of fuel particles from compacts #4 and #8 showed evidence of radial cracks within the porous buffer layer, but no defective particle were found or any evidence of specific TRISO particle failure mechanisms.

4.2.1.2. R2-K12

The R2-K12 irradiation test [Gontard 1990] was carried out in the R2-reactor located in Studsvik, Sweden, for 308 efpd beginning 28 November 1978 and ending 12 February 1980. The objectives of this experiment were: to test the reproducibility of manufacturing processes used for fuel elements of Standard Quality 1977 on other German reference fuel variants; establish fuel performance under 3000 MW(th) process heat concept irradiation conditions; in-reactor LTI-TRISO coating performance; and fuel performance comparison between the HEU $(Th,U)O_2$ LTI-TRISO variant and the two-particle system – HEU UC_2 TRISO fissile/ ThO_2 TRISO fertile (Variant 3 in Table 2). Four 60 mm diameter spherical fuel elements were irradiated in four independently instrumented capsules of the R2-K12 test rig. The upper two capsules contained the fuel elements with the HEU $(Th,U)O_2$ TRISO fuel variant and the bottom two contained elements with the HEU UC_2 TRISO fissile/ThO_2 TRISO fertile variant. Fuel particle batch EO 1607 was used in the mixed oxide elements together with the A3-27 type fuel matrix. The R2-K12 configuration data for capsules 1 and 2 with mixed oxide elements were presented in Table 18 and the in-reactor irradiation data provided in Table 17 and Figure 24.

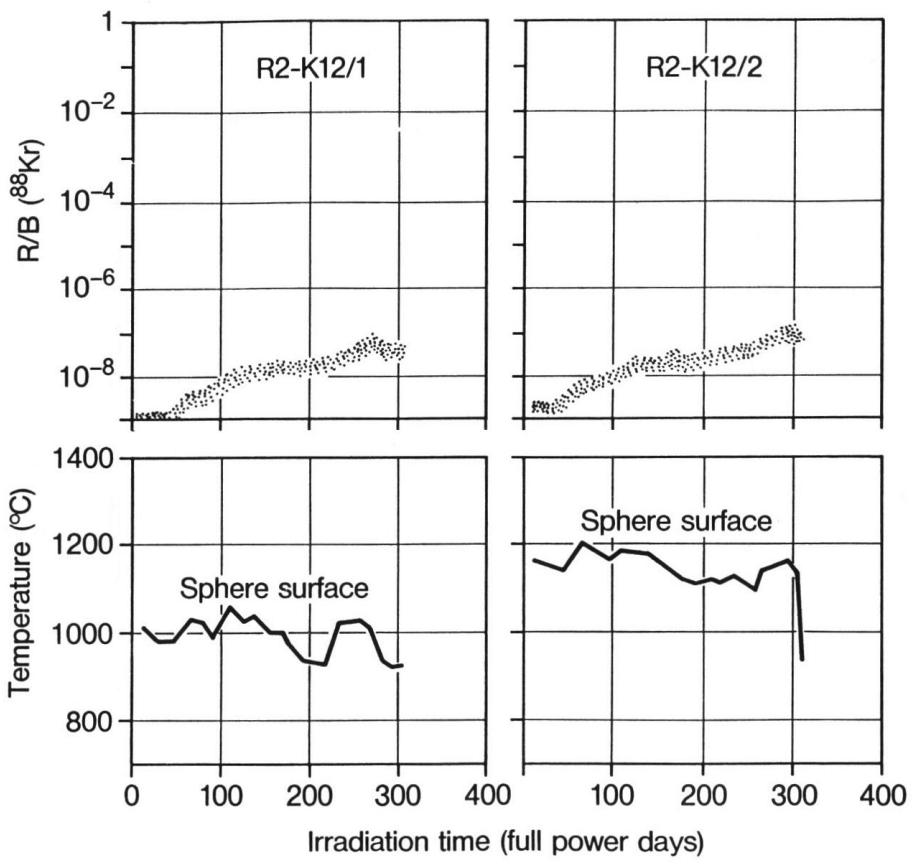

Figure 24. Gas release rates and fuel element surface temperatures in irradiation experiment R2-K12/1 and irradiation experiment R2-K12/2 [Gontard 1990].

Initial post-irradiation examination revealed that the release of cesium isotopes and silver to the graphite cups holding the fuel elements was significantly higher than predicted with the GETTER transport code and the German reference fission product transport data set [Muncke 1982, Acharya 1983]. The measured-to-calculated cesium release values were ~2 to ~9 times greater, with the largest differences in the higher temperature, higher burnup Capsule 2. Much larger differences were found for the silver isotope ^{110m}Ag; however, these differences were later traced to silver contamination within the capsule and graphite cups. The fuel element from Capsule 1 was partially deconsolidated to obtain a population of irradiated TRISO particles for further evaluation. Examination of the unbonded particles revealed two bare $(Th,U)O_2$ fuel kernels without coatings. Ceramographic examinations were performed on particles obtained from elements from both capsules. The results revealed typical fuel kernel features of porosity and metal inclusions, a reaction zone near the kernel/buffer layer interface and some tangential cracks along the buffer-IPyC interface. Only one particle was found with a radial crack in the buffer layer. No abnormalities were observed in the SiC or OPyC layers.

Both fuel elements were subjected to profile drilling along their diameters using an electrolytic deconsolidation procedure. Examination of the unbonded particles in the profile boring sections revealed no failed particles and a subsequent hot chlorination on the remaining portion of this element also revealed no failed particles. The fission product concentrations in the matrix material were also very small, near the detection limits. With the exception of silver, the measured release fractions for the fission product cesium (^{134}Cs and ^{137}Cs) were on the order of 1×10^{-6} to 9×10^{-6} from the fuel element and 1.6×10^{-3} to $\sim6\times10^{-3}$ in the TRISO coating. For silver, the measured release fraction from the TRISO coating was ~0.3% to ~2% in both the element and TRISO coating. The measured internal fractional release (based on ^{134}Cs and ^{137}Cs measurements) from the HEU $(Th,U)O_2$ fuel kernels were ~25% - 50% for both elements. The fractional release measurements from the fuel kernel, TRISO coating and element of the R2-K12 elements are listed in Table 22.

The evidence of failed particles found within several compacts is also evidenced in the BOL and EOL ^{88}Kr R/B release values provided in Table 17. This fact is further illustrated in the analysis of fission gas release data later in this section.

4.2.1.3. FRJ2-P23

The FRJ2-P23 irradiation test was carried out in the FRJ2-DIDO reactor located in Jülich, Germany for 177 efpd power days from 15 January 1979 through 23 September 1979. The primary objective of this experiment was to determine the fission product transport behavior of HEU $(Th,U)O_2$ TRISO coated fuel particles under irradiation conditions that exceeded maximum PNP/HHT limits in operating temperature and burnup. A total of 12 cylindrical compacts were irradiated, three each in four independently instrumented capsules of the FRJ2-P23 test rig. Each of the 12 cylindrical compacts were fabricated with particle batch EO 1607 and fuel matrix type A3-3. The three compacts in each of the bottom two irradiation capsules had a particle loading twice that of the compacts in the top two capsules. The FRJ2-P23 configuration data for four independent capsules were presented in Table 18 and the in-reactor irradiation data for each capsule were provided in Table 17. Figure 25 presents the in-reactor ^{88}Kr R/B released data, the mean compact operating temperatures, and the accumulated burnup as a function of time for the duration of the 177 day irradiation.

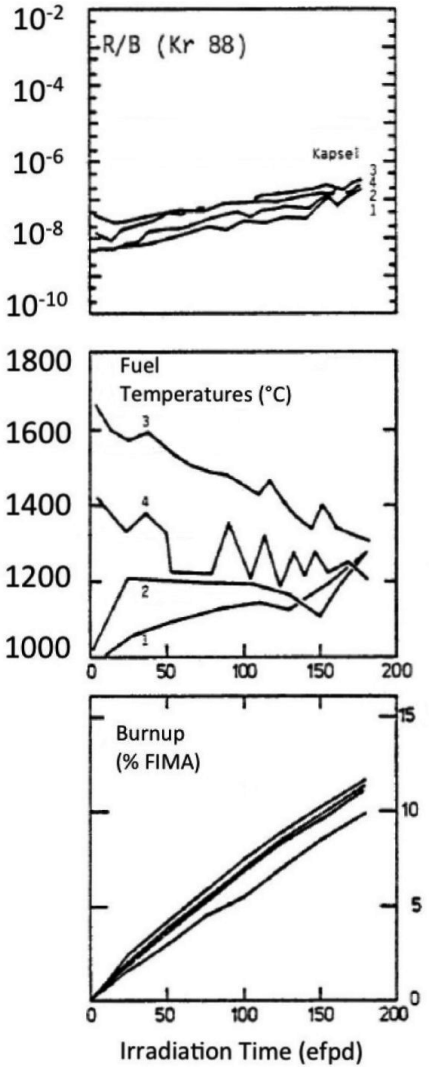

Figure 25. Gas release rates and irradiation conditions of fission product experiment FRJ2-P23 with four capsules containing three annular compacts each.

One specimen from each of the four irradiation capsules were subjected to:

(a) gas release measurement at 1000ºC (specimens #31, #36, #6, #17);

(b) electrolytic deconsolidation followed by ceramographic examination (specimens #32, #42, #13, #18) ; and

(c) electrolytic deconsolidation followed by fission product release measurements (specimens #33, #46, #24) or an IMGA measurement (specimen #14).

Fission product fractional release data are listed in Table 22 for the $(Th,U)O_2$ fuel kernel, TRISO coating and specimen for representative samples from each of the four test capsules of FRJ2-P23. The data are also representative of fuel operating temperatures from ~1060ºC up to ~1470°C. At the highest operating temperature of ~1470ºC, the fractional release of cesium (^{134}Cs and ^{137}Cs) is ~2% for both the TRISO coating and the fuel compacts. The fractional release for cesium in the $(Th,U)O_2$ fuel kernel at these temperatures is ~90%. Silver release in both the TRISO coating and fuel compact is ~40%. At the lower temperatures, cesium fractional release is ≤ 0.4% in the TRISO coating and ≤ 1.3×10^{-5} for the fuel compact. Silver fractional release is ~15% for both the TRISO coating and fuel compacts.

The unbonded HEU $(Th,U)O_2$ TRISO particles from specimen FRJ2-P23/14 from Capsule 3 were non-destructively examined using the IMGA system. A total of 1567 particles from batch EO 1607 were subjected to quantitative gamma spectrometry. Of this population, zero particles were identified as failed based on cesium loss (≤ 3 standard deviations of the mean $^{137}Cs/^{144}Ce \equiv$ failed particle). The IMGA results for this single specimen are summarized in Table 21.

4.2.1.4. FRJ2-K11

The FRJ2-K11 irradiation test was carried out in the FRJ2-DIDO reactor located in Jülich, Germany for 260 efpd from 27 April 1979 through 27 June 1980. The objectives of this test were: determine the fission product transport properties of HTGR production scale fuel elements under controlled irradiation conditions at or above the maximum design burnup and temperature for the PNP/HHT concept. Production scale elements from two AVR production campaigns with different HEU particle variants were selected for inclusion in FRJ2-K11. The FRJ2-K11 test rig contained two independently instrumented capsules vertically positioned one on top of another, each with space for two 60 mm diameter fuel elements. Two elements from the AVR XIII/3 Reload campaign, which containing the HEU UCO TRISO fissile and ThO_2 TRISO fertile particle variant were irradiated in the top capsule. In the bottom capsule, two elements from the AVR XV Reload campaign in which the HEU $(Th,U)O_2$ TRISO particles variant were irradiated. The fuel elements were similarly positioned within each capsule. Fuel performance for the two HEU variants was to be examined and compared under the controlled irradiation conditions with negligible fast neutron fluence. The FRJ2-K11 configuration data for the lower capsule two elements with HEU $(Th,U)O_2$ TRISO fuel were presented in Table 18 and the in-reactor irradiation data for this capsule were provided in Table 17. From EOL releases of short-lived fission gases, it is concluded that at most one particle may have failed in the lower capsule. Because they were not separately monitored, it is not know in which sphere.

The higher burnup element from FRJ2-K11/3 was subjected to an isothermal accident simulation test at a design temperature 1600ºC. Unfortunately, the actual temperature is thought to have been exceeded due to the loss of calibration of the control thermometer during the heat-up to test temperature. It is estimated that the actual isothermal temperature was well in excess (~200ºC higher) of 1600ºC during the ramp to temperature and a short-term annealing test (< 5 hr).

The fractional release data [Brown 1982] for the fuel element heated in excess of 1600ºC in an accident simulation test differs significantly than the non-heated element, especially for the TRISO coatings. The fractional release of cesium was ~25% for the TRISO coatings and

~30% for the $(Th,U)O_2$ fuel kernel in the heated element. By comparison, the cesium fractional release for the unheated element was ~3×10^{-4} for the TRISO coatings and ~20% for the fuel kernels. Cesium release in the matrix material is higher in the heated element, but only marginally as both are in the ~10^{-5} range. The silver release data from the TRISO coating of the heated element is about 3 times that in the unheated element – ~51% compared to ~17%. These data suggest that the isothermal accident simulation test had a significant effect on the behavior of the SiC layer of the TRISO coatings in the heated FRJ2-K11 element.

4.2.1.5. FRJ2-P25

The FRJ2-P25 irradiation test was also conducted at the FRJ2-DIDO reactor located in Jülich, Germany for 187 efpd from April 1980 through December 1980. The primary objective of this test was to investigate the fission product release from totally failed HEU particle variants under controlled irradiation conditions at or above the maximum design burnup and temperature for the PNP/HHT concept. The failed fuel was represented by a known quantity of laser-failed HEU particle variants within each test specimen. Total coating failure was achieved by laser-drilling through the IPyC, SiC and OPyC coatings into the buffer layer. Three cylindrical compacts containing HEU $(Th,U)O_2$ TRISO fuel particle batch EO 1607, each with 17 laser-failed particles from the same batch were irradiated in Capsule 2 of FRJ2-P25. Configuration data for the three cylindrical compacts in Capsule 2 of FRJ2-P25 were presented in Table 18 and the in-reactor irradiation data for this capsule were provided in Table 17. In-reactor krypton isotope R/B release rates are shown in Figure 26.

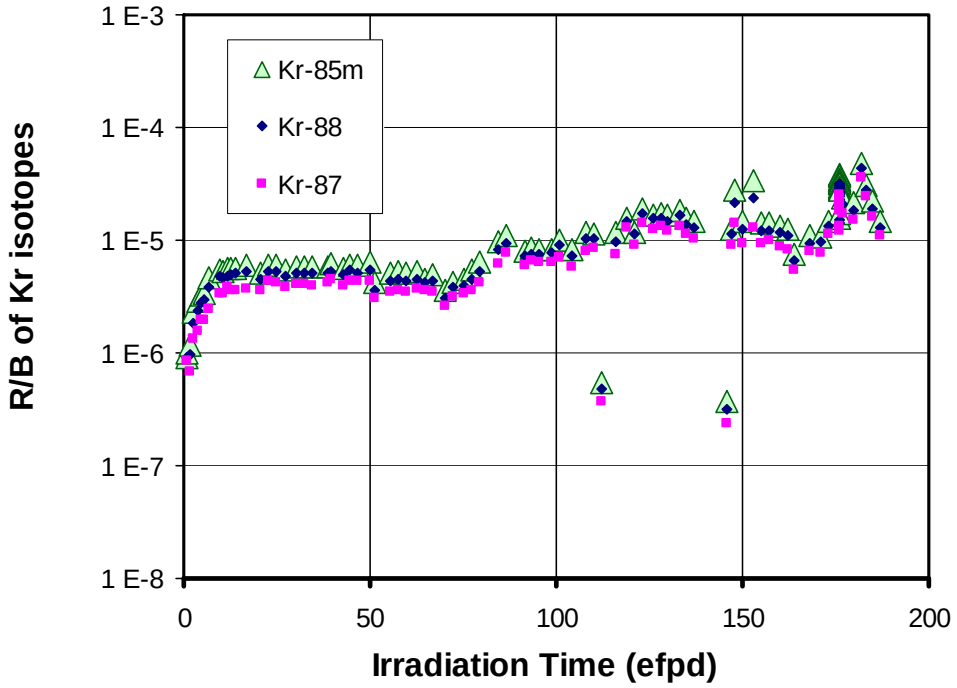

Figure 26. Release rates vs. irradiation time for short-lived krypton isotopes from FRJ2-P25/2 with ~1% laser-drilled simulated defective particles.

The evaluation of the noble fission gas release from failed HEU (TH,U)O_2 TRISO fuel particles, as represented by laser-failed TRISO coatings is presented in Chapter 4.2.2. Included there is the model for fission gas release for the HEU (Th,U)O_2 fuel kernel and its application to the interpretation of EOL fuel performance for the MTR accelerated irradiation tests.

Specimen #27 from FRJ2-P25/Capsule 2 was deconsolidated and the unbonded HEU (Th,U)O_2 TRISO particles from batch EO 1607 were non-destructively examined with the IMGA system. A total of 1695 particles were subjected to quantitative gamma spectrometry in the IMGA examination. Of this population, four particles were identified as having low $^{137}Cs/^{144}Ce$ activity ratios (≤ 3 standard deviations of the mean $^{137}Cs/^{144}Ce \equiv$ failed particle) and separated from the remaining population. These particles were subsequently identified as laser-failed particles inserted along with the nominal EO 1607 particles in this specimen during fabrication. After removing these four data sets from the population as non-representative, the examination revealed zero failed particles out of a population of 1691 irradiated particles from specimen FRJ2-P25/#27. The IMGA results for this specimen are summarized in Table 21.

4.2.1.6. R2-K13

The R2-K13 irradiation test [Gontard 1990] was executed in the R2-reactor in Studsvik, Sweden, for 517 efpd from March 1980 through September 1982, with a pause in irradiation from mid-December 1981 to early February 1982. This irradiation test was performed under the US/German Umbrella Agreement on Gas-Cooled Reactor Development [Lotts 1977, Turner 1983]. The primary objectives of the German portion of this test were:

- to investigate the irradiation performance of reference HEU (10Th,U)O_2 TRISO fuel particles from the German Standard Quality 1979;
- demonstrate low-particle failure under long-term MTR irradiation; demonstrate small fission product release from the German Standard Quality 1979 fuel particles;
- provide irradiated test specimens for post-irradiation design basis accident simulation tests;
- compare in-reactor fuel performance between the reference German HEU (Th,U)O_2 TRISO fuel and the reference U.S. two-particle system - HEU UCO TRISO fissile/ThO_2 TRISO fertile.

Two reference 60 mm diameter spherical fuel elements were irradiated in upper and lower independently instrumented capsules of the R2-K13 test rig. The two fuel elements were fabricated with the HEU (10Th,U)O_2 TRISO particle batch EO 1674 along with the A3-27 type fuel matrix. Each of the spherical elements were held in-place with graphite cups during irradiation, and the test rig was rotated 90º after every irradiation cycle to minimize radial fluence gradients through the capsules. The R2-K13 configuration data for capsules 1 and 4 with mixed oxide elements were presented in Table 18 and the in-reactor irradiation and release data are provided in Table 17. Figure 27 shows the in-reactor ^{88}Kr R/B release data and monitored fuel element surface temperatures for R2-K13/1 and /4 over the duration of the irradiation period.

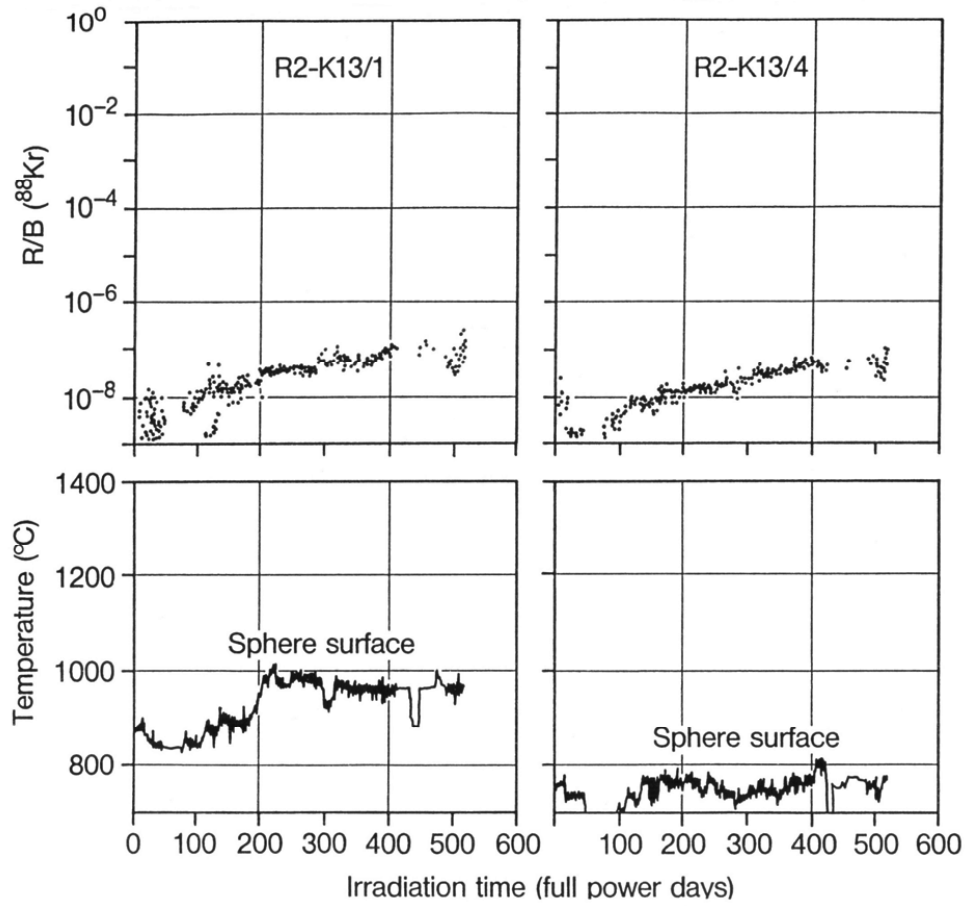

Figure 27. Gas release rates and fuel element surface temperatures [Gontard 1990] for spheres 1 and 4 in irradiation experiment R2-K13.

The high temperature fuel element from R2-K13/Capsule 1 was subjected to burnup measurements and then selected for a long-term isothermal accident simulation test at 1600ºC. The testing results and subsequent evaluations are presented in Chapter 5. The lower temperature element in R2-K13/Capsule 4 was also gamma counted for burnup determination and then subjected to an electrolytic profile boring examination across the diameter of the sphere. All of the individual particles of batch EO 1674 were collected, visually examined and their inventory measure using quantitative gamma spectrometry. Destructive examination of some fraction of the particle inventory revealed that $(Th,U)O_2$ fuel kernels of three distinct sizes made up the fuel particle batch EO 1674. This fact was not disclosed prior to evaluation and explained the systematic particle-to particle variation in radionuclide inventory. Fission product inventory (^{90}Sr, ^{134}Cs, ^{137}Cs) profiles, with the exception of ^{110m}Ag, in the fuel matrix were relatively flat across the diameter of the element from Capsule 4. Only ^{110m}Ag exhibited a peak in the matrix material near the center of the element.

Figure 28 (on left) shows the variation in radionuclide inventory in the coated particles of batch EO 1674 relative to their position along the diameter of the fuel element. Also shown in Figure 28 (on right) is the normalized distribution of the $^{134}Cs/^{137}Cs$ activity ratio which is indicative of the thermal flux profile the fuel element from R2-K13 experienced during irradiation.

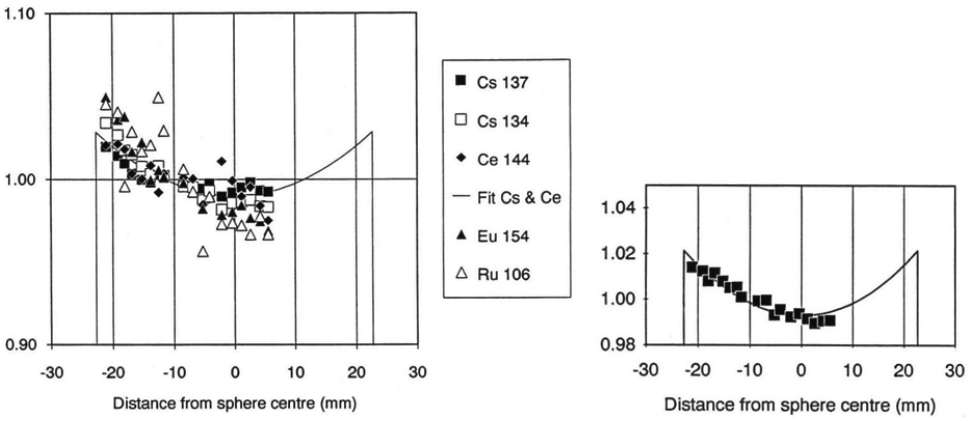

Normalized particle inventories across spherical fuel element

Normalized distribution of $^{134}Cs/^{137}Cs$ particle activity ratios

Figure 28. Radial distribution of coated particle fission product inventories [Gontard 1990] obtained after deconsolidation of the irradiated spherical fuel element R2-K13/4 with a burnup of 9.8% FIMA.

4.2.2. Prediction of Release Rates of Short-Lived Fission Gases

All of the above MTR accelerated tests maintained the capability to measure the release rates of gaseous fission products from the fuel under irradiation. Frequent monitoring of the individual test capsules occurred by taking a controlled volume of the sweep gas sample and gamma counting it to quantitatively measure the inventory of the short-lived gaseous Kr and Xe fission products as a function of irradiation time. The fission gas release-rate (Ri) can be computed directly from the sample volume, the purge gas flow rate at the time of sampling, and the activity of the released gas sample. Then by comparing the release-rate (R_i) to the birth-rate (B_i) of a particular isotope, the ratio $(R/B)_i$ provides a direct measure of the steady-state release behavior of the fuel. This is the standard method of monitoring and assessing in-reactor fuel performance.

By comparing the EOL ^{85m}Kr or ^{88}Kr R/B values with the R/B of a failed TRISO coated fuel particle, an estimate of the fraction of failed particles responsible for the fission gas release can be made:

$$\eta = \frac{\left(R_i / B_i\right)_{EOL}}{\left(R_i / B_i\right)_f} \qquad (1)$$

where

η is the fraction of failed particles;

$\left(R_i / B_i\right)_{EOL}$ is the ratio of EOL release rate over EOL birth-rate for isotope i;

$\left(R_i / B_i\right)_f$ is the ratio of the release rate over birth-rate for a defective or failed particle for isotope i.

The number of failed particles present at the EOL of an irradiation experiment is then the product of the failure fraction (η) and the particle population that the R/B_{EOL} represents. The $(R/B)_f$ for ^{85m}Kr was determined at a representative EOL $(Th,U)O_2$ fuel kernel temperature determined for each of the 11 independently swept irradiation test capsules.

The prediction of release rates for LEU UO_2 fuels is described in [IAEA 1997], but it is different for ThO_2 and $(Th,U)O_2$ fuels. The fractional release from in-reactor failed HEU $(Th,U)O_2$ TRISO particles was estimated through the analysis of the R/B data from laser failed EO 1607 particles in Capsule 2 of the FRJ2-P25 irradiation test. The release rate predictive model is given by:

$$\left(\frac{R}{B}\right)_f = g_F \left.\frac{R}{B}\right|_F + g_C \left.\frac{R}{B}\right|_C + g_P \qquad (2)$$

where

g_F, g_C, and g_P are model parameters with $g_F + g_C + g_P = 1$;

the suffixes F denote the fuel, C the graphite grains, and P the pores.

In the Equivalent Sphere Model [Booth 1957, Nabielek 1974], R/B is given by the relationship

$$\frac{R}{B} = 3\sqrt{\frac{D'}{\lambda}}\left(\coth\sqrt{\frac{\lambda}{D'}} - \sqrt{\frac{D'}{\lambda}}\right) \approx 3\sqrt{\frac{D'}{\lambda}} \qquad for \quad \lambda \equiv \frac{\ln 2}{\tau_{1/2}} >> D' \qquad (3)$$

where

$D' = D/a^2$ is the reduced diffusion coefficient, $[s^{-1}]$;

a is the fuel kernel radius, [m];

λ is the decay constant, $[s^{-1}]$; and

$\tau_{1/2}$ is the half-life, [s].

When T [K] is the irradiation temperature, the reduced diffusion coefficient can be expressed as

$$\log_{10} D' = a + b\frac{10^4}{T}$$

where T is the temperature, [K].

The model parameters [Thiel 1982] are provided in Table 19 based on analysis of the FRJ2-P25/2 data for the HEU (Th,U)O_2, The R/B data in Figure 26 are the in-reactor measured release rates for the short-lived Krypton isotopes, ^{85m}Kr, ^{87}Kr and ^{88}Kr, during irradiation FRJ2-P25/Capsule 2 with ~1% laser drilled defective particle coatings. Using the Thiel model [Thiel 1982] together with the parameters listed in Table 19, the release rates predictions for the krypton isotopes from a defective HEU (Th,U)O_2 fuel kernel were calculated as a function of irradiation temperature and are shown in Figure 29.

Table 19. Model parameters for prediction of short-lived fission gas release rates from defective/failed HEU (Th,U)O_2 fuel particles obtained from the analysis of the irradiation experiment FRJ2-P25/2 [Thiel 1982].

Element	**(Th,U)O_2 parameters**		**A3 matrix parameters**			**Pore parameters**
	a_F	**b_F**	**g_C**	**a_C**	**b_C**	**g_P**
Krypton	1.800	-1.639	0.029	-5.602	-0.284	0.0002
Xenon	7.95	-2.40	0.023	-6.85	-0.284	0.0002

The presence of heavy metal contamination in the A3 matrix material of fuel specimens will also contribute to measured fission gas release rate during in-reactor testing. This A3 matrix contamination consists of natural uranium and thorium and potentially enriched uranium from defective fuel during the fabrication process. The isotopic form of the contamination will, in general, be different from the fuel itself. This way, the R/B term for contamination needs a correction factor α:

$$\alpha = \frac{\frac{f_{Th} S_3 Y_{REF}}{Y_3} + f_u \frac{1+EF}{1+EC}\left(\frac{EC}{EF} S_5 \frac{Y_{REF}}{Y_5} + S_9 \frac{Y_{REF}}{Y_9}\right)}{\overline{Y}}$$

with

$$\overline{Y} = \frac{S_3 Y_3 + S_5 Y_5 + S_9 Y_9}{Y_{REF}}$$

where

Y3, Y5, Y9... are the Kr or Xe fission yields from ^{233}U, ^{235}U, ^{239}Pu,

$\overline{Y}$	is the weighted fission yield,
Y_{REF}	is the reference fission yield,
f_{Th}, f_U	are the thorium and uranium contamination fractions in the A3 matrix,
EF	is the $^{235}U/^{238}U$ ratio in fuel,
EC	is the $^{235}U/^{238}U$ ratio in contamination;
S	are the respective fission fractions from ^{233}U, ^{235}U, ^{239}Pu.

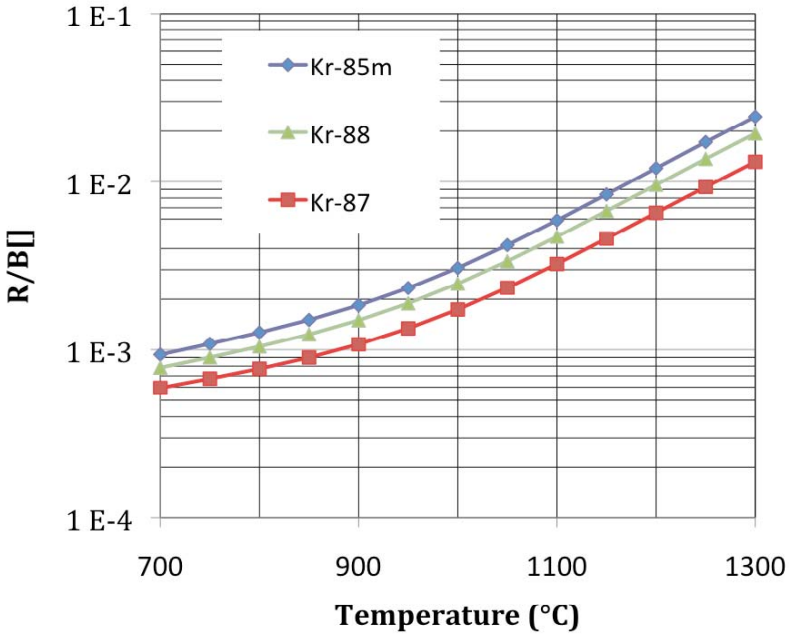

Figure 29. Model prediction of the release rate of short-lived Kr isotopes from bare (Th,U)O_2 kernels, defective or broken particles based on [Thiel 1982].

Figures 30 and 31 show the cycle-averaged, in-reactor ^{85m}Kr release rates from the spherical fuel elements R2-K13/1 and R2-K13/4, respectively, compared to the calculated contribution to R/B from the A3 matrix heavy metal contamination model in each capsule as a function of irradiation time. Based on these comparisons alone, the contamination model for fission gas release provides a reasonably good representation of the cycle-averaged in-reactor ^{85m}Kr R/B data for experiment R2-K13. These comparisons indicate that the cycle-averaged measured release in experiment R2-K13/1 and /4 can be reasonably reproduced using model predictions for the release of ^{85m}Kr from contamination only (true for all other short-lived Kr and Xe isotopes). Similar results were also expressed for experiments BR2-P25 and R2-K12/1 and /2.

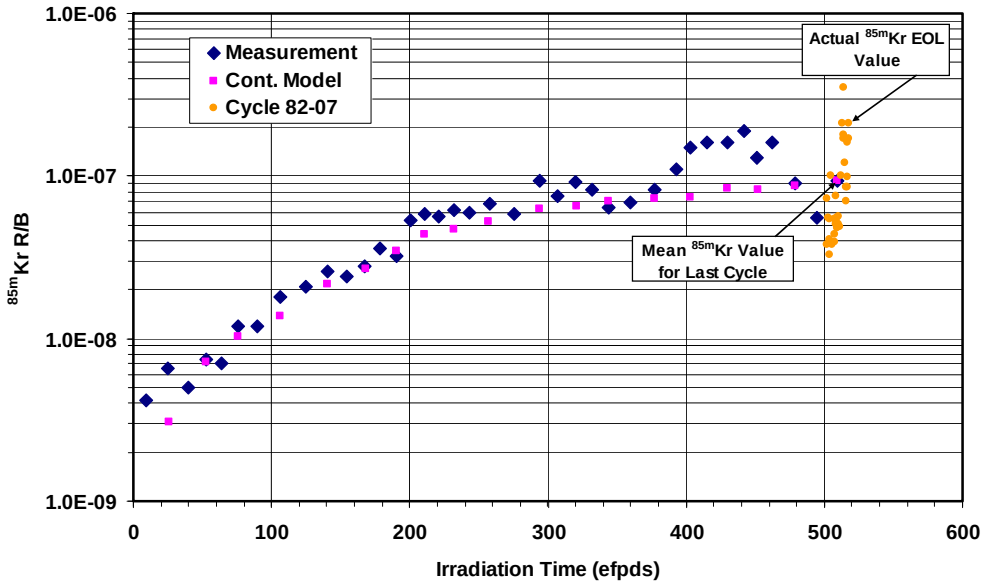

Figure 30. Comparison of measured and (HM only) predicted ^{85m}Kr R/B release data for R2-K13/1 as a function of irradiation time. Individual ^{85m}Kr R/B data for the last irradiation cycle are shown for reference.

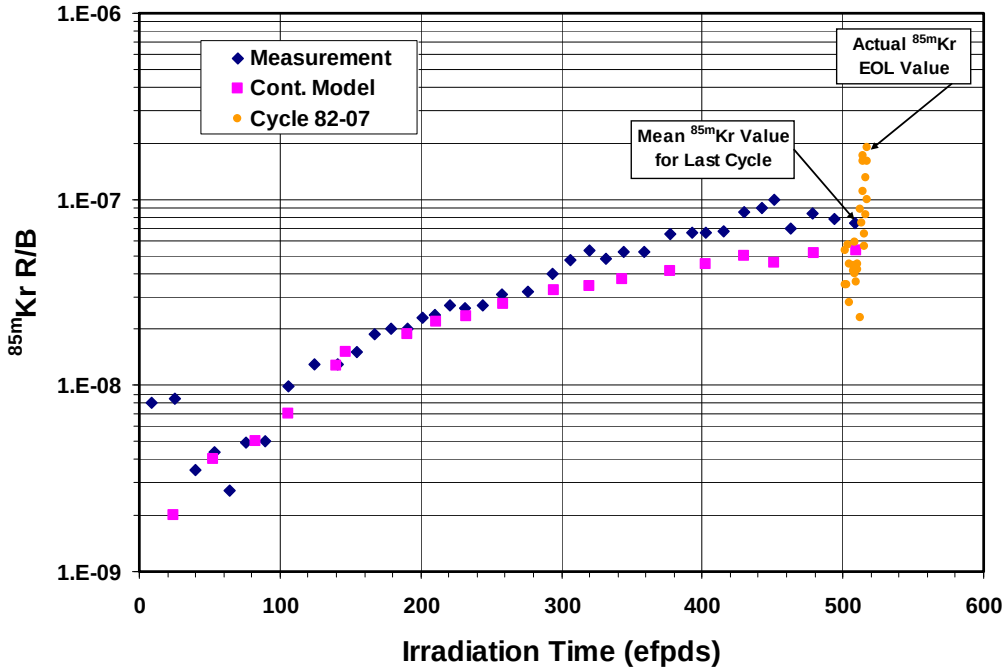

Figure 31. Comparison of measured and (HM only) predicted ^{85m}Kr R/B release data for R2-K13/4 as a function of irradiation time. Individual ^{85m}Kr R/B data for last irradiation cycle are shown for reference.

In addition to the cycle averaged ^{85m}Kr R/B data and A3-matrix heavy metal contamination model predictions, on each of Figure 30 and Figure 31 are plotted the individual ^{85m}Kr R/B data for the last irradiation cycle for the respective capsule. These data indicate a large spread in the ^{85m}Kr R/B values during the last irradiation cycle. The actual EOL ^{85m}Kr R/B value is not well represented by the cycle-averaged R/B data point for this last irradiation cycle. In R2-K13/1, the cycle-averaged ^{85m}Kr R/B value was 9.4×10^{-8} compared to the actual EOL ^{85m}Kr R/B value of 2.1×10^{-7} (difference of a factor of ~2). For R2-K13/4, the cycle-averaged ^{85m}Kr R/B value was 7.5×10^{-8} compared to the actual EOL ^{85m}Kr R/B value of 1.9×10^{-7} ($\leq$ 3 times difference). These differences are not great, but they can overlook the failure of one or two particles as is the case for R2-K13/4 where two failed particles were estimated at EOL. Similar mischaracterizations were also revealed for the fuel specimens in experiment BR2-P25. The parameters that were used for the A3-matrix HM contamination model predictions of are summarized in Table 20 below.

Table 20. Parameters for R/B predictions for A3-matrix heavy metal contamination model.

	BR2-P25	**R2-K12**	**R2-K13**
g U/ g graphite	4.5×10^{-9}	3×10^{-8}	3×10^{-8}
f_U	5.5×10^{-5}	5×10^{-6}	4×10^{-6}
Postulated HM ^{235}U enrichment [wt%]	10	1.2	1.2
f_{Th}	5.1×10^{-5}	4.6×10^{-6}	2×10^{-6}

4.2.3. Solid Fission Product Release from Intact and Defective Particles

Back in 1977, the HEU (Th,U)O_2 LTI-TRISO particles produced was the first high-quality fuel for HTGRs in Germany and was therefore characterized in great detail, both in manufacture, in irradiation and in accident conditions tests (where a new heating furnace, KÜFA, had to be built).

A significant effort was made within the German Fuel Development Program to assess fission product retention in intact HEU (Th,U)O_2 LTI-TRISO fuel particles as a function of temperature, time, burnup and fluence. Table 22 is a compilation of the measured fractional release data. From this table, the ^{137}Cs fractional release data for particle batch EO 1607 are plotted in Figure 32 in a simplified form as the differences in irradiation time, burnup and fluence accumulation are not considered. These results obtained in 1982-1984 are reasonably correlated with irradiation temperature. The fractional release data described in Table 22 were obtained in post-irradiation evaluations of irradiated fuel specimens containing the HEU (Th,U)O_2 TRISO coating batches EO 1607, EO 1674 and HT 150-160, 162-167.

Table 21. IMGA measurements for irradiated HEU (Th,U)O_2 TRISO particles from experiments BR2-P25, FRJ2-P23, and FRJ2-P25.

Experiment/ Specimen	Particle population examined	Number of failed particles	Failure fraction (Confidence limit)	
			η (50%)	η (95%)
Experiment BR2-P25				
BR2-P25/#3	1331	6	5.0×10^{-3}	8.9×10^{-3}
BR2-P25/#7	1291	8	6.7×10^{-3}	1.1×10^{-2}
Experiment FRJ2-P23				
FRJ2-P23/#14	1567	0	4.4×10^{-4}	1.9×10^{-3}
Experiment FRJ2-P25				
FRJ2-P25/#27	1691	0*	4.1×10^{-4}	1.8×10^{-3}
Summary				
HEU (Th,U)O_2 EO 1607	5880	14	2.5×10^{-3}	3.7×10^{-3}

* Four particles identified as purposely laser-failed (prior to irradiation) and removed from population.

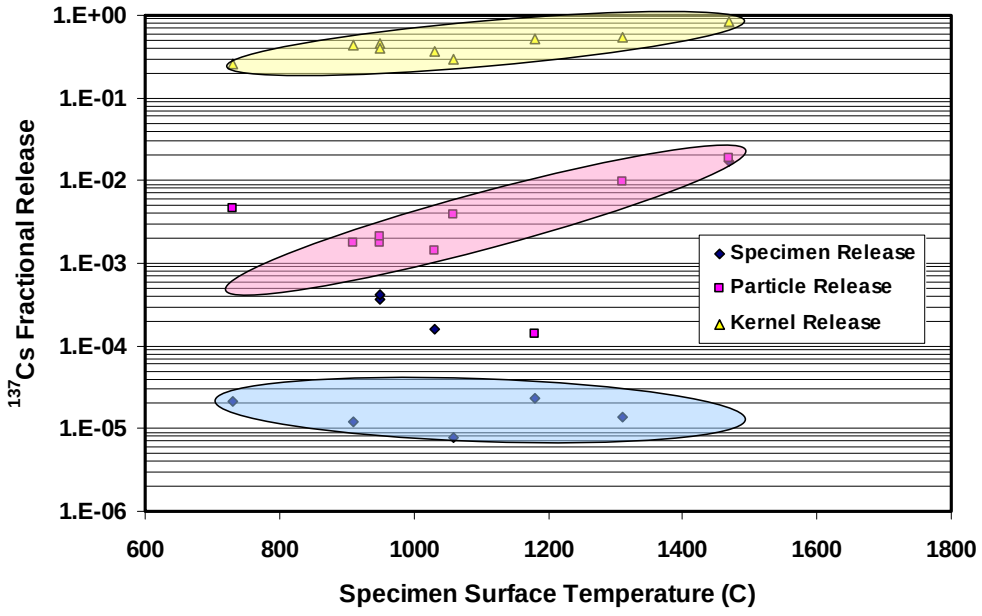

Figure 32. EOL releases of ^{137}Cs from (Th,U)O_2 fuel kernels, LTI-TRISO coated particles and from spheres/compacts.

Table 22. End of irradiation solid fission product release fractional released data obtained on HEU (Th,U)O_2 TRISO particle fuels [HBK 1984].

Test/ Specimen	Operating conditions			Measured fractional release							
				Fuel kernel		TRISO coating			Test specimen		
	Temp. [ºC]	Burnup [% FIMA]	Fluence [10^{25} n/m^2]	^{134}Cs	^{137}Cs	^{134}Cs	^{137}Cs	^{110m}Ag	^{134}Cs	^{137}Cs	^{110m}Ag
TRISO particle batch EO 1607											
BR2-P25/3	950	14.9	7.4	4.5×10^{-1}	4.5×10^{-1}	1.9×10^{-3}	1.8×10^{-3}	n.m.	1.4×10^{-4}	3.6×10^{-4}	n.m.
BR2-P25/7	950	15.6	8.1	4.9×10^{-1}	4.0×10^{-1}	2.0×10^{-3}	2.1×10^{-3}	n.m.	1.9×10^{-5}	4.1×10^{-4}	n.m.
R2-K12/1	730	11.1	5.6	3.0×10^{-1}	2.6×10^{-1}	5.9×10^{-3}	4.6×10^{-3}	3.4×10^{-3}	1.2×10^{-5}	2.1×10^{-5}	3.4×10^{-2}
R2-K12/2	910	12.4	6.9	5.1×10^{-1}	4.4×10^{-1}	1.6×10^{-3}	1.8×10^{-3}	1.4×10^{-2}	9.0×10^{-5}	1.2×10^{-5}	1.4×10^{-2}
FRJ2-P23/1	1060	11.3	1.1	3.2×10^{-1}	2.9×10^{-1}	1.6×10^{-3}	3.9×10^{-3}	1.5×10^{-1}	1.3×10^{-5}	7.9×10^{-6}	1.5×10^{-1}
FRJ2-P23/2	1180	12.5	1.4	5.9×10^{-1}	5.3×10^{-1}	7.1×10^{-5}	1.4×10^{-4}	1.4×10^{-1}	2.4×10^{-5}	2.3×10^{-5}	1.4×10^{-4}
FRJ2-P23/3	1470	11.9	1.4	9.1×10^{-1}	8.5×10^{-1}	2.2×10^{-2}	1.9×10^{-2}	4.0×10^{-1}	2.0×10^{-2}	1.7×10^{-2}	4.0×10^{-1}
FRJ2-P23/4	1310	12.1	1.4	6.2×10^{-1}	5.4×10^{-1}	1.1×10^{-2}	9.9×10^{-3}	4.6×10^{-2}	1.9×10^{-5}	1.4×10^{-5}	1.7×10^{-2}
FRJ2-P25/2	1030	11.6	1.4	4.1×10^{-1}	3.7×10^{-1}	1.5×10^{-3}	1.4×10^{-3}	-	2.3×10^{-4}	1.6×10^{-4}	1.3×10^{-1}
TRISO particle batch HT 150-160, 162-167											
FRJ2-K11/3	1010	9.0	~0.06	3.1×10^{-1}	2.9×10^{-1}	2.4×10^{-1}	2.6×10^{-1}	5.1×10^{-1}	8.2×10^{-5}	5.1×10^{-6}	4.7×10^{-2}
FRJ2-K11/4	1010	8.5	~0.05	1.6×10^{-1}	2.3×10^{-1}	3.2×10^{-4}	3.3×10^{-4}	1.7×10^{-1}	1.4×10^{-5}	4.0×10^{-6}	5.5×10^{-2}
TRISO particle batch EO 1674											
R2-K13/1	1170	10.2	8.5	n.m.	n.m.	n.m.	n.m.	n.m.	2.9×10^{-5}	1.1×10^{-5}	3.9×10^{-2}
R2-K13/4	980	9.8	6.8	n.m.	n.m.	n.m.	n.m.	n.m.	1.1×10^{-5}	3.2×10^{-6}	2.7×10^{-3}

n.m. = not measured

Several of the tests listed in Table 2 have also been used to provide the irradiated fuels necessary to establish essential fission product (Cs, Sr, Ag) transport parameters in kernel and coating materials [Stöver 1977, Allelein 1980, Amian 1983]. These and other parameters have been used for the prediction of particle failure with the PANAMA code and fission product release predictions with FRESCO both for irradiation experiments, accident simulation testing programs and design and licensing of HTGRs. Verification and validation have been conducted with these codes [Verfondern 2012]; their further development resulted in the new code STACY [Xhonneux 2012].

4.2.4. MTR Irradiation Performance Assessment

The BOL and EOL ^{85m}Kr R/B values, and for some the ^{88}Kr R/B values, are provided in Table 23 for the twelve independently monitored irradiation test capsules. Experiment FRJ2-P25/2 with ~1% was eliminated from the irradiation performance assessment because it contained intentionally laser-failed particles. Thus, only the in-reactor data from 11 test capsules were analyzed in detail. For each of the capsules from experiments R2-K12, FRJ2-K11, and R2-K13 in which reference 60 mm diameter fuel elements were irradiated, the BOL ^{85m}Kr R/B values were very low, in the 1.5×10^{-9} to 3.9×10^{-9} range. These are indicative of high-quality fuel elements with very low levels of heavy metal contamination (Th+U_{nat}) and free of defective particles. The EOL ^{85m}Kr R/B values for FRJ2-K11 and the two R2-K13 fuel spheres were all at the $\sim2\times10^{-7}$ level, whereas the EOL ^{85m}Kr R/B value for R2-K12 was at the $\sim4\times10^{-8}$ level. For the R2-K12 capsules, this is an increase by about one order of magnitude from BOL to EOL, and for R2-K13 and FRJ2-K11 an increase by about two orders of magnitude.

For experiment BR2-P25 which contained the small 20 mm-diameter fuel zone elements, the BOL ^{85m}Kr R/B value is 3×10^{-7} which would typically represent the presence of ~2 or more defective particles. For the four FRJ2-P23 test capsules, the BOL ^{85m}Kr R/B values are $\leq 10^{-7}$ values; however, the BOL irradiation temperatures are quite high compared to the other (Th,U)O_2 fueled experiments. The resulting R/B values may be caused by the higher temperatures and not the presence of defective fuel particles. At EOL, the BR2-P25 capsule ^{85m}Kr R/B values increased to the 10^{-6} range which is indicative of the presence of in-reactor failed fuel particles. The EOL ^{85m}Kr R/B values for the FRJ2-P23 capsules were $\sim2\times10^{-7}$ which would typically indicate one or more failed particles. However, the EOL temperatures still remained high which could affect these R/B values.

BOL and EOL failed particle fractions were calculated for each of monitored irradiation capsules based on their measured R/B values, best estimates of EOL irradiation temperatures, and the fission gas release model [Thiel 1982] for defective HEU (Th,U)O_2 fuel kernels in Equation 2. The results of these analyses are shown in Table 23. Defective fuel particles were identified in the BOL R/B data from the small 20 mm diameter fuel specimens in experiment BR2-P25, from at least one of the 60 mm diameter elements in FRJ2-K11, and from all the FRJ2-P25/2 test specimens which contained a laser drilled particles.

Table 23. Fuel Performance in accelerated MTR irradiation tests based on EOL ^{85m}Kr R/B values and the temperature dependent fractional release values for an exposed oxide fuel kernel [Thiel 1982].

Irradiation test/ capsule or sphere	Beginning of life		End of life			
	$\left(R/B\right)^{Kr-85m}_{BOL}$	Equiv. failed particles	$\left(R/B\right)^{Kr-85m}_{EOL}$	Contrib. due to contam ination	Equiv. in-reactor failed particles	Estimated failure fraction (upper 95% conf. limit)
BR2-P25/						
1-12	3.0×10^{-7} *	3	1.0×10^{-6}	negligible	5	5.9×10^{-4}
R2-K12/						
1	3.9×10^{-9}	0	3.2×10^{-8}	100% **	0	1.4×10^{-4}
2	3.5×10^{-9}	0	3.4×10^{-8}	100% **	0	
FRJ2-P23/						
1	$< 10^{-7}$ *	0	1.4×10^{-7}	100% **	0	1.2×10^{-4}
2	$< 10^{-7}$ *	0	1.9×10^{-7}	100% **	0	
3	$< 10^{-7}$ *	0	2.3×10^{-7}	100% **	0	
4	$< 10^{-7}$ *	0	2.1×10^{-7}	100% **	0	
FRJ2-K11/						
3,4	1.7×10^{-9}	0	2.7×10^{-7}	~50%	1	2.3×10^{-4}
FRJ2-P25/						
2	9.2×10^{-7}	51	1.5×10^{-5}	100% **	–	–
R2-K13/						
1	2.2×10^{-9}	0	2.1×10^{-7}	100% **	0	1.6×10^{-4}
4	1.5×10^{-9}	0	1.9×10^{-7}	negligible	2	
Total for entire HEU (Th,U)O_2 population (126,664)					8	1.1×10^{-4}
Total for HEU (Th,U)O_2 population in 60 mm diameter fuel elements (82,720)					3	9.4×10^{-4}
Total for HEU (Th,U)O_2 population in non-standard fuel specimens (43,950)					5	2.4×10^{-4}

* The short-lived fission gas ^{88}Kr R/B is shown for the experiments BR2-P25 and FRJ2-P23.

** A portion of EOL noble gas release is due to the breeding of fissile material into the initial uranium and thorium contamination in fuel matrix and capsule graphite materials.

At EOL, a total of eight in-reactor failed TRISO particles were estimated from the measured ^{85m}Kr and ^{88}Kr R/B values. Five were identified in the 20 mm diameter elements in BR2-P25, one in the two 60 mm diameter elements in FRJ2-K11, and two in the 60 mm diameter element in R2-K13/4. For the population of 126,664 (Th,U)O_2 TRISO particles analyzed, eight failed particles represents an expected in-reactor failure fraction of 6.32×10^{-5}; taking account of the finite sample size, this translates to a failure fraction limit of 1.14×10^{-4}, at the one-sided upper 95% confidence limit.

4.3 AVR Real-Time Irradiation Testing and Analysis

The AVR reactor (46 MW(th)) located in Jülich, Germany, was operated from 1967 through 1988 [Sauer 1990]. During the AVR's 21 years of operation, it provided invaluable information on spherical fuel element development, fuel particle development with many particle variants (kernel material, enrichments, coating designs) and various HTGR fuel cycles. More than 290,000 spherical fuel elements of five different types, containing more than 6×10^9 coated fuel particles, were inserted into its core. The distribution of various fuel element types within the AVR core as a function of operating history are shown in Figure 33 [Verfondern 2007, Nabielek 2008].

The AVR fuel reloads of particular importance relative to the HEU (Th,U)O_2 TRISO fuel particle system are AVR XV and AVR XX which were designated the AVR GO2 fuel type, Table 24. All of these elements were manufactured to NUKEM standard quality requirements in the period from 1978 through 1985. In an eight year period beginning in 1981 and again in 1985, these fuel elements were inserted into the AVR and experienced real-time HTGR operating conditions. At periodic intervals over the AVR's lifetime, a number of irradiated elements were randomly drawn from the core for post-irradiation evaluation and accident condition testing at the Research Center Jülich, Germany. A number of GO2 fuel elements were included in these random sample withdrawals. Post-irradiation evaluations included: fission product inventory measurements (burnup), out-of-reactor gas release measurements, failure fraction measurements and accident simulation testing. At the end of AVR operations in 1988, high-quality HTGR fuel elements containing HEU (Th,U)O_2 TRISO and LEU UO_2 TRISO coated fuel particles constituted more than half of the core inventory.

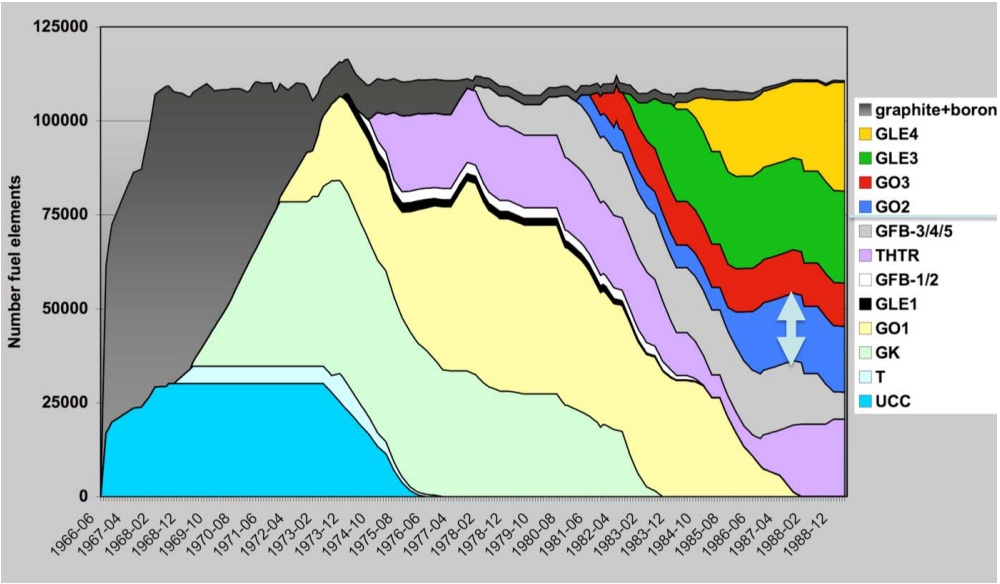

Figure 33. Distribution of spherical fuel element types in the AVR core as a function of operating history [Verfondern 2007, Nabielek 2008].

Table 24. High quality TRISO fuel elements inserted in the AVR Reactor over the period 1981 to 1987.

Fuel	AVR type	Reload	Initial insertion	No. of fuel elements in campaign
HEU $(Th,U)O_2$ TRISO	GO2	AVR XV	Feb. '81	6087
		AVR XX	Oct. '85	11,854
LEU UO_2 TRISO	GLE3	AVR XIX	July '82	24,615
	GLE4	AVR XXI	Feb. 84	20,250
		AVR XXI/2	Oct. 87	8740

The most limiting part of the AVR operating history has always been the actual operating temperatures experienced by the fuel elements as they traverse, on multiple passes, through the pebble-bed core during their irradiation lifetime. Predictions based on model calculations have been available, but no significant experimental measurements were made until the mid-1980s.

In 1986 a sophisticated, multi-element "melt wire experiment" was conducted and it was during this period that GO2 type elements were present in the AVR. Melt Wire Experiment HTA-8 was carried out in the AVR with specially designed graphite matrix spheres which incorporated a set 20 capsules, each containing a single melt-wire [Derz 1990, Gottaut 1990, Pohl 2009]. The melt-wires were fabricated of specific alloy composition that would melt if a precise temperature was exceeded. A total of 190 monitoring spheres were added into the AVR core through standard fuel loading procedures. Upon discharge, they were X-rayed to assess the momentary maximum peak temperatures experienced during their passage through the AVR.

Based on the melt-wire measurement results, the underlying temperature distribution was extracted by constructing a Quantile-Quantile plot [Koenker 2005] based upon the probability properties of the histogram distribution. Two Gaussian distributions with peak temperatures of 1100 ± 66°C and 1220 ± 100°C were found that define the variation of momentary maximum fuel element surface temperatures in the AVR between the inner core and outer core locations [Nabielek 2011]. Peak central temperatures were calculated to be 37.3°C and 75.6°C higher for the inner and outer locations, respectively. The resulting distributions of the peak temperatures experienced by AVR fuel elements are shown in Figure 34. It is important to note that these very high temperatures were experienced by a limited fraction of fuel element (at the very top of the core) only for a short period on each pass through the core of the AVR. These do not represent the nominal Type GO2 fuel element operating temperatures in the AVR.

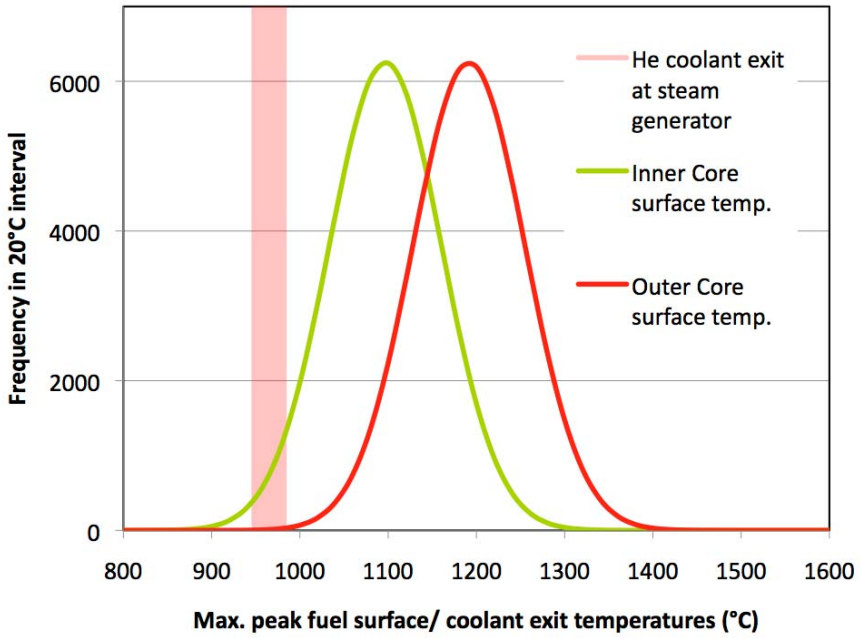

Figure 34. Two Gaussian distributions (1100±66°C and 1220±100°C) defining the variation of maximum fuel element surface temperatures in AVR between inner core and outer core [Nabielek 2011].

To assess the EOL performance of the AVR GO2 fuel elements with HEU (Th,U)O_2 TRISO fuel particles, a methodology was used based upon fission gas release measurements made during the gradual heatup in the early phase of accident condition testing [Schenk 1983, Schenk 1988, Schenk 1989]. This heatup process begins at room temperature, progresses over a series of heating-ramps to specific temperatures (300°C, 1050°C, and 1250°C) and hold periods until the desired simulation temperature is reached. Two of these hold points, 1050°C, and 1250°C, are designed to equilibrate the irradiated fuel particles in the fuel element at or near their prior irradiation temperature [Schenk 1978]. This allows the fuel to develop a stable internal environment before being heating to an elevated temperature, not previously experienced by the fuel particles. The 1050°C hold point was considered the mean working temperature for fuel specimens from accelerated MTR irradiation tests, and the 1250°C hold point was considered the typical working temperature for AVR fuel elements.

Throughout the accident simulation test, the test furnace is purged with a sweep gas and continuously monitored for release of the long-lived ^{85}Kr (10.76 yr half-life) fission gas. Detection of any significant activity in the sweep gas represents release from the fuel element and may be an indicator of the presence of failed or defective fuel particles.

Table 25 is a detailed list of eleven 60 mm diameter fuel elements containing HEU (Th,U)O_2 TRISO fuel elements that were subjected to accident simulation testing. Of these, nine were used to analyze AVR EOL irradiation performance. The two remaining elements are one element each from the MTR accelerated irradiation tests FRJ2-K11/3 and R2-K13/1.

Table 25. Noble gas ^{85}Kr release fractions measured during the heatup phase in accident simulation tests on AVR irradiated HEU (Th,U)O_2 fuel elements and irradiated spheres from the MTR tests R2-K13 and FRJ2-K11 [Schenk 1978, Schenk 1983, Schenk 1988, Schenk 1989].

Fuel element* (AVR sample No./ specimen No.)	**Burnup [% FIMA]**	**Measurement temperature of ^{85}Kr release [°C]**	**^{85}Kr release fraction**	**Peak temperature of accident simulation test [°C]**
KÜFA isothermal accident simulation tests				
AVR 70/26	8.2	1610**	$\leq 1.0\times10^{-6}$	1610
R2-K13/1	10.3	1250	$\leq 3.4\times10^{-7}$	1600
Graphite furnace tests				
AVR 70/15	7.1	1250	$\leq 7.0\times10^{-7}$	1500
AVR 70/7	7.3	1500**	$\leq 6.3\times10^{-7}$	1500
AVR 69/13	8.6	1800**	$\leq 5.4\times10^{-7}$	1800
AVR 74/24	11.2	1250	$\leq 5.4\times10^{-7}$	2100
AVR 74/20	11.9	1250	$\leq 1.6\times10^{-7}$	1900
FRJ2-K11/3	10.0	1600**	$\leq 5.1\times10^{-6}$	1600
Ramp accident simulation tests in graphite furnace				
AVR 69/28	6.8	1530**	$\leq 6.8\times10^{-7}$	2150
AVR 70/18	7.1	2130**	$\leq 6.5\times10^{-6}$	2400
AVR 74/17	10.3	1250	$\leq 1.4\times10^{-7}$	2500
Accident simulation tests on LEU UO_2 MTR and HTR-Modul Proof Test elements (for comparison)				
HFR-K3/1	7.7	1250	$< 5.6\times10^{-8}$	1600
HFR-K3/3	10.2	1250	1.5×10^{-7}	1800
FRJ2-K13/2	8.1	1250	5.3×10^{-7}	1600
FRJ2-K13/4	7.8	1250	4.5×10^{-8}	1600 / 1800
HFR-K6/2	9.7	1050	1.0×10^{-8}	1600
HFR-K6/3	9.8	1050	3.2×10^{-6}	1600

* The AVR Sample No. represents the sequential sample of elements withdrawn for the AVR core for surveillance purposes; the Specimen No. is the order in which this element was withdrawn.
** No detectable release at 1250°C.

Figure 35 presents the fractional release data for the 11 fuel elements. Two elements, one GO2 designated AVR 70/26 and one from R2-K13 were subjected to isothermal tests of 1600°C, six elements, five AVR GO2 elements and one element from FRJ2-K11 were subjected to isothermal tests at temperatures of 1500ºC (2), 1600ºC, 1800ºC, 1900ºC and 2100ºC; and three AVR GO2 elements subjected to ramp tests ranging from 2150ºC to

2500°C. Included in the figure , for comparison purposes, are ^{85}Kr fractional release measurements made on six MTR and HTR-Modul Proof Test elements that were subjected to similar design basis accident simulation testing, but contained modern LEU UO_2 TRISO coated particle fuels.

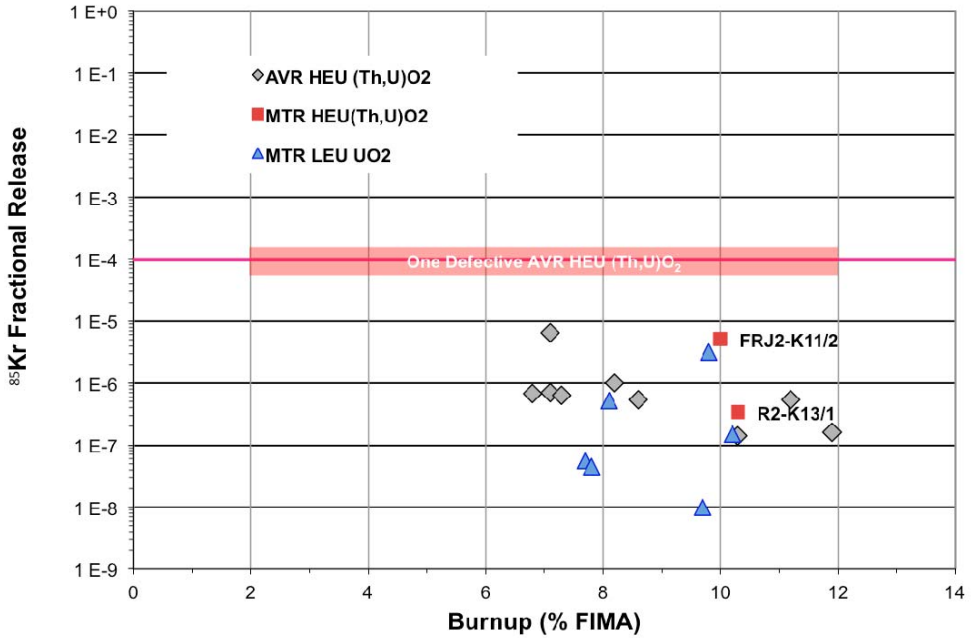

Figure 35. Noble gas ^{85}Kr fractional release monitored during accident simulation testing of AVR type GO2 fuel elements with HEU (Th,U)O_2 TRISO fuel (black symbols) compared with similar data obtained in MTR tests (red + blue symbols).

Figure 36 shows the ^{85}Kr fractional release measured on the three AVR GO2 fuel elements subjected to constant heating ramp tests ranging from 2150°C to 2500°C. The level of one particle failure is ~9.5×10^{-5} (black horizontal line).

The ^{85}Kr fractional release data presented in Figure 35 and Figure 36 are indicative of the EOL performance for the AVR GO2 fuel elements. For the six AVR GO2 elements subjected to isothermal accident tests, the release data were measured at the 1250°C hold period during the ramp-up to test temperature and are directly representative of EOL AVR performance. In cases where there was no detectable release at 1250ºC, the release measurements recorded are at the beginning of the soak temperature phase (elements AVR 70/26, AVR 70/7, and AVR 69/13). For those elements subjected to a constant heating ramp to temperatures > 2150°C, two elements (AVR 70/18 and AVR 74/17) had no detectable release at 1250ºC. The release fraction data shown for these elements represents the first detectable data and the temperature at which they were recorded. All of the AVR GO2 release data in Table 25 were used to estimate EOL performance – namely zero in-reactor failures during the real-HTGR environment of the AVR reactor.

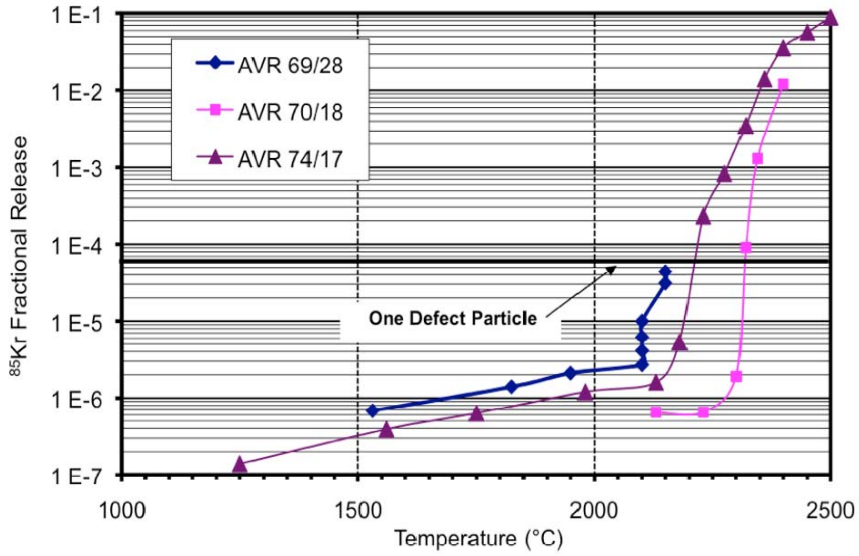

Figure 36. Fractional release of ^{85}Kr measured during accident simulation testing of AVR-GO2 fuel elements containing HEU (Th,U)O_2 TRISO fuel as function of heating temperature [Schenk 1983, Schenk 1988].

Based on the ^{85}Kr fractional release data from nine accident simulation tests on AVR GO2 elements, their performance at the time of discharge from the AVR was excellent. Most of the release data, with few exceptions, are $< 10^{-6}$ in the temperature range of 1250°C to well beyond 1800°C. The ^{85}Kr release fraction of a single HEU (Th,U)O_2 TRISO particle in an AVR GO2 element at these temperatures is ~9.5×10^{-5}. The AVR GO2 elements fractional release data also compare well with ^{85}Kr release data from accident simulation testing of MTR irradiated specimens for those with HEU (Th,U)O_2 TRISO particles and those with LEU UO_2 TRISO particles [Nabielek 2010].

Collectively, the nine AVR GO2 fuel elements represent a population of ~94,320 HEU (Th,U)O_2 TRISO coated particles, and with no observed in-reactor failure at discharge. This EOL performance represents an expected failure level of zero; taking account of the finite sample size, this translates to a failure fraction limit of 3.2×10^{-5}, at the 95% confidence limit.

4.4 Performance Assessment under Normal Operating Conditions

The in-reactor performance assessment for the HEU (Th,U)O_2 TRISO fuel system is based on five MTR accelerated irradiation tests (Table 18, with the exception of FRJ2-P25/Capsule 2) and the nine AVR GO2 type elements evaluated in this section. The five MTR tests contained a total of 30 irradiated fuel specimens with a total population of 126,664 (Th,U)O_2 TRISO particles. These fuel specimens were irradiated over a temperature range of 750ºC to 1600ºC, achieved peak burnups in the range of 8.5% to 15.6% FIMA, and accumulated fast neutron fluences (E > 16fJ) in the range of $< 1\times10^{25}$ to 8.5×10^{25} n/m^2. At EOL, a total of eight

in-reactor failed TRISO particles were estimated from the measured ^{85m}Kr and ^{88}Kr R/B values. Five were observed somewhere in the twelve 20 mm-diameter fuel zone elements in BR2-P25, one between the two 60 mm diameter elements in FRJ2-K11, and two in the 60 mm diameter element R2-K13/4. These results can be broken down in the following assessment of in-reactor performance:

- overall an in-reactor failure level of 1.1×10^{-4}, at the upper 95% confidence limit for all the $(Th,U)O_2$ TRISO fuel irradiated in the five MTR irradiation experiments;

- for the population of HEU $(Th,U)O_2$ TRISO particles irradiated in six standard 60 mm diameter fuel elements MTR irradiation experiments (FRJ2-K11, R2-K12 and -K13), three failures in a population of 82,720, yields a in-reactor failure level of 9.4×10^{-5}, at the upper 95% confidence limit; and

- for the population of HEU $(Th,U)O_2$ TRISO particles irradiated in non-standard fuel specimens, five failures in a population of 43,950, yields a failure level of 2.4×10^{-4}, at the upper 95% confidence limit.

Approximately 17,940 AVR GO2 type elements were manufactured and inserted into the AVR beginning in 1981 and again in 1985. Collectively these elements represent ~6.2% of all the fuel elements irradiated in the AVR. The AVR GO2 elements contained ~10,480 HEU $(Th,U)O_2$ TRISO particles per element. Over the period 1981 through 1988, a number of these elements were removed from the AVR core for post-irradiation evaluation and design basis accident simulation tests. As part of this surveillance effort, nine of the AVR GO2 elements with a burnup range from 7.1% to 11.9% FIMA accumulated under real-time HTGR conditions, were subjected to isothermal and constant heating ramp annealing tests. These nine standard elements represent a population of ~94,320 HEU $(Th,U)O_2$ TRISO coated particles. Fission gas release fractions (^{85}Kr), monitored in the heat-up phase of these tests, were used to evaluate their irradiation performance upon discharge from the AVR. Based on the analysis of these data, there were no in-reactor particle failures. These results lead to the following EOL assessment of their irradiation performance in the AVR:

- overall, an AVR in-reactor failure level of 3.2×10^{-5}, at the upper 95% confidence limit, and

- confirms that the real-time performance results for HEU $(Th,U)O_2$ TRISO fuel are somewhat better than the in-reactor performance observed in accelerated MTR testing.

Taken collectively, the MTR irradiation tests and the real-time AVR irradiations show a total of eight in-rector particle failures out of ~220,990 HEU $(Th,U)O_2$ TRISO particles examined. This yields a total in-reactor failure level for the HEU $(Th,U)O_2$ TRISO fuel system of 6.5×10^{-5}, at the one-sided upper 95% confidence level. These performance results are summarized in Table 26.

Table 26. Irradiation testing statistical evaluation for HEU (Th,U)O_2 TRISO coated fuel particles subjected to accelerated MTR irradiation tests and the real-time environment of the AVR.

Reference HTGR spherical elements and fuel bodies with HEU (Th,U)O_2 TRISO particles		No. fuel bodies	No. coated particles (N)	No. in-reactor failed particles (n)	Expected failure fraction (=n/N)	One-sided upper 95% confidence limit
Irradiation testing	MTRs	30	~126,670	8		
	AVR	9	~94,320	0		
	Total	39	~220,990	8	3.6×10^{-5}	6.5×10^{-5}

4.5 In-Reactor Performance Comparison with other HTGR Fuel Designs

As shown in Table 2, two additional HTGR fuel designs employing the TRISO-coating were under development within the German program in the period 1977 to 1985. These were:

- a two particle system consisting of a HEU UCO TRISO fissile particle and a ThO_2 TRISO fertile particle, Variant 3 for the PNP/HHT concepts, during the mid-to-late 1970s and early 1980s; and
- the LEU UO_2 TRISO particle variant which became the German reference HTGR fuel design for the LEU Program beginning in 1980 and continued afterwards.

The fuel development efforts for both fuel systems included a full complement of qualification tests carried out in accelerated MTR testing coupled with large, full-scale industrial manufacturing campaigns and irradiation testing in the real-time AVR. All of the irradiation tests identified in Table 2 were executed successfully; however, the level of effort dedicated to evaluating their irradiation performance was much diminished with respect to the UCO TRISO/ThO_2 TRISO system. By the time, many of these MTR irradiation tests were completed, Germany's switch to the LEU Program was complete and efforts to fully evaluate their irradiation performance were abandoned.

The successful development of the LEU UO_2 fuel system within the German program and the irradiation performance results for the LEU UO_2 TRISO fuel particle design have been well-documented [Burck 1988, Nabielek 1990, Gontard 1990, Petti 2010, Nabielek 2010]. The LEU UO_2 fuel system was licensed in Germany in the 1990s for the HTR-Modul concept [Interatom 1988] and it remains today a viable fuel concept for HTGR application worldwide.

A comparison between the in-reactor performance of the HEU (Th,U)O_2 TRISO fuel system and the LEU UO_2 TRISO fuel system is provided in Table 27. Since both fuel systems were subjected to similar development efforts, this comparison is straightforward. Both fuel systems were tested in qualification tests carried out in European MTRs and both were the subject of two large fabrication and irradiation campaigns in the AVR. Comparing the operating conditions during irradiation shows a similar burnup and accumulated fast fluence range. The major difference was that the peak operating temperatures in the MTR tests were

in the 1200ºC to 1600ºC range for the HEU (Th,U)O_2 fuels as compared to the 1100ºC to 1200ºC for the LEU UO_2 fuels. This operating temperature difference may explain why the (Th,U)O_2 fuels have a higher in-reactor failure level of ~6.5×10^{-5} as compared to ~2.1×10^{-5} for the LEU UO_2 fuels.

Table 27. Comparison of in-reactor fuel performance between the HEU (Th,U)O_2 TRISO and the LEU UO_2 TRISO fuel systems.

Standard HTGR spherical elements and fuel bodies with (Th,U)O_2 TRISO particles		**No. fuel bodies**	**No. coated particles (N)**	**No. in-reactor failed particles (n)**	**Expected failure fraction (=n/N)**	**One-sided upper 95% confidence limit**
LEU UO_2 TRISO						
Irradiation testing	MTRs Standard Non-stand	 19 45	 276,680 80,572	 0 9		
	AVR	24	393,600	0		
	Total	88	750,852	9	1.2×10^{-5}	2.1×10^{-5}
HEU (Th,U)O_2 TRISO						
Irradiation testing	MTRs Standard Non-stand	 6 24	 82,720 43,950	 3 5		
	AVR	9	94,320	0		
	Total	39	220,990	8	3.6×10^{-5}	6.5×10^{-5}

5. ACCIDENT SIMULATION

Fuel temperatures under the unrestricted-core-heatup accident scenario envisioned for the large HTGR plant concepts such as the PNP and HHT do lead to a nuclear shutdown because of the large negative temperature coefficient in the core. However, the afterheat production resulting from fission product decay in combination with a loss of forced circulation may lead to unrestricted core heatup. For the large PNP/HHT concept HTGR plants, fuel temperatures can go to 2500°C or higher. In contrast, the smaller modular HTGRs, with their tall, small diameter core automatically limits the maximum temperature to ~1600°C. The coolant in both the large PNP/HHT plants and in the modular HTGRs is still helium.

5.1. Accident Simulation Test Facilities

These high temperature accident scenarios were simulated in the hot cell test furnaces located at the Research Center Jülich (FZJ), Germany. Accident simulation was accomplished by externally heating irradiated spherical fuel elements under a purged helium environment. The He purge circuit incorporated the capability for continuous on-line measurement of ^{85}Kr release from the heated fuel in external cold traps. Figure 37 is a schematic of the hot-cell furnace configuration that was developed [Schenk 1978, Schenk 1983, Schenk 1988, Schenk 1989, Nabielek 1989, Schenk 1990] and used for accident simulation testing of irradiated spherical fuel elements, some of which contained HEU (Th,U)O_2 LTI-TRISO fuel particles. Prior to 1984, a graphite high-temperature furnace (so-called "A-Test" annealing furnace) described in Figure 38 was the primary furnace employed. The "A-Test" furnace facility provided the capability of constant heatup ramps to a peak temperature, as high as 2500°C. Continuous fission gas release monitoring was possible but the release of solid fission products could only be estimated by measuring the difference in key solid fission product inventories before and after the accident simulation test.

In the early 1980s, irradiated fuel elements containing high-quality HEU (Th,U)O_2 and LEU UO_2 TRISO fuel particles were becoming available for experimental post-irradiation evaluation. At about this same time, researchers at the Research Center Jülich were experiencing repeated temperature control problems with the standard "A-Test" furnace annealing facility. These losses in temperature control problems were a direct result of annealing tests performed on lesser quality fuel elements from early AVR and THTR production campaigns. As a result of these high solid fission product releases, the "A-Furnace" facility's control system became compromised. Thus, the need was generated for a new high-temperature heating facility with state-of-the-art fission product detection capabilities to quantify gaseous and solid fission product behavior during accident condition testing based on new HTGR design basis events.

The new accident simulation facility was designed to demonstrate the passive safety characteristics of smaller, modular HTGR concepts. The high-temperature furnace in this facility was a tantalum furnace allowing heating tests up to 1800°C with a built-in cold-finger apparatus (KÜFA=Kühlfinger-Anlage). Inclusion of the cold-finger assembly added the capability of a semi-continuous measurement of solid fission product release in addition to the continuous gas release monitoring without having to interrupt the heating test. Figure 39 is a full schematic of the tantalum heating furnace showing the cold-finger apparatus, fuel element placement within the furnace heating zone, and the major components of the KÜFA facility.

Figure 40 is a schematic of fission product release detection capabilities of the KÜFA facility and the handling of the deposition plates. The KÜFA facility has been relocated to and is now operated at the Institute of Transuranium (ITU) in Karlsruhe, Germany, (a European Commission research center) and it retains its state-of-the-art capabilities today.

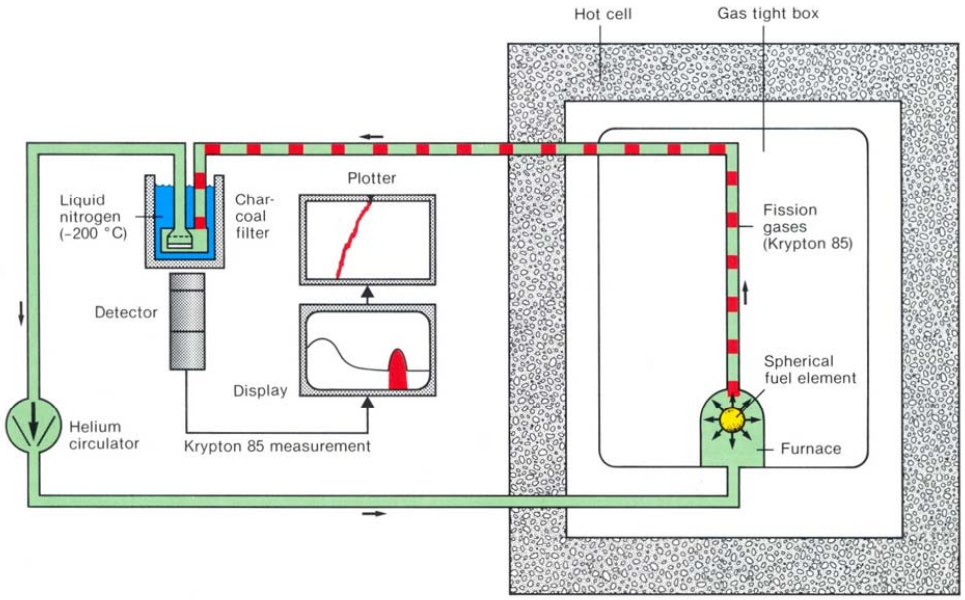

Figure 37. Hot-cell setup for accident simulation tests with irradiated fuel elements.

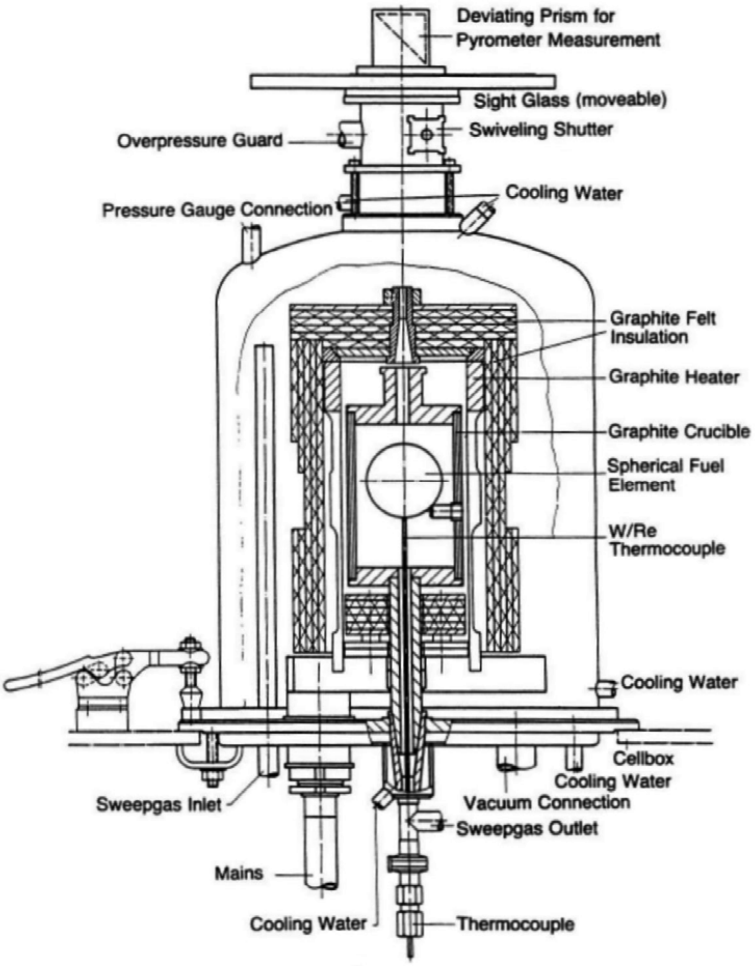

Figure 38. Graphite heating furnace, designated "A-Test" apparatus for core heatup accident simulation testing of fuel spheres up to 2500°C [Schenk 1983].

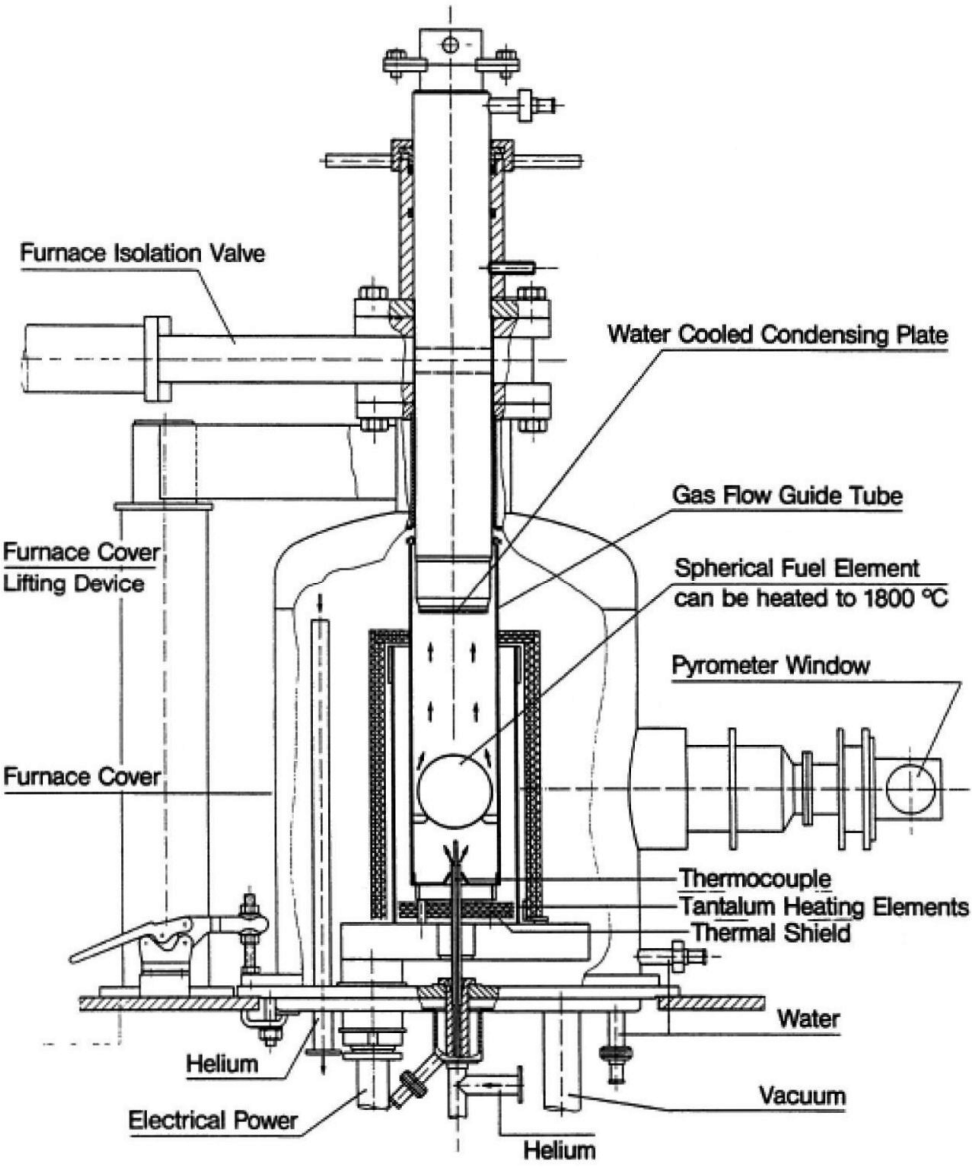

Figure 39. The KÜFA: a tantalum heating furnace with a water cooled cold-finger for accident simulations tests up to 1800°C.

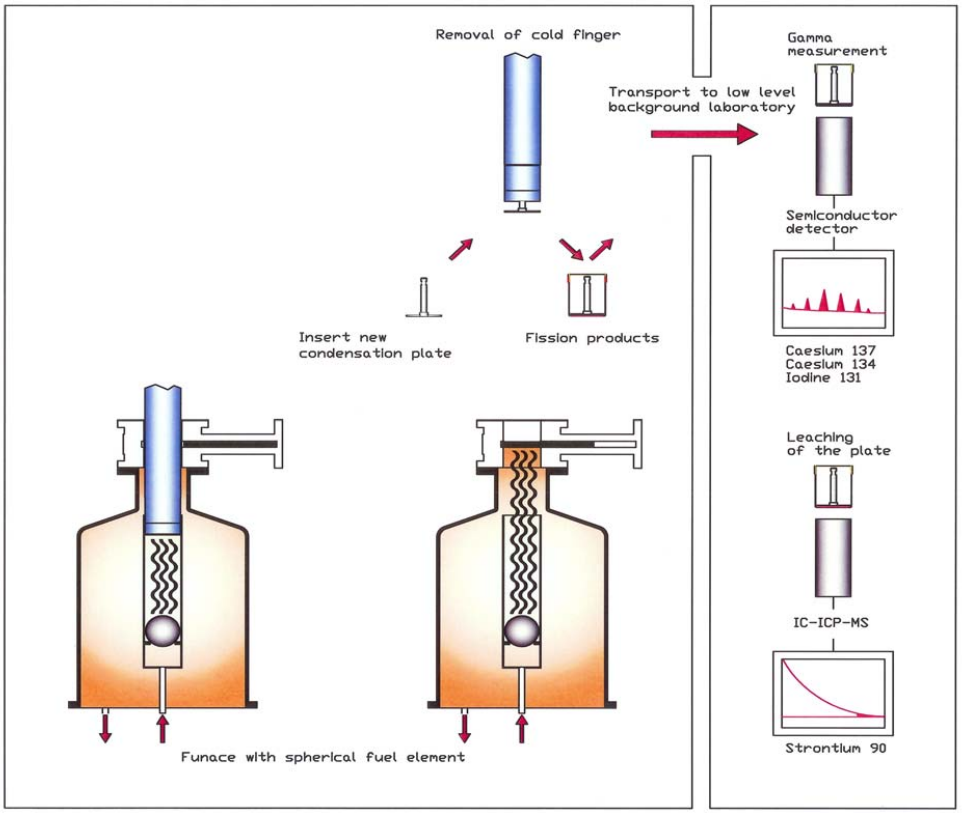

Figure 40. KÜFA operational diagram of the exchange of the cooled steel condensation plate and its analysis by gamma-spectrometry and ICP mass-spectrometry [Toscano 2010, Freis 2010, Freis 2010b].

The fuel element heatup methodology [Schenk 1988] developed for accident simulation testing at the Research Center Jülich is shown in Figure 41. Typically the heating profile for smaller, modular HTGR concepts like the HTR-Modul would be limited to 1600ºC or 1800ºC, and accident simulation testing would be carried out in the KÜFA facility. Heating profiles for large HTGRs like the PNP or HHT concepts would be to higher temperatures up to 2500ºC, and such accident simulation testing would generally be performed in the "A-Test" furnace facility. The hold points at 1050ºC and 1250ºC were established for equilibration to re-adjust the fuel to their prior EOL irradiation conditions. The ^{85}Kr gas release data measured at these hold point temperatures can be used to estimate the fuel element's EOL performance in terms of the presence of failed fuel particles in the prior irradiation. This type of analysis was carried out on HEU (Th,U)O_2 TRISO fuels (Table 25 and Figure 35) and previously for LEU UO_2 TRISO fuels [Nabielek 2010] successfully, and is particularly useful for AVR irradiated fuel elements where no in-reactor R/B data are available.

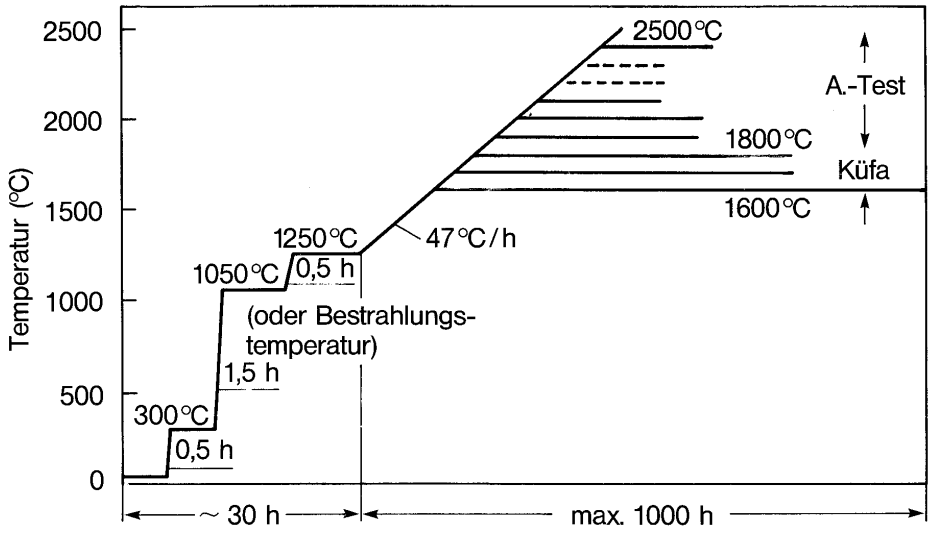

Figure 41. Typical temperature/time profile in the ramp-up to isothermal accident condition heating tests with the 1250°C equilibration period being used to determine the particle failure level at the end of the preceding irradiation.

The accident simulation tests conducted on reference 60 mm diameter irradiated spherical fuel elements with HEU (Th,U)O_2 TRISO fuels include:

- two isothermal accident simulation tests performed in the KÜFA test facility at temperatures of ~1600ºC;
- six isothermal accident simulation tests in the "A-Test" furnace at temperatures of 1500ºC (2), 1600ºC, 1800ºC, 1900ºC, 2100ºC; and
- three constant temperature ramp (47ºC/hr) simulation tests also performed in the "A-Test" facility – one element each to 2150ºC, 2400ºC, and 2500ºC.

A total of eleven irradiated fuel elements with (Th,U)O_2 TRISO fuel were subjected to accident conditions tests and are characterized along with their irradiation conditions prior to the heating tests in Table 28. The results from one of the accident simulation tests, FRJ2-K11/Sphere 3 were not included in this performance evaluation because of a loss of temperature control during heatup to the planned accident simulation temperature. (Indications were that the final heating temperature, based on the observed solid fission product release results (see Table 25), was considerable higher than the intended 1600ºC.) Nine of the accident simulation tests contained the HEU (Th,U)O_2 TRISO particle batch HT 150-160, 162-167 within GO2 type fuel elements and were part of the AVR XV Reload. The remaining irradiated fuel element subjected to accident testing contained the HEU (Th,U)O_2 TRISO particle batch EO 1674, and was irradiated in the MTR accelerated experiment R2-K13/Capsule 1. Both of these particle batches were characterized in Table 6

and the fuel elements in Table 10. The primary difference between the AVR GO2 fuel elements and the R2-K13 elements were the heavy metal loadings. The AVR GO2 elements had an N value (Th/^{235}U ratio) of 5.00 with a total heavy metal loading of 6.140 g/element compared to an N value of 10.02 for the R2-K13 fuel elements with a total heavy metal loading of 11.367 g/element. The enrichment of the HEU (Th,U)O_2 TRISO fuel particles in the AVR GO2 elements was 92.48 wt% ^{235}U compared to 89.01 wt% ^{235}U for the particles in the R2-K13 elements. The AVR GO2 elements and the R2-K13 were both fabricated with the same type A3-27 graphite matrix.

Table 28. Irradiation conditions and HEU (Th,U)O_2 TRISO fuel particle batches contained in the irradiated spherical fuel elements subjected to accident simulation testing.

Fuel element	**(Th,U)O_2 particle batch**	**Irradiation conditions**			**Peak temperature of accident simulation test [ºC]**
		Temperature [ºC]	**Burnup [% FIMA]**	**Fluence [10^{25} n/m^2, E>16 fJ]**	
KÜFA test facility					
AVR 70/26	HT 150-160, 162-167	900-1200	8.2	2.0	1610
R2-K13/1	EO 1674	1000 - 1200	10.3	8.3	1600
"A-Furnace" test facility					
AVR 70/15	HT 150-160, 162-167	900-1200	7.1	1.7	1500
AVR 70/7	HT 150-160, 162-167	900-1200	7.3	1.8	1500
AVR 69/13	HT 150-160, 162-167	900-1200	8.6	2.1	1800
AVR 74/24	HT 150-160, 162-167	900-1200	11.2	2.7	2100
AVR 74/20	HT 150-160, 162-167	900-1200	11.9	2.9	1900
AVR 69/28	HT 150-160, 162-167	900-1200	10.0	1.7	2150
AVR 70/18	HT 150-160, 162-167	900-1200	6.8	1.7	2400
AVR 74/17	HT 150-160, 162-167	900-1200	7.1	2.5	2500
FRJ2-K11/ Sphere 3*	HT 150-160, 162-167	900-1166	10.3	0.062	1600

* Results for the 1600ºC accident condition test for FRJ2-K11/Sphere 3 were discarded because of the loss of temperature control during the heatup portion of the test.

Table 29. Accident Simulation test results for irradiated reference fuel elements containing HEU (Th,U)O_2 TRISO fuel particles.

Fuel element	Burnup [% FIMA]	Heating program			Release fractions				
		T_{max} [°C]	1250°C to T_{max} [h]	Heating time [h]	^{85}Kr	^{134}Cs	^{137}Cs	^{90}Sr*	^{110m}Ag*
AVR 70/7	7.3	1500 1500 1500	1.5 1.5 1.5	100 50 50 total: 200	$< 7\times10^{-6}$ $< 7\times10^{-6}$ $< 7\times10^{-6}$ $< 2\times10^{-5}$	$< 2\times10^{-2}$ $< 2\times10^{-2}$ $< 2\times10^{-2}$ $< 2\times10^{-2}$	$< 2\times10^{-2}$ $< 2\times10^{-2}$ $< 2\times10^{-2}$ $< 2\times10^{-2}$	–	–
AVR 70/15	7.1	1500 1500	7 1.5	90 50 total: 140	$< 8\times10^{-5}$ $< 3\times10^{-6}$ $< 8\times10^{-5}$	$< 2\times10^{-2}$ $< 2\times10^{-2}$ $< 2\times10^{-2}$	$< 2\times10^{-2}$ $< 2\times10^{-2}$ $< 2\times10^{-2}$	–	–
AVR 70/26	8.2	1610	1.5	312	$< 1\times10^{-5}$	**	$< 3\times10^{-5}$	$< 1.7\times10^{-5}$	$< 1.9\times10^{-2}$
R2-K13/1	10.3	1600	7.5	1000	$< 3.5\times10^{-4}$	$< 1.6\times10^{-2}$	$< 1.5\times10^{-2}$	$< 1.2\times10^{-3}$	~1
AVR 69/13	8.6	1800	14 2.5 3.5 12	10 10 22 50 total: 92	$< 1\times10^{-6}$ $< 1\times10^{-6}$ $< 3\times10^{-5}$ $< 9\times10^{-3}$ 9.0×10^{-3}	$< 1\times10^{-2}$ $< 1\times10^{-2}$ $< 1\times10^{-2}$ 5×10^{-1} 5.0×10^{-1}	$< 1\times10^{-2}$ $< 1\times10^{-2}$ $< 3\times10^{-2}$ 4.8×10^{-1} 4.8×10^{-1}	–	–
AVR 74/20	11.9	1900	15	50	$< 2.1\times10^{-2}$	$< 4.2\times10^{-1}$	$< 4.3\times10^{-1}$	–	–
AVR 74/24	11.2	2100	18	30	$< 1\times10^{-1}$	$< 5.0\times10^{-1}$	$< 5.0\times10^{-1}$	–	–
AVR 69/28	6.8	2150	58	6	$< 4\times10^{-5}$	$< 2.2\times10^{-1}$	$< 2.2\times10^{-1}$	–	–
AVR 70/18	7.1	2400	28	Ramp	$< 1.2\times10^{-2}$	**	$< 8.2\times10^{-1}$	–	–
AVR 74/17	10.3	2500	27	Ramp	$< 1.2\times10^{-1}$	$< 8.3\times10^{-1}$	$< 8.3\times10^{-1}$	–	–

* Measured only in two tests conducted in KÜFA facility.
** Not evaluated/inexact measurement

The complete set of fission product release data obtained from accident simulation tests on irradiated fuel elements containing HEU (Th,U)O_2 TRISO fuel particles are given in Table 29. The ^{85}Kr release results were obtained from the cold traps in the gas circuit. Solid fission product releases were measured in two different ways: in tests performed in the KÜFA facility, measurements were made on the cold finger plates; in tests performed in the "A-Test" facility, the loss of inventory was obtained by measurement of the spherical fuel element inventory before and after the heating procedure.

5.2. Observations from the Ramp Tests to 2500ºC

The three ramp tests on AVR GO2 fuel elements AVR 69/28, AVR 70/18 and AVR 74/17 were previously shown in Figure 36. The ^{85}Kr fission gas release fractions were in the ~6×10^{-7} to < 3×10^{-6} range to temperatures beyond 2050ºC. These release data are far below the inventory of a single particle indicating no HEU (Th,U)O_2 TRISO particle failure at the time of their discharge from the AVR. Figure 42 is a comparison of ^{85}Kr fission gas release data for two of the AVR GO2 elements in Figure 36 (AVR 70/18 and AVR 74/17) with similar data obtained during accident simulation ramp tests on AVR GLE3 fuel elements (AVR 70/19 and AVR 74/8) containing LEU UO_2 TRISO particles. The ^{85}Kr fractional release data, as a function of heating temperature, are comparable for all four AVR irradiated elements. The GO2 elements with HEU (Th,U)O_2 fuels had a significantly higher burnup – 7.1% and 10.3% FIMA, compared to 2.2% and 2.9% FIMA for the LEU UO_2 fueled elements. No particle failure is indicated up to temperatures above 2050ºC for any of the four elements tested.

As the ramp temperature exceeds ~2100ºC, the ^{85}Kr fractional release curves make a dramatic shift upward and continues to rise as the temperature increases. At temperatures above 2100ºC, the release curve quickly reaches a level indicative of catastrophic particle failure. As shown in Figure 42, this occurs in the (Th,U)O_2 TRISO fuel as well as in the UO_2 TRISO fuel at nearly the same temperature. This dramatic change in performance is due to a serious deterioration of the TRISO coatings on fuel particles caused by the onset of SiC thermal decomposition. At very high temperatures, 1800°C to 2200°C, the SiC layer will decompose into its constituent elements [Ikawa 1978, Benz 1981, Nabielek 1983]:

$$SiC(s) \rightarrow Si(g) + C(s).$$

The Si(g) vaporizes away leaving a porous carbon material behind. Studies [Benz 1982] in the temperature range of 1600°C to 2200°C on unirradiated fuel particles with and without their OPyC coatings have described this decomposition process in an Arrhenius relationship characterized by a thinning rate for the SiC layer given by

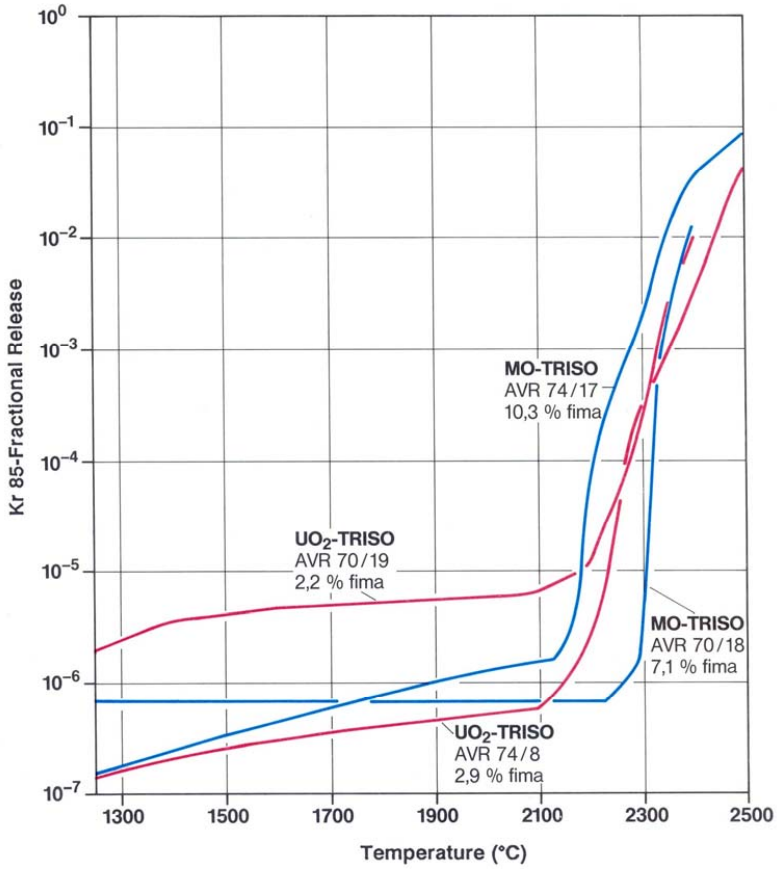

Figure 42. Comparison of the ^{85}Kr fractional release from irradiated AVR GO2 (HEU (Th,U)O_2 TRISO) and AVR GLE3 (LEU UO_2 TRISO) fuel elements as a function of temperature during accident simulation ramp tests [Schenk 1988].

$$k = k_o e^{-\frac{Q}{RT_c}}$$

where

k is the empirically derived SiC decomposition rate [m/s];

Q is the activation energy, = 556 kJ/mol [Benz 1981];

T is temperature [K];

R is the universal gas constant = 8.3145 J/mol/K; and

k_o is a frequency factor dependent on coated particle batch and manufacturing conditions.

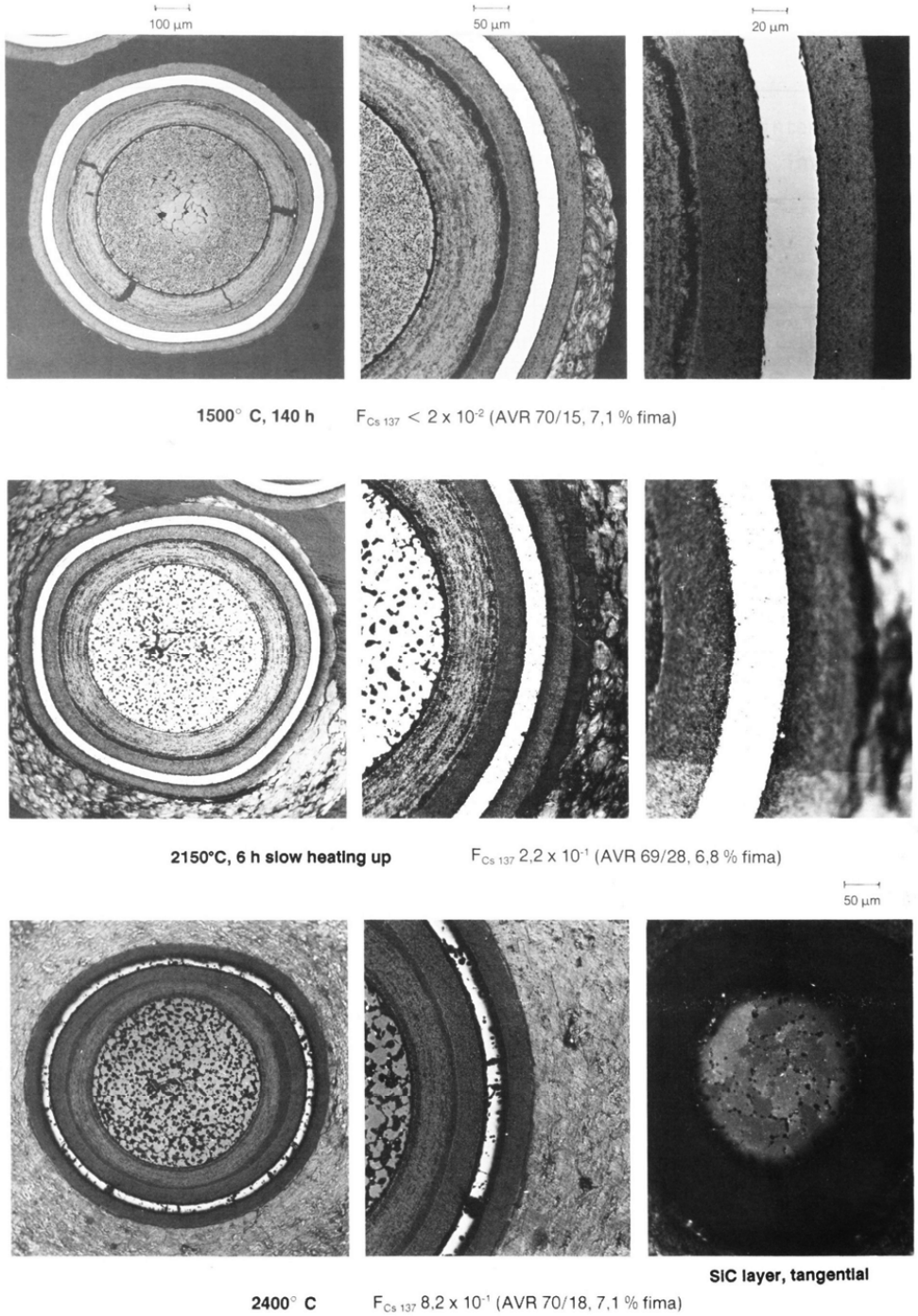

Figure 43. Ceramographic sections of AVR GO2 fuel elements containing HEU (Th,U)O_2 TRISO fuel particles heated in accident condition simulation tests [Schenk 1988].

At HTGR normal operating temperatures of < 1200°C, the SiC decomposition rate is negligibly small and is not a contributor to particle failure. Even at anticipated accident conditions of 1600°C for hundreds of hours, SiC decomposition is insignificant. Figure 43 shows this visible deterioration of the SiC layer observed in the TRISO coatings heated to temperatures > 2100°C, compared to similar TRISO coatings heated to temperatures of 1500°C.

5.3. Observations from Isothermal Tests in Temperature Range of 1500ºC to 2100ºC

Six isothermal accident simulation tests were conducted in the "A-Test" furnace facility on AVR GO2 fuel elements AVR 70/15, AVR 70/7, AVR 69/13, AVR 74/24, AVR 74/20 and the FRJ2-K11/3 fuel element with burnups ranging from 7.1% to 11.9% FIMA. Figure 44 shows the ^{85}Kr fractional release data for all of these elements as a function of accident simulation temperature. All of these elements were heated at a constant rate of ~50ºC/h until their design isothermal soak temperature was achieved. At this point temperature was maintained at this soak temperature for the prescribed time. The details of the heating program for each of these six fuel elements were presented in Table 29. Three elements – AVR 70/7 (1500ºC), AVR 70/15 (1500ºC) and AVR FRJ2-K11/3 (1600ºC) had isothermal soak temperatures ≤ 1600ºC. Elements AVR 70/15 and FRJ2-K11/3 appear to have failed particles present at the end of their respective isothermal phase of the accident simulation. For these two elements, the ^{85}Kr fractional release data increased several orders of magnitude during this phase and were close to or exceeded the level of one equivalent particle failure (Figure 44). As noted previously, the results for FRJ2-K11/3 are thought to have been compromised because of loss of temperature control during the heatup phase of testing in the "A-Test" facility.

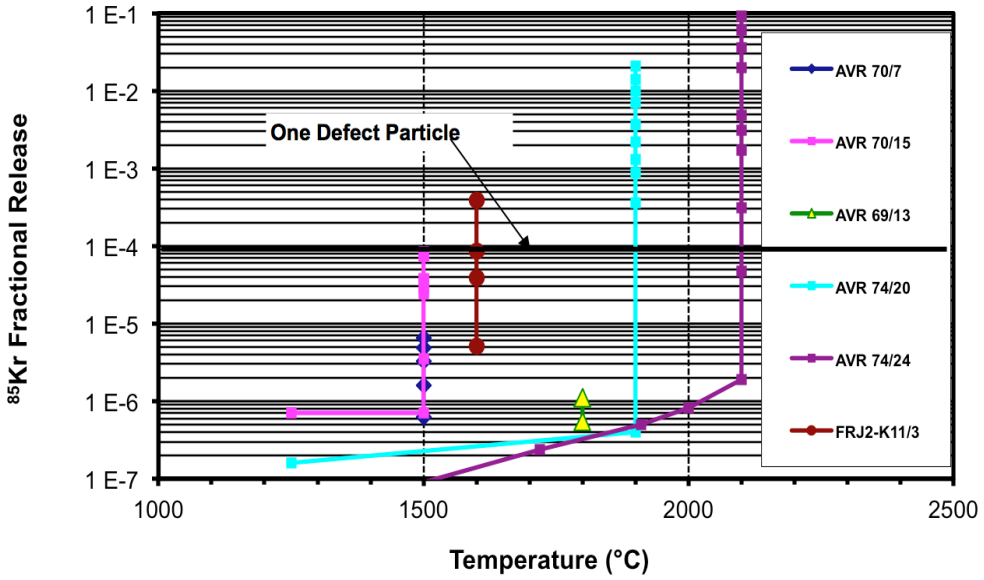

Figure 44. Noble gas ^{85}Kr fractional release measured during isothermal accident simulation tests conducted on six AVR type GO2 fuel elements with TRISO (Th,U)O_2 TRISO fuel particles.

The remaining elements – AVR 69/13 (1800ºC), AVR 74/20 (1900ºC) and AVR 74/24 (1500ºC) all had isothermal soak temperatures ≥ 1600ºC. Each of these elements also exhibited a definitive rise in their ^{85}Kr fractional release at the end of the isothermal phase of the accident simulation. Elements AVR 74/20 and AVR 74/24 had significant numbers of failed particles present at this point. AVR 69/13 experienced some increase in ^{85}Kr release but the isothermal heating phase was too short to fail any particles.

The ^{85}Kr fractional release data are consistent with the cesium release fractions measured on all AVR GO2 fuel elements. All of the cesium fractional release data are in the $< 2\times10^{-2}$ to $\sim5\times10^{-1}$. Figure 45 is a ceramographic section of AVR GO2 element 69/13 after completing its accident simulation test. The ceramography showed no evidence of corrosion in the SiC layer or any detrimental effects due to the 92 h exposure at temperatures of 1800ºC. The only observable effect was some cracking in the overcoating layer surrounding the TRISO particle.

5.4. Performance Evaluation of 1600°C Heating Tests

The KÜFA heating facility for accident condition testing was installed and made operational in 1982-83. Fortunately, some of the first irradiated fuels available for evaluation in the KÜFA facility (1984) were fuel elements containing HEU $(Th,U)O_2$ TRISO fuel particles. Two 1600°C isothermal heating tests were performed on the GO2 fuel element AVR 70/26 and the fuel element from R2-K13/Capsule 1. Pre-irradiation characterization data on the fuel particle batches and the as-manufactured fuel elements are available in Table 6 and Table 10, respectively. The EOL irradiation conditions for the two elements were presented in Table 28 and the heating programs for each were presented in Table 29. The fractional release results for the key fission products ^{85}Kr, ^{90}Sr, ^{137}Cs, and ^{110m}Ag are shown in Figure 46 for the R2-K13/1 and AVR 70/26 accident simulation test.

Fuel element AVR 70/26 was heated from its equilibration temperature to 1600°C over a period of 1.5 hours and then held at 1600°C for 312 hours. From the start of the heatup process to the cool down, the noble gas ^{85}Kr fractional release was continuously monitored. Solid fission products – ^{90}Sr, ^{137}Cs and ^{110m}Ag were monitored semi-continuously throughout the heatup and the isothermal heating phases. The AVR 70/26 fractional release data presented in Figure 48 represents a contiguous release profile for the entire test.

The fuel element from R2-K13/Capsule 1 was heated from equilibration to 1600°C over 7.5 h and then held at 1600°C for 1000 h. This is the longest accident simulation test completed in the KÜFA heating facility to date. Noble gas ^{85}Kr fractional release was continuously monitored throughout the test from start to cool down, and the solid fission product releases were monitored semi-continuously throughout the heatup and the isothermal heating phases. The contiguous release profiles for R2-K13/1 shown in Figure 46 are in detail for the first 500 hours and then only the endpoint release values.

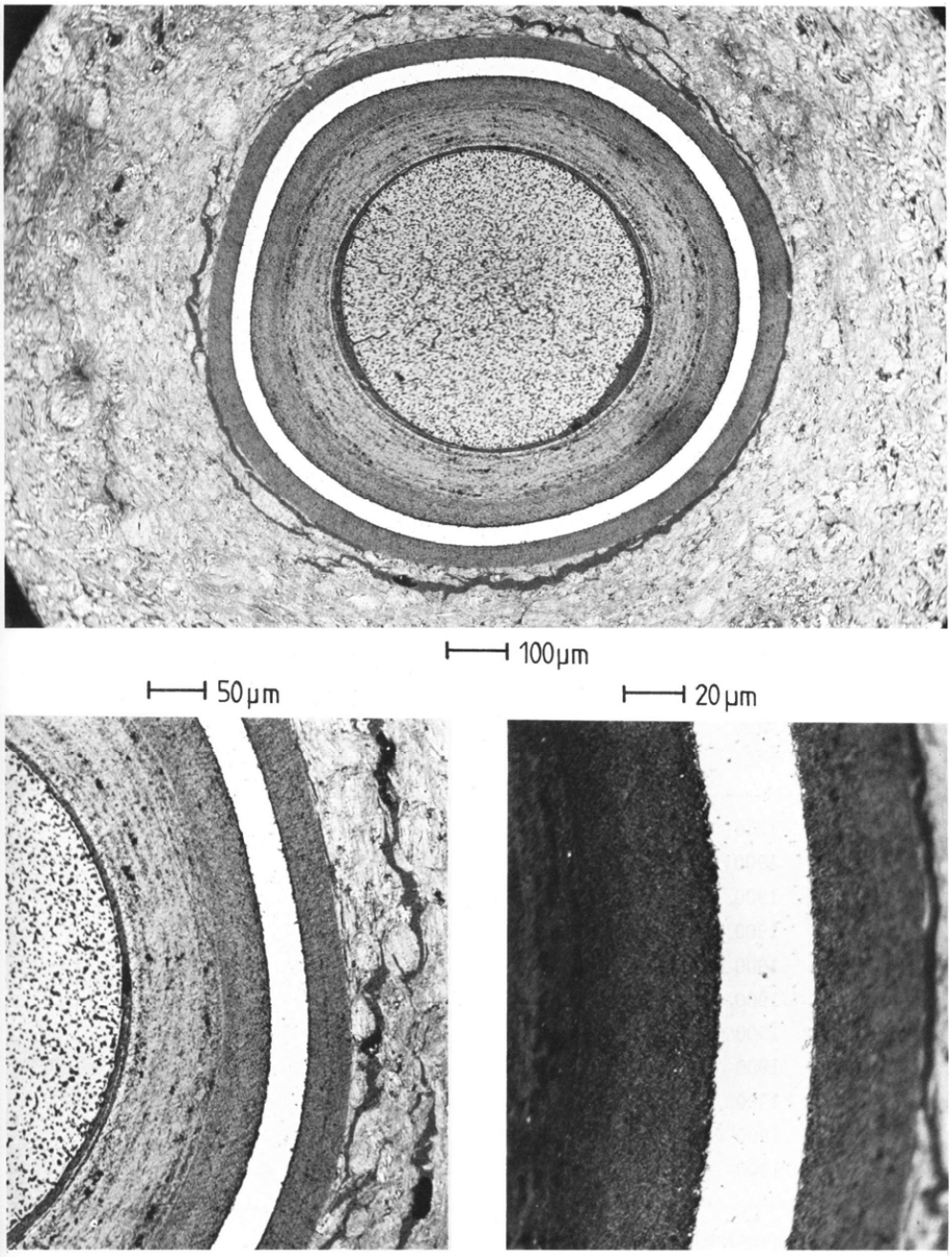

Figure 45. Ceramographic sections of TRISO mixed oxide particle from AVR GO2 fuel element 69/13 irradiated to 8.6% FIMA and heated for 92 hours at 1800°C [Schenk 1989].

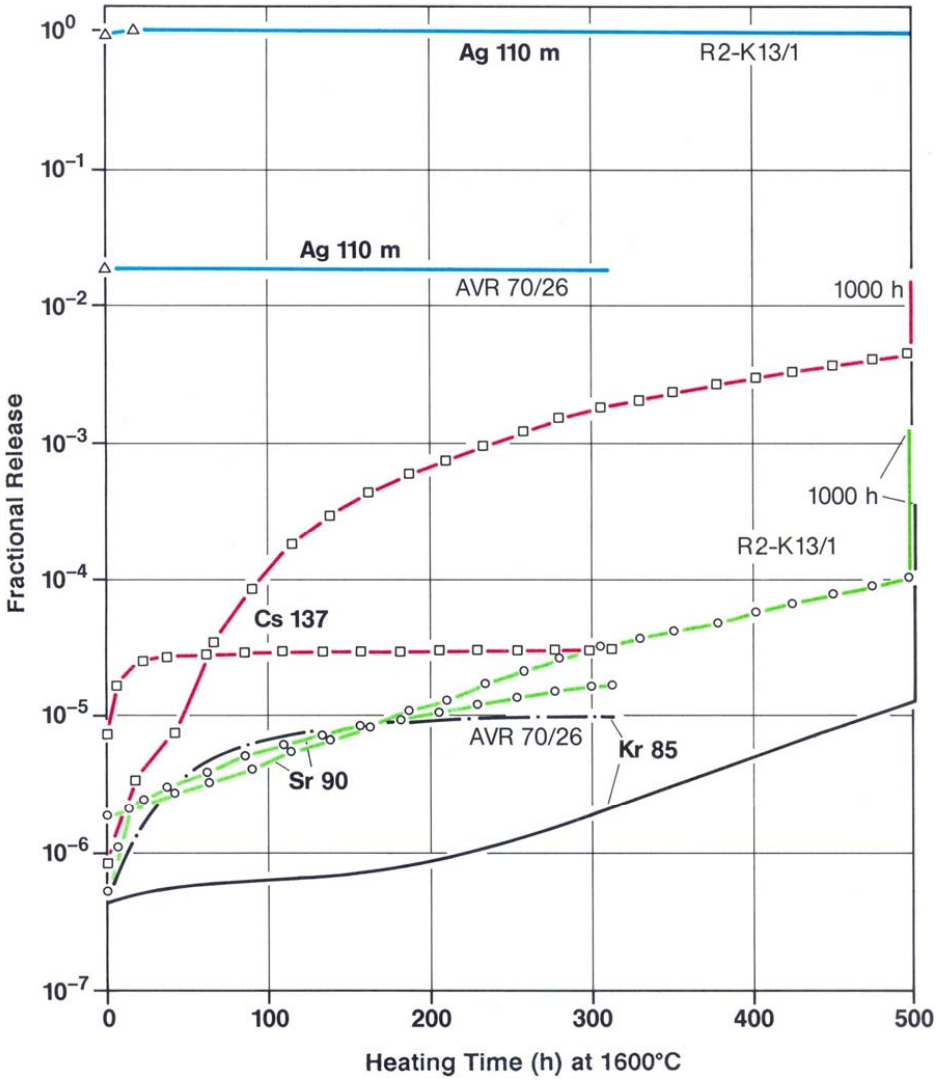

Figure 46. Fission product release fractions measured during 1000 h (R2-K13/1) and 312 h (AVR 70/26) isothermal heatup tests at 1600°C from fuel elements with HEU (Th,U)O_2 TRISO particles [Schenk 1988].

The fractional release data during the heatup phase between equilibration at 1250ºC to the isothermal heating phase at 1600°C are shown in Figure 47 for AVR 70/26 and R2-K13/1. The fractional release profiles are essentially flat over this 350ºC rise in temperature for the R2-K13/Capsule 1 fuel element. At the beginning of the isothermal heatup phase the ^{85}Kr, ^{90}Sr, and ^{137}Cs release fractions are all significantly < 10^{-5}. Only the fractional release values for the activation product ^{110m}Ag are high. At the beginning of the isothermal heating, the GO2 fuel element AVR 70/26 had released ~2% of its ^{110m}Ag inventory and the R2-K13/Capsule 1 fuel element has released close to 100% of its original ^{110m}Ag inventory.

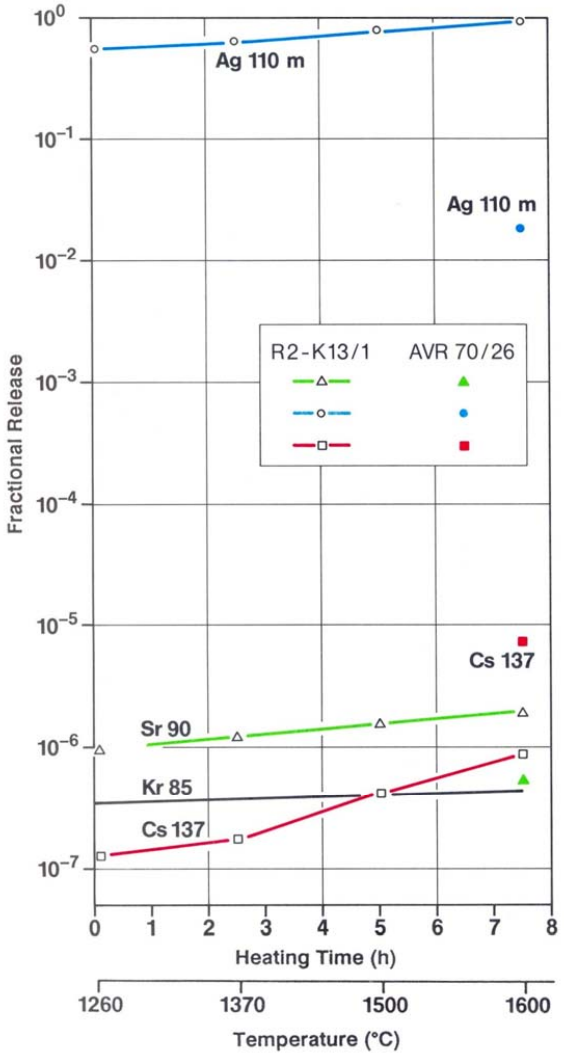

Figure 47. Fractional release data monitored during the heatup phase between equilibration and the isothermal heating temperature at 1600°C in heatup tests with fuel elements AVR 70/26 (endpoints only) and R2-K13/1 [Schenk 1988].

Figure 48 presents the noble gas ^{85}Kr fractional release for AVR 70/26 and R2-K13/1 for the first 200 hours of their 1600ºC isothermal accident simulation tests [Schenk 1988, Schenk 1989]. The fractional release for AVR 70/26 remained $< 10^{-5}$ for the duration of its 312 hours of isothermal heating. In R2-K13/1, the ^{85}Kr fractional release started out at $< 10^{-6}$ and remained below 10^{-6} for the first 200 hours. The ^{85}Kr fractional release data from other AVR GO2 type elements subjected to accident condition simulation tests with HEU $(Th,U)O_2$ TRISO fuels are also shown in Figure 48; the release fraction for R2-K13/1 is significantly lower than for the AVR GO2 fuel elements for the first 200 hours of heating at 1600°C.

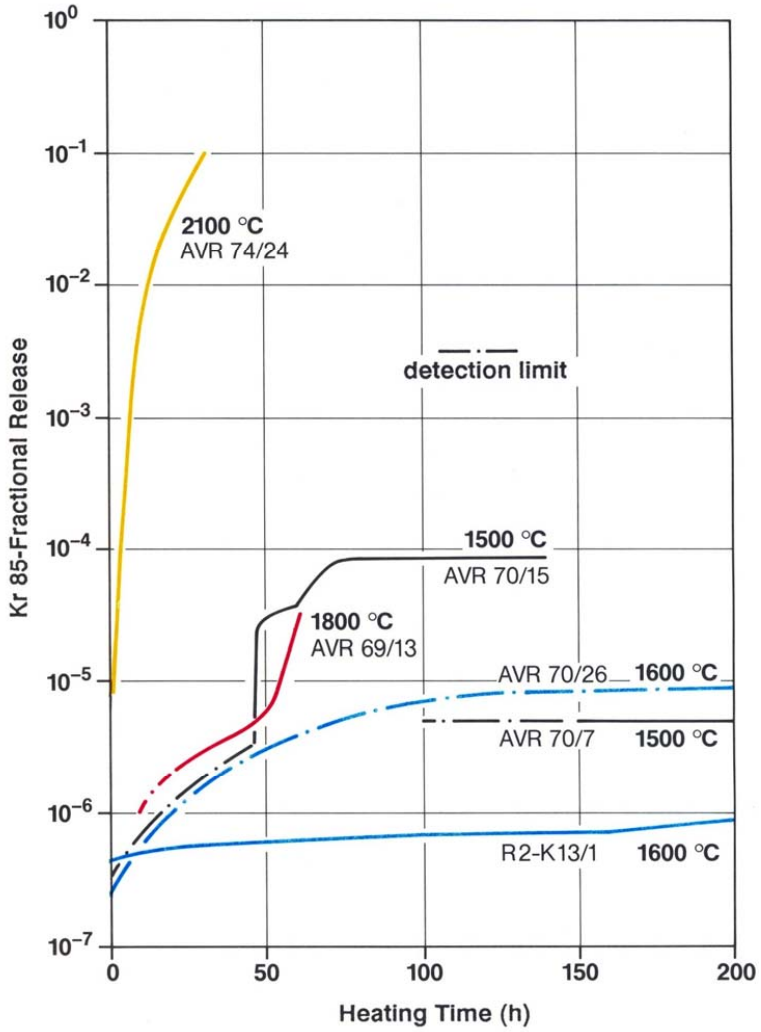

Figure 48. Noble gas ^{85}Kr fractional release, for AVR 70/26 and R2-K13/1 remained < 10^{-5} well beyond 200 hours at 1600ºC indicating no particle failure in either element [Schenk 1988].

The ^{137}Cs fractional release data monitored for AVR 70/26 and R2-K13/1 are shown in Figure 49 and their profiles are quite different from the very beginning of the isothermal heating phase. The ^{137}Cs fractional release from the GO2 fuel element AVR 70/26 rises initially at the beginning of the 1600ºC heating phase and then flattens out quickly at ~3×10^{-5} after ~30 hours of heating. In R2-K13/1, the ^{137}Cs fractional release starts out at an about 10 times lower value than for AVR 70/26 and begins to rise immediately with the 1600ºC heating phase. After ~60 hours of heating at 1600ºC, the R2-K13/1 ^{137}Cs fractional release fraction exceeds the fractional release in the AVR 70/26 element and continues to increase throughout the remainder of the heating phase.

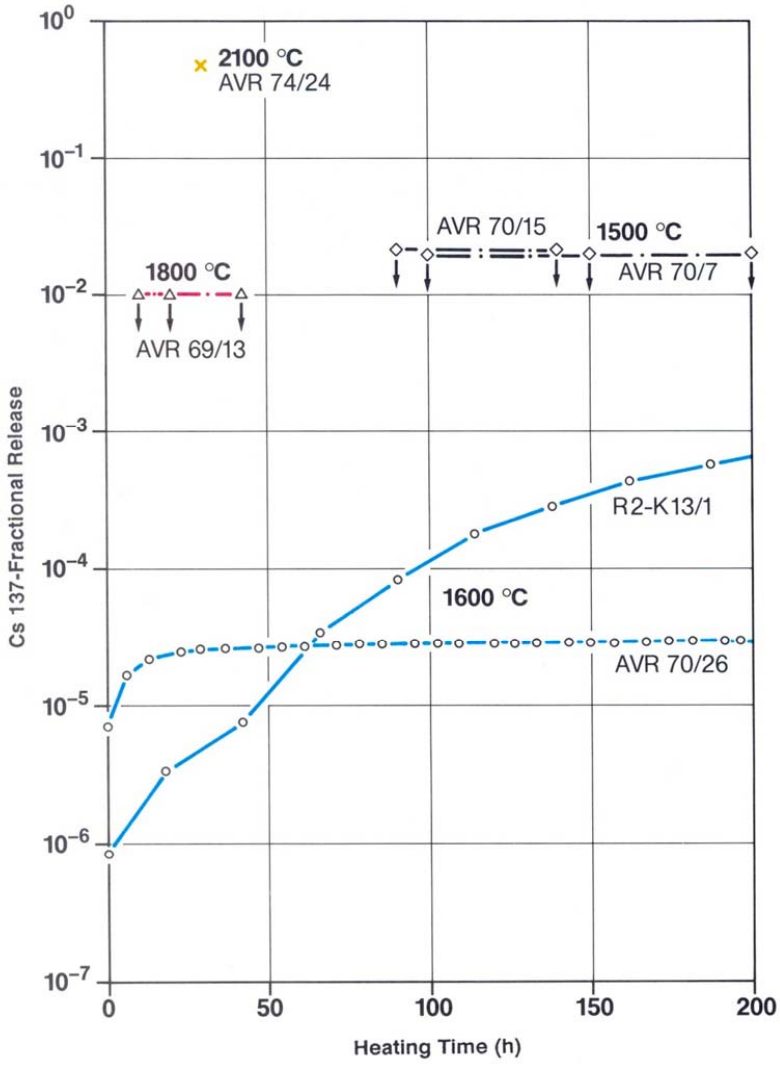

Figure 49. Fractional release of ^{137}Cs from fuel elements AVR 70/26 and R2-K13/S with HEU (Th,U)O_2 TRISO fuel particles [Schenk 1988].

The ^{137}Cs fractional release rate data plotted in Figure 50 illustrates the different phenomena that are occurring in the AVR 70/26 and R2-K13/1 fuel elements while undergoing the same type of accident simulation testing. The shapes of the two release rate curves shown here are indicative of quite different behavior for the HEU (Th,U)O_2 TRISO fuel particles and subsequent cesium source terms in these two elements. The lower curve for AVR 70/26 is representative of a depleting source for cesium, and conversely, the upper curve for R2-K13/1 is characteristic of an increasing cesium source.

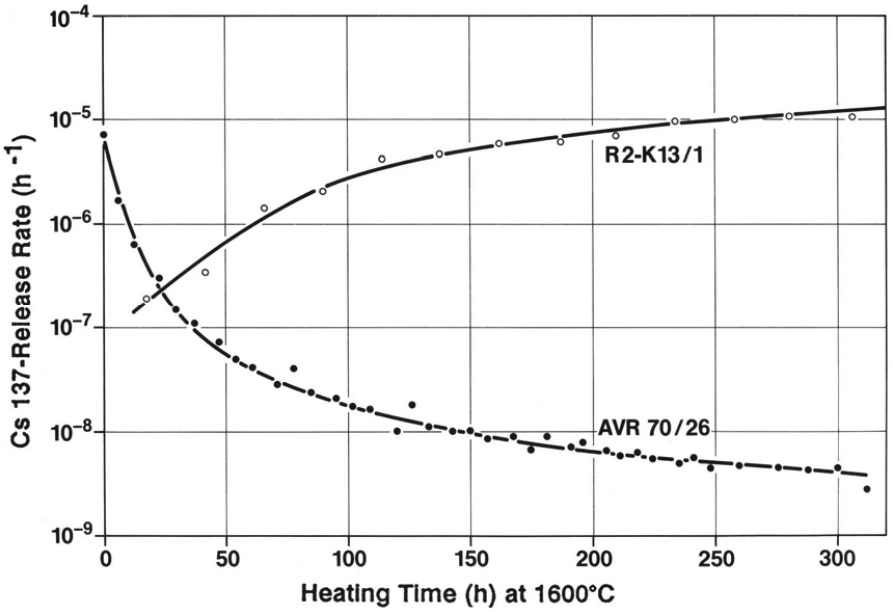

Figure 50. Fractional release rate for ^{137}Cs measured during accident simulation testing of irradiated fuel elements AVR 70/26 and R2-K13/1 [Schenk 1988].

What is happening is that the depleting cesium source in the AVR 70/26 fuel element is located in the fuel matrix. This source term is a result of as-fabricated heavy metal contamination and additional cesium contamination picked up from years of service in the AVR. At 1600°C they are both being driven off by the high temperature heating process. As the isothermal heating process continues the A3-27 fuel matrix continues to loose cesium through this purification. It also means that the HEU $(Th,U)O_2$ TRISO fuel particles in AVR 70/26 remain intact, retaining their ^{137}Cs inventory not allowing any diffusive release through the TRISO coatings during this heating process. The exact opposite is happening in the R2-K13/Capsule 1 fuel element. The increasing source term is diffusive ^{137}Cs release through the SiC and PyC layers in TRISO coatings of the HEU $(Th,U)O_2$ fuel particles. This occurs even though the fuel particles appear to be intact as there is no indication of increased ^{85}Kr release or any bursts of activity. However, the SiC layers of these particles have failed as evidenced by their significant cesium loss.

There are two different HEU $(Th,U)O_2$ TRISO particle batches being tested in these two elements. The GO2 element AVR 70/26 contains the particle batch designated HT 150-160, 162-167, and the R2-K13/1 element contains particle batch EO 1674. The most significant characterization difference between these two particle batches is their N values; particles in AVR 70/26 have a $Th/^{235}U$ ratio of 5.00 and the R2-K13/1 particles have a $Th/^{235}U$ ratio of 10.02. The other important fact is that the irradiation conditions are different in that the operating temperatures in the AVR 70/26 element were probably on average lower than in the R2-K13 experiment because of the cycling effect in the AVR. And, the accumulated fluence in the AVR 70/26 element is by a factor of about 4 lower at 2.0×10^{25} n/m^2 compared to 8.3×10^{25} n/m^2, E>16fJ. The burnup of the R2-K13/1 element is also ~25% higher at 10.3% FIMA compared to AVR 70/26 element.

5.5 Accident Condition Performance Assessment

Based on the evaluation of the accident simulation testing conducted on irradiated reference fuel elements containing HEU (Th,U)O_2 TRISO fuel particles the following important items must be taken into consideration:

- The graphite "A-Test" furnace facility has a solid fission product detection limit of one or several percent of the inventory. Furthermore, the results from the 1400ºC-1800°C isothermal accident simulation tests are unreliable because of uncertainty in the temperature determination caused by repeated failures in the automated temperature control system.

- AVR GO2 fuel elements (and other modern HTGR fuel elements) are soaked with cesium on the surface because of the large number of releasing elements that remained in the AVR from early AVR and THTR production campaigns. However, they do not actively release Cs during prolonged heating from the particles within the elements. This is due to the lower average operating temperatures in the AVR and lower accumulated fast fluence by comparison to spherical fuel elements irradiated in high-flux MTRs.

- Reference spherical fuel elements irradiated in MTRs are much cleaner and release fission product at a much lower level as compared to AVR irradiated elements. However, with continued heating, these elements with higher operating temperatures and higher accumulated fast fluences exhibit active diffusive release of solid fission products from intact TRISO particles within the fuel elements.

- Typically, krypton fractional releases always lag behind the cesium release because of the additional holdup provided by the PyC layers in TRISO coatings.

With the assumption that the accumulated ^{85}Kr release fraction is an indicator of particle failure (50% internal release at 1600°C, near 100% internal release at 1800°C), the evolution of particle failure as demonstrated in the accident simulation tests is shown in Figure 51. Maintaining the maximum accident temperature below 1600ºC dramatically avoids particle failure for several hundred hours.

In summary, full (100%) retention of gaseous and solid fission products (exception: silver) was demonstrated up to and including 1600°C for ~60 hours in R2-K13/1 element and 100, 200, up to 300 hours for the AVR GO2 elements. Beyond these conditions, solid fission product retention is influenced by high operating temperatures and high fast fluence levels accumulated in prior irradiation testing.

The statistical evaluation of particle failure is summarized in Table 30. While the accident test results are extremely good, the coincidence of the late construction of the KÜFA furnace with the change-over to LEU resulted in only two useful tests with (Th,U)O_2 fuels. This low number of accident condition tests limits the confidence in the results.

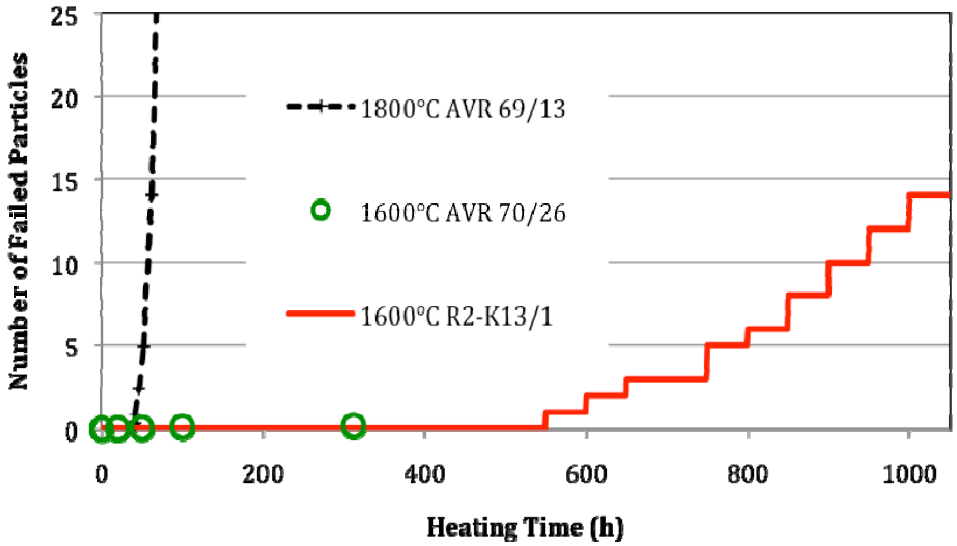

Figure 51. Number of failed particles estimated in accident condition heating tests with HEU (Th,U)O_2 TRISO fuel elements as a function of heating time.

Table 30. Statistical evaluation of HEU (Th,U)O_2 TRISO fuel particle failure fractions during accident simulation tests at 1600°C up to 550 hours and constant heat-rate ramp tests to temperatures of 2400-2500ºC.

Standard HTGR spherical elements and fuel bodies with (Th,U)O_2 TRISO particles		**No. fuel bodies**	**No. coated particles N**	**No. in-reactor failed particles n**	**Expected failure fraction =n/N**	**One-sided upper 95% confidence limit**
Accident testing	R2-K13/1 during the first 550 h	1	20,050	0	0	0
	AVR GO2 from Reload XV*	4	41,920	0	0	0
	Total	5	61,970	0	0	4.8×10^{-5}

* AVR 70/26 in KÜFA; AVR 69/28, AVR 70/18 and AVR 74/17 in "A-Test" furnace ramp tests.

6. PERFORMANCE LIMITS FOR THE HEU (TH,U)O_2 TRISO FUEL SYSTEM

Performance data on the HEU (Th,U)O_2 TRISO fuel system generated within the German Fuel Development Program during the period 1977 to 1990 were evaluated in three areas: fuel manufacture, in-reactor testing and accident simulation testing. Collectively, the performance results from 67 spherical fuel elements and 27 specially designed irradiation test specimens were evaluated for this assessment. This represents ~487,480 TRISO particles from manufacturing, ~220,990 TRISO particles that were irradiation tested, and ~61,970 TRISO particles subjected to accident simulation testing.

Table 31 presents a statistical analysis of all the manufacturing, irradiation and accident testing performance results in terms on the number of defective and failed fuel particles observed in the totality of the HEU (Th,U)O_2 TRISO fuel test specimens. These experimental results are summarized below in Table 32 and in Figure 52.

The data presented in the Table 31 will in all practical circumstances be compared with the fuel performance requirements for today's modern HTGR concepts that require a high degree of passive safety and stringent licensing requirements. However, the HEU (Th,U)O_2 TRISO fuels of this study were manufactured and tested some 30 years ago for HTGR design concepts in Germany that were directed towards process heat applications (PNP) and direct cycle electricity production (HHT). Instead of small, modular HTGRs of primary interest today, these (Th,U)O_2 TRISO fuels were destined for large HTGR plant designs of 3000 MW(th), with a pre-stressed concrete pressure vessels, and multiple inlet and outlet on-line refueling systems. The large HTGR plant design operating conditions are similar to those of today's HTGR designs with respect to operating temperature, burnup and accumulated fast fluence. However, in the area of accident mitigation, modern HTGR concepts are far superior to the large PNP/HHT HTGR concepts of the 1970s and early 1980s.

Target values for particle performance [HBK 1979] that represented guidelines for the development of fuel systems for the PNP and HHT concepts in the mid-to-late 1970 in Germany are listed in Table 33. The one-sided 95% upper confidence limits derived in manufacture and in irradiation testing are by a factor of about 3 lower than target specifications of the time [HBK 1979, Kania 1980b]. In comparison to modern HTGR fuel quality requirements, the PNP/HHT requirements are slightly higher (actual values higher), but they are severe and for Fuel Variant 2, (Th,U)O_2 TRISO, the cumulative EOL failure fraction requirement from all contributions (fabrication, matrix contamination and irradiation-induced failure) for a PNP/HHT fuel element is $\leq 2.9\times10^{-4}$. Note that there is no specification for fuel performance under accident conditions in Table 33 and there are no statistical requirements presented (confidence levels).

Table 31. Final HEU (Th,U)O_2 TRISO fuel performance evaluation consisting of limiting fractions of defects during manufacture and failures during irradiation and accident testing.

Standard HTGR spherical elements and fuel bodies with (Th,U)O_2 TRISO particles		**No. fuel bodies**	**No. particles in a fuel body**	**No. coated particles N**	**No. defective/ failed particles n**	**Expected failure fraction n/N**	**One-sided upper 95% confidence limit**
Manufacture	GO2 from AVR Reload XV	16	10,480	167,680	5	3.0×10^{-5}	
	GO2 from AVR Reload XX	30	10,660	319,800	0	0	
	$Total_{manu}$	**46**	**-**	**487,480**	**5**	**1.0×10^{-5}**	**2.2×10^{-5}**
MTR irradiation	BR2-P25/1-12	12	1490	17,880	5	2.8×10^{-5}	
	R2-K12/1	1	10,830	10,830	0	0	
	R2-K12/2	1	10,830	10,830	0	0	
	FRJ2-P23/1-4	12	1707 / 2638	26,070	0	0	
	FRJ2-K11/3-4	2	10,480	20,960	1	4.8×10^{-5}	
	R2-K13/1	1	20,050	20,050	0	0	
	R2-K13/4	1	20,050	20,050	2	1.0×10^{-4}	
	$Total_{MTR}$	-	-	126,670	8	6.1×10^{-5}	
AVR irradiation	AVR XV GO2	9	10,480	94,320	0	0	
All irradiation	**$Total_{MTR+AVR}$**	**-**	**-**	**220,990**	**8**	**3.6×10^{-5}**	**6.5×10^{-5}**
Accident testing	R2-K13/1 up to 550h	1	20,050	20,050	0	0	
	GO2 from AVR XV*	4	10,480	40,920	0	0	
	$Total_{Accid}$	**5**	**-**	**61,970**	**0**	**0**	**4.8×10^{-5}**

* consisting of one KÜFA test AVR 70/26 and 4 ramp tests AVR 70/18, AVR 74/17, AVR 74/20, AVR 74/24, see Chapter 5 on accident testing.

Table 32. Statistical analysis of particle failure fractions due to manufacture, irradiation, and accident testing performance.

	Expected failure fraction	**Failure fraction at the 95% confidence limit**
Manufacture	1×10^{-5}	$0\ldots2.2\times10^{-5}$
In-reactor performance	3.6×10^{-5}	$0\ldots6.5\times10^{-5}$
Accident condition performance	0	$0\ldots4.8\times10^{-5}$

Table 33. Target specifications for particle and fuel element performance for the particle variants applicable to the PNP/HHT HTGR concepts [HBK 1979].

	PNP/HHT fuel element performance targets with HEU fuels			
	Variant 1	**Variant 2**	**Variant 3**	
Particle type				
Kernel diameter [µm]	400	500	200	500
Composition	$(Th,U)O_2$	$(Th,U)O_2$	UC_2 (UCO)	ThO_2
Coating design	HTI-BISO	LTI-TRISO	LTI-TRISO	LTI-TRISO
Fuel element				
Heavy metal [g/element]	11.24	11.24	11.24	
^{235}U [g/element]	0.96	0.96	0.96	
Matrix contamination	1×10^{-4}	3×10^{-5}	3×10^{-5}	3×10^{-5}
As-fabricated defects	1×10^{-4}	6×10^{-5}	1×10^{-4}	6×10^{-5}
Irradiation-induced failures	2×10^{-4}	2×10^{-4}	1×10^{-4}	2×10^{-4}
Irradiation conditions	*PNP-3000*	*HHT-Demo*	*Test limits*	
Duration [d]	1160	1100	2000	
Burnup [% FIMA]	9.9 – 11.2	10.4 – 11.2	14	
Fluence [E>0.1 MeV, m^{-2}]	$3.1\text{-}4.5\times10^{25}$	$3.1\text{-}4.5\times10^{25}$	$3.1\text{-}4.5\times10^{25}$	
Central max. temp [ºC]	1020	1014	1200	
Max. FE power [kW]	2.9	2.7	4.5	

Comparing the HEU $(Th,U)O_2$ TRISO fuel particle statistical data in Table 31 with the requirements in Table 33 shows that

- Relative to manufacture, the experimental data is lower than the contamination requirement by a factor of ~3 at the upper 95% confidence level, 2.2×10^{-5} vs. 9×10^{-5}.
- For irradiation-induced failure, the experimental data again is lower than the requirement by a factor of ~3 at the 95% confidence level, 6.4×10^{-5} vs. 2×10^{-4}.
- In the late 1970s, an unrestrained-core-heatup event was the dominant accident scenario for large HTGR concepts, and this compares to the experimental data of 4.8×10^{-5} for accident temperatures ≤ 1600ºC.

These comparisons are striking, especially for the period when these fuels were fabricated, irradiation tested and experimentally evaluated.

As observed in previous performance assessments [Nabielek 2010], non-reference test specimens prepared specially to meet HTGR irradiation test rigs (mini-spheres, cylindrical compacts and coupons) configuration restrictions are often the primary source of in-reactor failed particles. The fabrication processes developed for the HTGR pebble-bed reference 60 mm diameter spherical fuel elements have been finely tuned over the years and proved to be by far the best and most representative configuration for irradiation testing of HTGR coated particle fuels. In a conservative manner, considering only the experimental performance results obtained on reference spherical elements, a somewhat improved statistic for irradiation testing is realized, where the failure statistics drops to 3.8×10^{-5}. The $(Th,U)O_2$ TRISO fuel failure statistics, based only on the experimental results from reference HTGR fuel elements are presented in Table 34 and Figure 52.

Table 34. Performance statistics for the HEU $(Th,U)O_2$ TRISO fuel system based on the experimental results obtained from 66 spherical fuel elements in the German HTGR Fuel Development Program (see also Figure 52).

Standard HTGR spherical elements with $(Th,U)O_2$ TRISO particles	**Total No. fuel bodies**	**Total No. coated particles N**	**Total No. failed particles n**	**Expected failure fraction n/N**	**One-sided upper 95% confidence limit**
Manufacture	46	487,480	5	1.0×10^{-5}	2.2×10^{-5}
Irradiation	15	177,040	3	1.7×10^{-5}	4.4×10^{-5}
Accident	5	61,970	0	0	4.8×10^{-5}

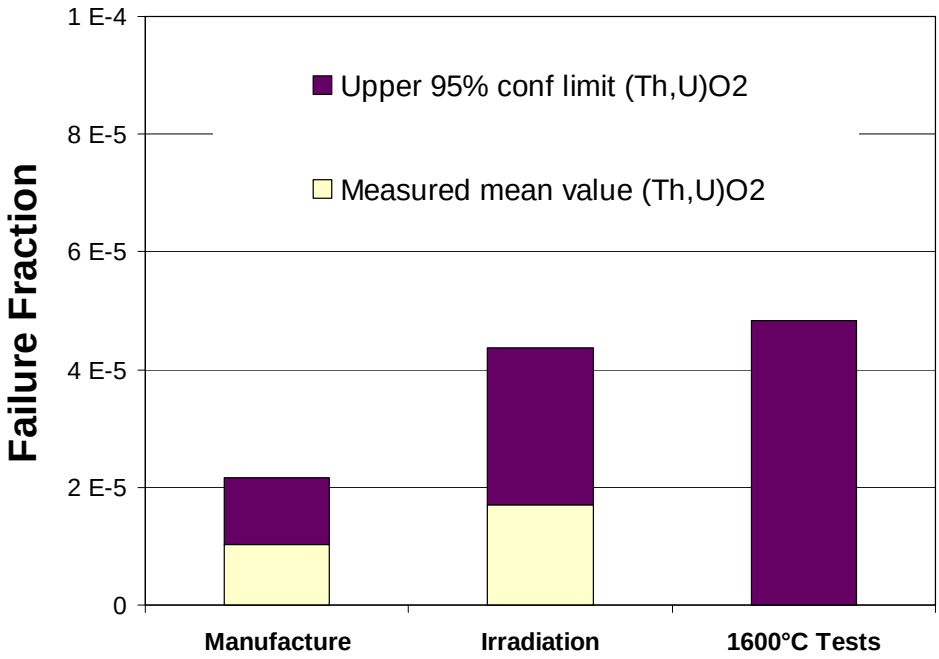

Figure 52. Final HEU (Th,U)O_2 TRISO fuel performance assessment of experimental values in manufacturing defects, irradiation and accident induced failures, and their one-sided upper 95% confidence limits.

With modern HTGR fuels, present state-of-the-art requirements dictate:

- near complete retention of fission products at their source – the intact TRISO coated particles with no standard particle failure during normal operating conditions at temperatures < 1250°C, and for accident conditions at temperatures ≤ 1600°C;
- very low levels of contamination in the outer PyC layer (≤ 10^{-5}) of the particle and in the fuel element graphitic matrix (~10^{-5}); and
- low levels of as-fabricated defective fuel particles (~10^{-5}) with missing or defective coatings.

In this manner, the source term in an HTGR is dominated by defective fuel particles produced during manufacture and only by their failure during irradiation or in accidents. Many of the irradiation and accident conditions tests conducted between 1977 and 1990 have demonstrated excellent fuel behavior, and their final performance assessment is limited only by sampling statistics. The performance statistics for the HEU (Th,U)O_2 TRISO fuel system, as illustrated in Table 34, are in perfect concert with those state-of-the-art requirements for present-day High Temperature Reactor concepts.

7. SUMMARY AND CONCLUSIONS

Thorium is of interest for its widespread availability and the good irradiation behavior of Th and (Th,U) oxide and carbide compounds as fuels in nuclear power systems. Early development of all large HTGRs employed the thorium-uranium (^{233}U) HEU fuel cycle, but after 1980 all HTGR development switched to the uranium-plutonium fuel cycle with low-enriched uranium of $\leq 20\%$ enrichment. Currently, there is a renewed interest in thorium utilization.

Following completion of fuel development work for AVR and THTR with HTI-BISO coated particles in Germany, the German fuel development program embarked on a new program on advanced HTGR concepts aimed at process heat application and direct-cycle electricity generation. The operating/ maintenance requirements for these new PNP/HHT concepts required a clean primary circuit, especially for the HHT direct-cycle concept with the gas turbine in the primary circuit. Thus, already in 1978-84, fuel quality requirements that led to the modern HTGR particle quality standards were established for low contamination and low defect particle levels in the manufacture of spherical fuel elements with TRISO particles. The combination of an LTI inner and outer PyC layers with a strong, stable SiC layer not only improved clean manufacturing conditions, but the TRISO coating design provided increased mechanical strength to the coated particle and a high degree of fission product retention, not previously known with HTI-BISO coatings.

Improved performance with the HEU $(Th,U)O_2$ TRISO fuel system was successfully demonstrated in three primary areas: manufacturing, irradiation testing, and accident simulation testing. In terms of demonstrating performance for advanced HTGR applications, the experimental failure statistics from manufacture and irradiation testing were lower than particle failure requirements specified for the PNP and HHT designs. Then, in the mid-1970s, there were no passive safety requirements specified for the PNP/HHT as they were large HTGR plant designs and the unrestrained core heatup event beyond 2000°C was the dominant accident scenario.

Based on the performance statistics compiled from the period from 1977 through 1990, the following assessment of HEU $(Th,U)O_2$ TRISO fuel system can be presented:

- Forty-six (46) reference HTGR fuel elements from manufacturing, containing 487,480 TRISO fuel particles were evaluated using reference Quality Control methods. The results yielded a combined contamination and defective particle fraction 2.2×10^{-5} at the upper 95% confidence level. This value is lower that the PNP/HHT specification value by a factor of ~3 and is below the LEU UO_2 specification for the German HTR-Modul of 6.5×10^{-5}.

- In-reactor testing under normal operating conditions, included accelerated MTR irradiation experiments (comprising 126,664 TRISO particles) in six reference fuel elements and 24 special fuel specimens, and testing of reference AVR GO2 elements (94,320 TRISO particles) in nine fuel elements from the real-time AVR environment. These results yielded an in-reactor failure level under normal operating conditions of 6.5×10^{-5} at the upper 95% confidence level. If only reference fuel elements are considered, the in-reactor failure level is 4.4×10^{-5} with a 95% confidence level. Both of these levels are well below the PNP/HHT

specification by a factor of > 3, and are significantly lower than the in-reactor operation requirement for the German HTR-Modul at 2×10^{-4}.

- Accident simulation testing carried out on five reference fuel elements (representing 61,970 TRISO particles) yielded at failure level of 4.8×10^{-5} at the upper 95% confidence level. This failure level represents the expected fraction of failed fuel particles at accident conditions ≤ 1600ºC. This level is less than the German HTR-Modul target value of 5×10^{-4} for temperatures ≤ 1620ºC.

The experimental performance statistics for the HEU $(Th,U)O_2$ TRISO fuel system obtained with only standard HTGR 60 mm diameter fuel elements are in agreement with similar results obtained on reference fuel elements with the LEU UO_2 TRISO fuel system as shown in Table 35 and Figure 54. The LEU UO_2 TRISO fuel system was also developed under the same German HTGR Fuel Development Program for the HTR-Modul concept. The consistency of the results demonstrates the success of a dedicated effort over two decades with high funding levels and intensive cooperation between industry, research centers and academia. Both fuel designs compare well against the requirements for the German HTR-Modul concept.

Table 35. Comparison of the performance statistics obtained on reference HTGR 60 mm diameter fuel elements containing HEU $(Th,U)O_2$ TRISO fuel with similar statistics on elements containing LEU UO_2 TRISO fuel (see also Figure 53).

Standard HTGR spherical elements with $(Th,U)O_2$ TRISO particles	**Total No. fuel bodies**	**Total No. coated particles N**	**Total No. failed particles n**	**Expected failure fraction n/N**	**One-sided upper 95% confidence limit**
HEU $(Th,U)O_2$ TRISO					
Manufacture	46	487,480	5	1.0×10^{-5}	2.2×10^{-5}
Irradiation	15*	177,040*	3	1.7×10^{-5}	4.4×10^{-5}
Accident	5	61,970	0	0	4.8×10^{-5}
LEU UO_2 TRISO					
Manufacture	175	2,202,200	86	3.9×10^{-5}	4.7×10^{-5}
Irradiation	43	670,280	0	0	4.5×10^{-6}
Accident	19	287,480	5	1.7×10^{-5}	3.7×10^{-5}

* Six MTR tests with 82,720 particles plus nine AVR tests with 94,320 particles

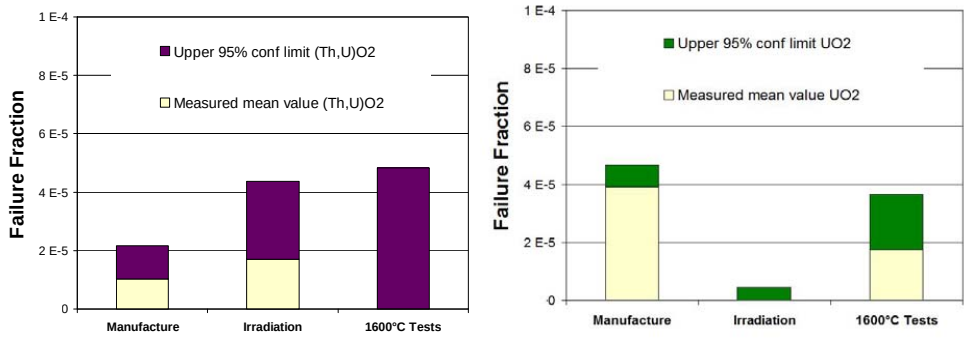

Figure 53. Comparison of final TRISO fuel performance assessment of experimental values in manufacturing defects, irradiation and accident induced failures, and their one-sided upper 95% confidence limits for HEU (Th,U)O_2 (left) and LEU UO_2 (right).

The objective of this effort was to perform a performance assessment on the HEU (Th,U)O_2 TRISO Fuel system based on the results obtained in the German Fuel Development Program over the period from 1977 to 1990. In was during the early part of this period that the HEU (Th,U)O_2 TRISO particle concept was developed. This assessment focused on three primary areas of (Th,U)O_2 TRISO fuel development: manufacturing, irradiation testing and accident simulation testing (more commonly known as "annealing studies" during this period). The successful completion of the present effort was in part due to the large quantity of literature and documentation that were made available on the manufacture and testing of (Th,U)O_2 fuels from the Research Center Jülich (Forschungszentrum Jülich) (FZJ) in Germany.

REFERENCES

Acharya R., Analysis of the R2-K12 Irradiation Experiment. Document 906636, Issue 3, General Atomics, San Diego, CA, 1983.

Allelein H.-J., Spaltproduktverhalten – speziell Cs-137 – in HTR TRISO Brennstoffteilchen. Report Jül-1695, Research Center Jülich, 1980.

Amian W., Stöver D., Diffusion of Silver and Cesium in Silicon Carbide Coatings of Fuel Particles for HTRs. *Nuclear Technology* **61**:475, 1983.

Bäumer R., Kalinowski I., Röhler E., Schöning J., Wachholz W., Construction and Operating Experience with the 300-MW THTR Nuclear Power Plant. *Nuclear Engineering and Design* **121**:155-166, 1990.

Benz R., Naoumidis A., Stability of Unirradiated Triso-Coated UC_2-UO_2 Particles with Different UC_2 Contents at Elevated Temperatures. *Journal of Nuclear Materials* **97**:15 1981.

Benz, R., Kinetics of Decomposition of CVD SiC in Modified TRISO-coated Fuel Particles at Temperatures of 1600 to 2200°C, Technical Note IRW-TN-124/82, Research Center Jülich, 1982.

Booth A.H., A Method of Calculating Fission Gas Diffusion from UO_2 Fuel and Its Application to the X-2-f Loop Test. Report CRDC-721, AECL No. 496, Atomic Energy of Canada Limited, Chalk River, Ontario, 1957.

Brown P.E., Inns A.J., Post-Irradiation Examination of Spherical Fuel Elements from Irradiation Experiments FRJ2-K10 and K11, Report AERE-G2240, UKAEA, Harwell, 1982.

Burck W., Krautwasser P., Datensatz zum Bestrahlungsverhalten von hochangereicherten (Th,U)-Mischoxid-Brennstoffteilchen mit SiC Zwischenschicht. Internal Report, IRW-IB-13/88, Research Center Jülich, 1988.

Dahlberg R.C., Turner R.F., Goedell W.V., Fort St. Vrain Core Design Characteristics. *Nuclear Engineering International* **14**:163, 1969.

Delle W.W., et al., Quality Control Procedures for HTGR Fuel Element Components. Report Jül-1333, Research Center Jülich, 1976.

Derz H., Gottaut H., Pohl P., Pott G., The Determination of the Maximum Coolant Temperature in the AVR Core. Internal Report HTA-IB-3/90, Research Center Jülich, 1990.

Fortescue P., Bell F.R., Duffield R.B., Hexagonal Fuel Element, U.S. Patent Application No. 485,811, Filed September 8, 1965.

Freis D., Störfallsimulationen und Nachbestrahlungsuntersuchungen an kugelförmigen Brennelementen für Hochtemperaturreaktoren. PhD Thesis University RWTH Aachen, 2010.

Freis D., Bottomley D., Ejton J., Weerd W. de, Kostecka H., Toscano E.H., Postirradiation Testing of High Temperature Reactor Spherical Fuel Elements under Accident Conditions. *Journal of Engineering for Gas Turbines and Power* **132**(4), 2010b.

Gontard R., Mehner A.-W., Vorbestrahlungsbericht für das Experiment R2-K12. Internal Report HBK-IB-7/81, Research Center Jülich, 1981.

Gontard R., Nabielek H., Performance Evaluation of Modern HTR TRISO Fuels. Internal Report HTA-IB-05/90, Research Center Jülich, 1990.

Gottaut H., Krüger K., Results of Experiments at the AVR Reactor. Nuclear Engineering and Design 121:143, 1990.

Greneche D., et al., Rethinking the Thorium Fuel Cycle: An Industrial Point of View. Proc. ICAPP 2007, paper 7367, Nice, France, 2007.

Gruppelaar H., (Ed.), Thorium as a Waste Management Option. Final Report EUR-19142.EN, Commission of the European Communities, Directorate-General Science, Research and Development, Luxembourg, 2000.

Hantke H.-J., Performance of High Quality HTR-LEU Fuel Elements with TRISO Coated Particles – A Summary Report. Internal Report HTA-IB-7/92, Research Center Jülich, 1992.

Hauer M., Bröcker P., HOBEG Abnahmeprüfzeugnis AVR XV nach DIN 50049-3.1.B, Zeugnis Nr. 716/3193/78 from 7 September 1978, HOBEG, Hanau, 1978.

Hauer M., Bröcker P., HOBEG Abnahmeprüfzeugnis AVR XX nach DIN 50049-3.1.B, Zeugnis Nr. 57/5561/83 from 20 May 1983, HOBEG, Hanau, 1983.

HBK, HBK Projektbericht 1978. Internal Report HBK-IB-1/79, page 25, Research Center Jülich, 1979.

HBK, HBK Projektbericht 1983. Internal Report HBK-IB-1/84, Research Center Jülich, 1984.

Heit W., Pebble Bed Fuel Element Research and Development and Industrial Production in Germany. Proc. HTR-TN Int. HTR Fuel Seminar, Brussels, 2001.

HHT, HHT-NINT-Anlagenkonzept 1000 MW – Abschlussbericht, Hochtemperaturreaktor Heliumturbine Groβer Leistung, Volume 1, Research Center Jülich, 1977.

Hrovat M., Nickel H., Koizlik K., Über die Entwicklung eines Matrixmaterials zur Herstellung gepresster Brennelemente für Hochtemperatur-Reaktoren. Report Jül-969, Research Center Jülich, 1973.

Hrovat M., Huschka H., Mehner A.-W., Warzawa W., Spherical Fuel Elements for Small and Medium Sized HTRs. *Nuclear Engineering and Design* **109**:253, 1988.

Huschka H., Vygen P., Coated Particles: Requirements and Status of Fabrication Technology. *Nuclear Technology* **35**:228, 1977.

IAEA, Fuel Performance and Fission Product Behavior in Gas Cooled Reactors. Report IAEA-TECDOC-978, International Atomic Energy Agency, Vienna, 1997.

IAEA, High Temperature Gas Cooled Reactor Fuels and Materials. Report IAEA-TECDOC-1645, International Atomic Energy Agency, Vienna, 2010.

IAEA, Advances in HTGR Fuel Technology. Report IAEA-TECDOC-1674, International Atomic Energy Agency, Vienna, 2012.

IAEA, Role of Thorium to Supplement Fuel Cycles of Future Nuclear Energy Systems. Nuclear Energy Series No. NF-T-2.4, International Atomic Energy Agency, Vienna, 2012b.

Ikawa K., Kobayashi F., Iwamoto K., Failure of Coated Fuel Particles during Thermal Excursion above 2000°C. *Journal of Nuclear Science and Technology* **15**:774, 1978.

Interatom, Hochtemperaturreaktor-Modul-Kraftwerksanlage Sicherheitsbericht. Siemens Internal report, Erlangen-Bensberg, 1988.

Ivens G., Wimmers M., The AVR as Test Bed for Fuel Elements. In: 21 Years of Successful Operation for a Future Technology, Association of German Engineers (VDI)) - The Society for Energy Technologies (Publ.), VDI-Verlag Düsseldorf, 1990.

Kadner M., Baier J., Production of Fuel Kernels for HTR Fuel Elements. *Kerntechnik* **18**:413, 1977.

Kania M.J., Valentine K.H., The Irradiated-Microsphere Gamma Analyzer (IMGA) – An Integrated System for HTGR Coated Particle Fuel Performance Assessment. Report ORNL-5606, Oak Ridge National Laboratory, 1980.

Kania M.J., Nickel H., Performance Assessment of the $(Th,U)O_2$ HTI-BISO Coated Particle under PNP/HHT Irradiation Conditions, Report Jül-1685, Research Center Jülich, 1980b.

Koenker R., Quantile Regression. ISBN-10: 0521608279, Cambridge University Press, 2005.

Kugeler K., Kugeler M., Niessen H., Hohn H., Design of a 3000 MW(th) High Temperature Reactor for Process Heat Applications. *Nuclear Engineering and Design* **34**:33-50, 1975.

Kuijper J.C., et al., Plutonium and Minor Actinide Management in Thermal High-Temperature Gas-Cooled Reactors. Publishable Final Activity Report of the PUMA Project, Contract Number: FP6-036457, Report EUR 24865, Brussels, 2010.

Liang T.X., Recent R&D of HTR Fuel in INET. Presentation at the IAEA Technical Meeting on HTR Fuel and Fuel Cycle, Vienna, 6-9 September 2010.

Liu B., Fabricating Process and Quality Control Diagram of the Fuel Element. Presentation at the Institute of Nuclear and New Energy Technologies, Tsinghua University, Beijing, 27 May 2011.

Lotts A.L., Holman F., Balthesen E., Turner R., "HTGR Fuel and Fuel Cycle Technology", IAEA Conference on Advanced Reactors, Salzburg, Austria, May 1977.

Muncke G., Freisetzungsrechnung fester Spaltprodukte R2-K12. Internal Report DB 1261, Hochtemperatur-Reaktorbau (HRB), Mannheim, 1982.

Nabielek H., Hick H., Wagner-Löffler M., Voice E.H., Performance Limits of Coated Particle Fuel – Part III: Fission Product Migration in HTR Fuel. Report DPR 828/III, OECD DRAGON Project, Winfrith, 1974.

Nabielek H., Naoumidis A., Goodin D.T., and Ikawa K., High Temperature Behavior of HTR Fuel Particles. Proc. Jahrestagung Kerntechnik, pages 000-000, Berlin, 1983.

Nabielek H., Schenk W., Heit W., Mehner A.-W., Goodin D.T., The Performance of HTR Fuel Particles at Extreme Temperatures. *Nuclear Technology* **84**:62, 1989.

Nabielek H., Kühnlein W., Schenk W., Heit W., Christ A., Ragoss H., Development of Advanced HTR Fuel Elements. *Nuclear Engineering and Design* **121**:199, 1990.

Nabielek H., Verfondern K., Kania M.J., Fuel and Fission Products in the AVR Reactor. Proc. HTR2008, paper 0000, Washington D.C., 2008.

Nabielek H., Verfondern K., Kania M.J., HTR Fuel Testing in AVR and in MTRs. Proc. 5th Int. Top. Meeting on High Temperature Reactor Technology HTR2010, paper 064, Prague, 2010.

Nabielek H., Predicted Maximum AVR Fuel Temperatures Derived from the 1986 Melt-Wire Experiment. Technical Note, 2011.

Petti D., Maki J., Hunn J., Pappano P., Barnes C., Saurwein J.J., Nagley S., Kendall J., Hobbins R., NGNP Fuel Qualification White Paper. Report INL/EXT-10-18610, Rev. 0, Idaho National Laboratory, 2010.

Pohl P., Experimental Evaluation of the AVR Melt-Wire Test. Technical Note, Arbeitsgemeinschaft Versuchsreaktor GmbH, Jülich, 2009.

Sauer E. (Ed.), AVR-Experimental High Temperature Reactor: 21 Years of Successful Operation for a Future Technology. Association of German Engineers VDI, Düsseldorf, 1990.

Schenk W., Untersuchungen zum Verhalten von beschichteten Brennstoffteilchen und Kugelbrennelementen bei Störfalltemperaturen. Report Jül-1490, Research Center Jülich, 1978.

Schenk W., Störfallsimulation an bestrahlten Kugelbrennelementen bei Temperaturen von 1400 bis 2500°C. Report Jül-1883, Research Center Jülich, 1983.

Schenk W., Pitzer D., Nabielek H., Fission Product Release Profiles from Spherical HTR Fuel Elements at Accident Temperatures. Report Jül-2234, Research Center Jülich, 1988.

Schenk W., Nabielek H., Kugelbrennelement mit TRISO-Partikeln bei Störfalltemperaturen. Report Jül-Spez-487, Research Center Jülich, 1989.

Schenk W., Pott G., Nabielek H., Fuel Accident Performance Testing for Small HTRs. Journal of Nuclear Materials 171:19, 1990.

Schulten R., Bellermann W., Braun H., Schmidt H.W., Setzwein A., Stürmer W., Der Hochtemperaturreaktor von BBC/Krupp. Die Atomwirtschaft, 1959.

Schulten R., Pebble bed HTRs. *Annals of Nuclear Energy* **5**:357, 1978.

Schulze R.E., Schulze H.A., Rind W., Graphite Matrix Materials for Spherical HTR Fuel Elements. Report Jül-Spez-167, Research Center Jülich, 1982.

Stöver D., Hecker R., Cesium Release Data for BISO-Coated Particles. *Nuclear Technology* **35**:465, 1977.

Stansfield O.M., Evolution of HTGR Coated Particle Fuel Design. Energy 16:33-45, 1991.

Thiel J., Gasfreisetzung aus Defektpartikeln im Experiment FRJ2-P25. Internal Report DB 1583, Hochtemperatur-Reaktorbau (HRB), Mannheim, 1982.

Toscano E.H., Private Communication, 2010.

Turner R.F., US/FRG Umbrella Agreement for Cooperation in GCR Development: Fuel, Fission Products and Graphite Subprogram – Quarterly Status Report III/83. Document No. GA-A17337, General Atomics, San Diego, CA, 1983.

Verfondern K., Status of German Spent HTGR Fuel Research. Proc. IAEA-TM on Safety Aspects of Modular HTGRs, Beijing, 2007.

Verfondern K., Cao J., Liu T., Allelein H.-J., Conclusions from V&V Studies on the German Codes PANAMA and FRESCO for HTGR Fuel Performance and Fission Product Release. Proc. HTR2012, paper 3-007, Tokyo, 2012.

Vorreyer M., Leushacke D.F., Th/U-Fuel Cycle for HTGRs. ProNuclear Seminar 1978, Internal Report, HBK-IB-2/78, Research Center Jülich, 1978.

WNA, Thorium. World Nuclear Association, http://www.world-nuclear.org/info/inf62.html, 2011.

Xhonneux A., Allelein H.-J., Development of an Integrated Fission Product Release and Transport Code for Spatially Resolved Full-Core Calculations of V/HTRs. Proc. HTR2012, paper 5-009, Tokyo, 2012.

Zhao H., Liang T.X., Zhang J., He J., Zhou Y., Tang C.H., Manufacture and Characteristics of Spherical Fuel Elements for the HTR-10. *Nuclear Engineering and Design* **236**:643, 2006.

LIST OF ACRONYMS

AVR	Arbeitsgemeinschaft Versuchsreaktor GmbH
BISO	Bi-isotropic
BOL	Beginning-of-life
BR2	MTR in Mol, Belgium
CVD	Chemical vapor deposition
EOL	End-of-Life
FRJ2	MTR in Jülich (DIDO), Germany
HEU	High-enriched uranium
HHT	High temperature reactor with helium turbine
HTGR	High Temperature Gas-Cooled Reactor
HTI	High-temperature isotropic
IMGA	Irradiated microsphere gamma analyzer
INET	Institute of New and Nuclear Energy Technology, Beijing
KÜFA	Kühlfinger-Anlage (Cold-finger apparatus)
LEU	Low-enriched uranium
LTI	Low-temperature isotropic
LWR	Light water reactor
MEU	Medium-enriched uranium
MTR	Material Test Reactor
PNP	Prototype nuclear process heat reactor
PyC	Pyrocarbon
QC/QA	Quality control/Quality Assurance
R2	MTR in Studsvik, Sweden
R/B	Ratio of release rate to birth rate
SiC	Silicon carbide
THTR	Thorium High Temperature Reactor
TRISO	Tri-isotropic
UCO	Mixture of UO_2 and UC_2

Band / Volume 161
Thermal Shock Behaviour of Different Tungsten Grades under Varying Conditions
O. M. Wirtz (2013), XIV, 130 pp
ISBN: 978-3-89336-842-6

Band / Volume 162
Effects of ^{137}Cs and ^{90}Sr on structure and functional aspects of the microflora in agricultural used soils
B. Niedrée (2013), XII, 92 pp
ISBN: 978-3-89336-843-3

Band / Volume 163
Lidar observations of natural and volcanic-ash-induced cirrus clouds
C. Rolf (2013), IX, 124 pp
ISBN: 978-3-89336-847-1

Band / Volume 164
CO2-Abscheidung, -Speicherung und -Nutzung:
Technische, wirtschaftliche, umweltseitige und gesellschaftliche Perspektive
Advances in Systems Analysis 2
W. Kuckshinrichs; J.-F. Hake (Eds.) (2012), iv, 354 pp
ISBN: 978-3-89336-850-1

Band / Volume 165
Interest Mediation and Policy Formulation in the European Union
Influence of Transnational Technology-Oriented Agreements on European Policy in the Field of Carbon Capture and Storage
Advances in Systems Analysis 3
O. Schenk (2013), XIII, 253 pp
ISBN: 978-3-89336-852-5

Band / Volume 166
Versagensverhalten plasmagespritzter Mg-Al-Spinell-Schichten unter Thermozyklierung
S. M. Ebert (2013), X, 173 pp
ISBN: 978-3-89336-853-2

Band / Volume 167
Coupled modeling of water, vapor and heat in unsaturated soils - Field applications and numerical studies
C. Steenpaß (2013), X, 123 pp
ISBN: 978-3-89336-854-9

Band / Volume 168
An analysis of the global atmospheric methane budget under different climates
A. Basu (2013), v, 110 pp
ISBN: 978-3-89336-859-4

Band / Volume 169
Experimental determination of the partitioning coefficient of nopinone as a marker substance in organic aerosol
B. Steitz (2013), 132 pp
ISBN: 978-3-89336-862-4

Band / Volume 170
Ion Beam Treatment of Functional Layers in Thin-Film Silicon Solar Cells
W. Zhang (2013), xi, 191 pp
ISBN: 978-3-89336-864-8

Band / Volume 171
Pulvermetallurgische Herstellung von porösem Titan und von NiTi-Legierungen für biomedizinische Anwendungen
M. Bram (2013), X, 238 pp
ISBN: 978-3-89336-866-2

Band / Volume 172
IEK-3 Report 2013. Langlebige Elektrochemische Verfahrenstechnik
(2013), ca. 185 pp
ISBN: 978-3-89336-868-6

Band / Volume 173
Combined Steady State and High Cycle Transient Heat Load Simulation with the Electron Beam Facility JUDITH 2
Th. Loewenhoff (2013), XVI, 108 pp
ISBN: 978-3-89336-869-3

Band / Volume 174
High-Quality Thorium TRISO Fuel Performance in HTGRs
K. Verfondern, H. Nabielek, M.J. Kania, H.-J. Allelein (2013), viii, 109 pp
ISBN: 978-3-89336-873-0

Weitere ***Schriften des Verlags im Forschungszentrum Jülich*** unter
http://wwwzb1.fz-juelich.de/verlagextern1/index.asp

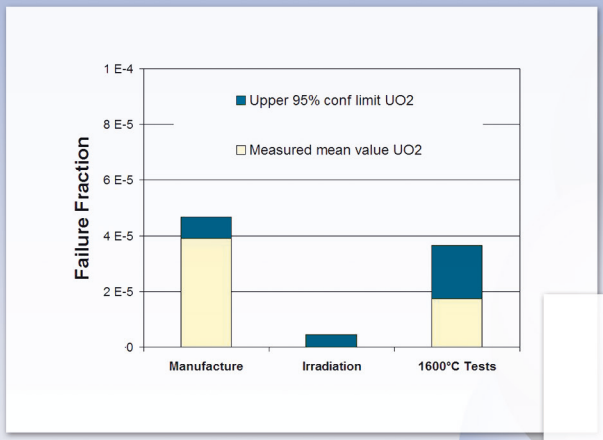

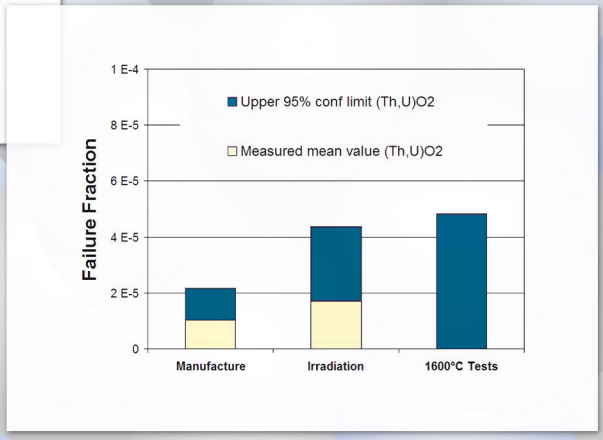

Energie & Umwelt / Energy & Environment
Band / Volume 174
ISBN 978-3-89336-873-0

JÜLICH
FORSCHUNGSZENTRUM